Biochemical Characterization of a Novel Lysosomal Membrane Protein Disrupted in Renal Carcinoma 2 (DIRC2)

Dissertation

in fulfillment of the requirement for the degree “Dr. rer. nat”

of the Faculty of Mathematics and Natural Sciences

at Kiel University

submitted by

Lalu Rudyat Telly Savalas

Kiel 2011

Referees:

1. Prof. Dr. Paul Saftig

2. Prof. Dr. Matthias Leippe

Date of oral examination : 13.05.2011

Approved for publication : 24.05.2011

Signed: Dean

Herewith I declare that:

1. Apart from the supervisor`s guidance, the contents and design of this dissertation are my own work.
2. This thesis has not been in partially or wholly as part of a doctoral degree to another examining body.
   Parts of this work have been submitted for scientific publication
3. This thesis has been prepared according to the Rules of Good Scientific Practice of the German Research Foundation.

Kiel, March 9, 2011

Lalu Rudyat Telly Savalas

Acknowledgement

I would like to thank to Prof. Dr. Paul Saftig and Dr. Bernd Schroeder who guided me throughout my PhD thesis.

I would like to express my grateful to the Saftig´s present and former members: Eeva-Liisa Eskelinen, Karine Reiss, Seenu, Beimi, Marc, Alex, Christina Wehling, Marion, Jenny, Kathi, Micha, Judith, Marlies, Inez, Fr. Z, Michelle, Johann, Janna, Sebastian, Raffi, Andrea, Nur, Jockel, Hannes, Silvio, Christian Raab, Mirka.

I would especially thank to the DAAD (Deutsher Akademischer Austaushdienst), the Directorate of Higher Education, Republic of Indoensia, the Rector of University of Mataram and the Dean of the Faculty of Teacher Training and Education, University of Mataram, Indonesia for facilitating my study in Germany.

I am heartily indebted by the encouragement from my former teachers and lecturers: pak Supardi, Dr. Dessy Natalia.

Thank you to the former and present PPI Kiel colleagues.

Thank you to *Ibunda* Baiq Nai´mah and Siti Syamsiyah serta *Ayahanda* Ahmad Ramli and Sri Bintoro Hadiwidjojo, to my brothers and sisters Rully el Faraby, Very el Viera, Yudi Islami Firdaus, *Mba* Uun, *Mba* Fivi, *Dek* Hudaya, *Dek* Ibadurrahman, *Dek* Hanif.

I would like to thank to my lovely wife Jannatin Àrdhuha and our sons Mukhlis and Hasan Abdulhaq, who fueled me up to accomplish this work.

Table of contents

List of Figures

List of Tables

Abbreviations

α	anti or alpha
µ	micro
µg	micro gram
βGC	beta-Glucocerebrosidase
µL	micro Liter
µm	micro meter, 10^{-6} meter
µM	micro molar
µg	micro gram
ADP	Adenosine diphosphate
Amp	Ampicilin
AP	Adaptor protein, Alkaline phosphatase
ARF	ADP-ribosylation factor
ATP	Adenosine triphosphate
BCA	Bicinchoninic acid
bp	base pair
BSA	Bovine serum albumin
CD63	Cluster of differentiation 63
CD68	Cluster of differentiation 68
CD-MPR	Cation dependent MPR
cDNA	complementary Deoxyribose nucleic acid
CI-MPR	Cation independent MPR
CLN7	Ceroid-lipofuscinosis 7
cm	centimeter
CTNS	Cystinosin
CtsB	Cathepsin B
CtsL	Cathepsin L
CtsD	Cathepsin D
DEPC	Diethylpyrocarbonat
DIRC2	Disrupted in renal carcinoma
DMEM	Dulbecco´s modified eagle medium
DMSO	Dimethyl sulphonyl
DMSZ	Deutsche Sammlung von Mikroorganismen und Zellkulturen/German Collection of Microorganisms and Cell Cultures
DNA	Deoxyribonucleotide acid
dNTPs	deoxynucleotide triphosphates
E. coli	*Escherichia coli*
ECL	Enhanced chemiluminescence
EDTA	Ethylene diamine tetraacetic acid
EmrD	*E. coli* multidrug resistance protein D
Endo H	Endoglycosidase H
ER	Endoplasmic reticulum

FCS	Fetal calf serum
FLVCR	Feline leukemia virus subgroup C cellular receptor
GalNAc	*N*-Acetylgalactosamine
GFP	Green fluorescence protein
GGA	Golgi-localized γ-ear containing ARF
GlcNAc	*N*-Acetylglucosamine
GLUT	Glucose transporter
HA	Hemagglutinin
HCl	Hydrochloric acid
HEPES	4-(2-hydroxyethyl)-1-piperazineethanesulfonic acid
kbp	kilo base pair
KCl	Kalium chloride
kDa	kilo Dalton
kg	kilo gram
KH_2PO_4	Kalium dihydrogen phosphate
L	Liter
LacY	Lactose permease from *E. coli*
LAMPs	Lysosomal associated membrane proteins
LB	Lysogenic Broth
LBPA	Lysobiphosphatidic acid
LC-MS/MS	Liquid chromatography-Mass spectrometry/Mass spectrometry
LIMPs	Lysosomal integral membrane proteins
m	meter, milli
M	Molar
mA	milli Ampere
MCS	Multi cloning site
mCtsB	mouse cathepsin B
mCtsL	mouse cathepsin L
MFS	Major facilitator superfamily
MFSD8	Major facilitator superfamily domain containing 8
mg	milli gram
MHC	Major histocompability complex
min	minute
mL	milli Liter
mM	milli Molar
MPR300	Mannose-6-phosphate receptor 300 kDa
MPR46	Mannose-6-phosphate receptor 46 kDa
MPS IIIC	Mucopolysaccharidosis IIIC
mRNA	messenger RNA
MS	Mass spectrometry
MVB	Multivesicular body
Na_2HPO_4	Dinatrium hydrogen phosphate
NaCl	Natrium chloride

NaOAc	Natrium acetic acid
NaOH	Natrium hydroxide
ng	nano gram
NH_4Cl	Ammonium chloride
O. formigenus	*Oxalobacter formigenus*
^oC	Celcius degree
PBS	Phosphate buffered saline
PCR	Polymerase chain reaction
PDI	Protein disulfide isomerase
Pfu	*Pyrococcus furiosus*
pH	potentia Hydrogenii
PMSF	Phenylmethylsulfonyl fluoride
PNGase F	Peptide-N4-(N-acetyl-beta-glucosaminyl) asparagine amidase
PNS	Post nuclear supernatant
RNA	ribonucleotide acid
rpm	rotation per minute
RT-PCR	Reverse transcription PCR
s	second
SARS-CoV	Severe acute respiratory syndrome coronavirus
SDS	Sodium dodecyl sulfate
SDS-PAGE	Sodium dodecyl sulfate polyacrylamide gel electrophoresis
SH3	Src homology 3
siRNA	small interfering RNA
SLC	Solute carrier (protein)
SSB	single-strand DNA binding
SV40	Simian virus 40
TAE	Tris-acetate-EDTA
Taq	*Thermus aquaticus*
TBS	Tris-buffered saline
TEMED	Tetramethylethylenediamine
TGN	*trans*-Golgi network
TIP47	Tail interacting protein of 47 kDa
TMDs	Transmembrane domains
Tris-Cl	Tris-chloride
U	Unit
V	Volt
V-ATPase	Vacuolar-type H^+-ATPase
VHS domain	domain present in Vps27p, Hrs, Stam protein

Summary

The human *Disrupted In Renal Carcinoma* 2 (DIRC2) protein consists of 478 amino acids and is a putative member of the major facilitator superfamily. Bioinformatic analysis suggested that DIRC2 has twelve transmembrane spanning domains. Both ends of DIRC2 are facing the cytosolic milieu. By immunofluorescence and subcellular fractionation analysis, it could be shown that DIRC2 localizes to lysosomes.

The sequence of DIRC2 exhibits a dileucine lysosomal targeting motif of the [DE]XXXL[LI] type and two tyrosine-based lysosomal targeting sequences of the YXXØ type at its N- and C-terminus, respectively. Mutation of these lysosomal sorting motifs followed by analysis of the mutants by immunofluorescence showed that the dileucine motif at the N-terminus is indispensable for lysosomal targeting, whereas the two tyrosine-based lysosomal targeting motifs are irrelevant to lysosomal targeting of DIRC2. Linear sequence analysis of DIRC2 also revealed two potential N-glycosylation sites. By using a N209A mutant and PNGase F digestion, it could be demonstrated that only Asn-209 in loop5 is utilized.

Immunoblot detection of either overexpressed or endogenous DIRC2 in HeLa cells showed that DIRC2 is processed into two asymmetric fragments. Proteolysis of DIRC2 takes place in lysosomes and can be prevented by ER retention or redirection of newly synthesized DIRC2 to the plasma membrane. The present study also showed that processing of DIRC2 depends on the activity of the lysosomal protease cathepsin L. However, DIRC2 is only partially processed in mouse liver deficient in cathepsin L, indicating that the role of cathepsin L in the proteolysis of DIRC2 in cathepsin L deficient mouse liver may be compensated by other still unknown proteases. The exact cleavage site of DIRC2 by cathepsin L still needs to be determined but the proteolysis is likely to take place between residue 214 and 261.

Downregulation of DIRC2 with siRNAs in HeLa cells did not detectably influence lysosomal functions, as assessed by the activity of lysosomal enzymes or the expression level of lysosomal proteins. While the function of DIRC2 is currently unknown, the need for (or the consequence of) DIRC2 proteolysis remains unclear. Since under steady state

condition the bulk of both overexpressed and endogenous DIRC2 are observed in processed form, it seems unlikely that the observed proteolysis corresponds to degradation. Hence, the possibility that the proteolytic processing modulates the function of DIRC2 cannot be excluded. Initial functional analysis of the full length form of DIRC2, expressed in *Xenopus oocytes*, indicated that DIRC2 is an electrogenic transporter protein. However the actual substrate of DIRC2-mediated transport is still unknown.

Zusammenfassung

Das humane Protein *Disrupted In Renal Carcinoma 2* (DIRC2) besteht aus 478 Aminosäuren und ist ein vermeintliches Mitglied der Major-Facilitator-Superfamilie. Bioinformatische Analysen lassen vermuten, dass DIRC2 ein zwölf Transmembrandomänen umfassendes Protein ist, dessen Enden beide im Cytosol liegen. Mit Hilfe von Immunfluoreszenzexperimenten und subzellulärer Fraktionierung konnte gezeigt werden, dass DIRC2 eine lysosomale Lokalisation besitzt.

DIRC2 weist drei lysosomale Zielsequenzen auf. Neben einem Dileucinmotiv des [DE]XXXL[LI]-Typs sind zwei tyrosinbasierte YXXØ-Sequenzen jeweils am N- und C-Terminus enthalten. Mutationen innerhalb dieser Sortierungsmotive, gefolgt von anschließender immunfluoreszenzbasierter Analyse, zeigten die Notwendigkeit des N-terminalen Dileucinmotifs, nicht aber der YXXØ-Motive für den zielgerichteten Transport von DIRC2 zu den Lysosomen. Weitere Sequenzanalysen von DIRC2 ergaben zwei potentielle N-Glykosylierungsstellen. Unter Verwendung einer DIRC2-N209A Mutante und deren Deglykosylierung mittels PNGase F konnte gezeigt werden, dass nur dieses Asn-209 glykosyliert vorliegt.

Immunoblotanalysen des überexprimierten oder endogenen DIRC2 in HeLa-Zellen zeigten, dass eine Prozessierung des Proteins in zwei asymmetrische Fragmente erfolgt. Die Proteolyse von neusynthetisiertem DIRC2 findet in den Lysosomen statt und kann durch eine ER-Retention oder einen umgeleiteten Transport zur Plasmamembran verhindert werden. Die Untersuchung zeigte außerdem, dass die DIRC2-Prozessierung von der lysosomalen Protease Cathepsin L abhängt. Eine jedoch weiterhin stattfindende partielle DIRC2-Prozessierung in Lebern Cathepsin L-defizienter Mäuse könnte auf eine Kompensation von Cathepsin L durch andere, noch nicht identifizierte Proteasen hindeuten. Die genaue Cathepsin L-Schnittstelle im DIRC2 Protein muss zwar noch aufgeklärt werden, konnte aber auf einen Bereich zwischen den Aminosäureresten 214 und 261 eingegrenzt werden.

Durch eine siRNA-induzierte Verhinderung der DIRC2-Expression in HeLa-Zellen konnte kein messbarer Effekt auf die Aktivität lysosomaler Enzyme, sowie die

Expressionsspiegel lysosomaler Proteine festgestellt werden. Die genaue Funktion von DIRC2 bleibt also weiterhin unklar und somit auch die Notwendigkeit (oder die Konsequenz) der Proteolyse von DIRC2. Jedoch scheint es unwahrscheinlich, dass die Proteolyse nur auf den Abbau von DIRC2 zurückzuführen ist, da unter *steady state*-Bedingungen der Hauptanteil, sowohl des überexprimierten, als auch des endogenen DIRC2 in prozessierter Form vorliegt. Demnach kann eine Modulierung der Funktion, durch proteolytische Prozessierung nicht ausgeschlossen werden. Kürzlich begonnene, funktionell Analysen des unprozessierten, in *Xenopus oocyten* exprimierten DIRC2, deuteten darauf hin, dass es sich bei dem Protein um ein elektrogenes Transporterprotein handeln könnte. Allerdings sind dessen mutmaßliche Substrate bis jetzt unbekannt.

1. Introduction

1.1 Lysosomes

Lysosomes are acidic membrane-bound cytoplasmic organelles that serve as a major degradative compartment in eukaryotic cells. They were first described by de Duve over 50 years ago (de Duve 1955, de Duve 1959), and were also termed "suicide bags", referring to their potential function as subcellular particles responsible for protein turnover. Until the discovery of the ubiquitin-proteasome system, lysosomes were thought to be the sole major players in intracellular protein degradation or turnover (Chiechanover 2005). The discovery of the ubiquitin-proteasome system has indeed changed the knowledge in the field of protein degradation. However, this advance did not marginalize the study of lysosomes, because it turned out that varieties of biomacromolecules, such as glycoconjugates, lipids, and nucleic acids, are also degraded within the lysosome, followed by the releasing their building blocks and transporting the catabolic products back to the cytoplasm for reuse (Cuervo and Dice 1998).

Both endogenous and exogenous macromolecules can be delivered to lysosomes through the biosynthetic, autophagic, and endocytic pathway, respectively (Figure 1.1). The degradative function of these organelles is carried out by around 50 acid hydrolases within their lumen, such as proteinases, lipases and glycosidases. The acidic nature of lysosomes is due to the activity of the vacuolar H^+-type ATP-ase which pumps protons into the lysosomal lumen and thereby maintains the pH at 4.5-5 (Mellman et al 1986). Lysosomes also serve as the destination for cytoplasmic constituents taken up via autophagy which are targeted for degradation and recycling. Lysosomes also have a role in the downregulation of cell surface receptors, inactivation of pathogenic organisms, repair of the plasma membrane after wounding, and loading of processed antigens onto MHC class II molecules (Storch and Braulke 2005).

1.2 Targeting of Lysosomal Proteins

The correct localization of both soluble lysosomal proteins and membrane proteins results from highly regulated sequential events. The best characterized lysosomal targeting

pathway for soluble lysosomal proteins is the mannose-6-phosphate receptor pathway. Additionally, there is also a mannose-6-phosphate receptor independent pathway. For lysosomal membrane proteins, certain motifs owned by these proteins have been known to be decisive for their lysosomal fate (reviewed by Braulke and Bonifacino 2009, Saftig and Klumperman 2009).

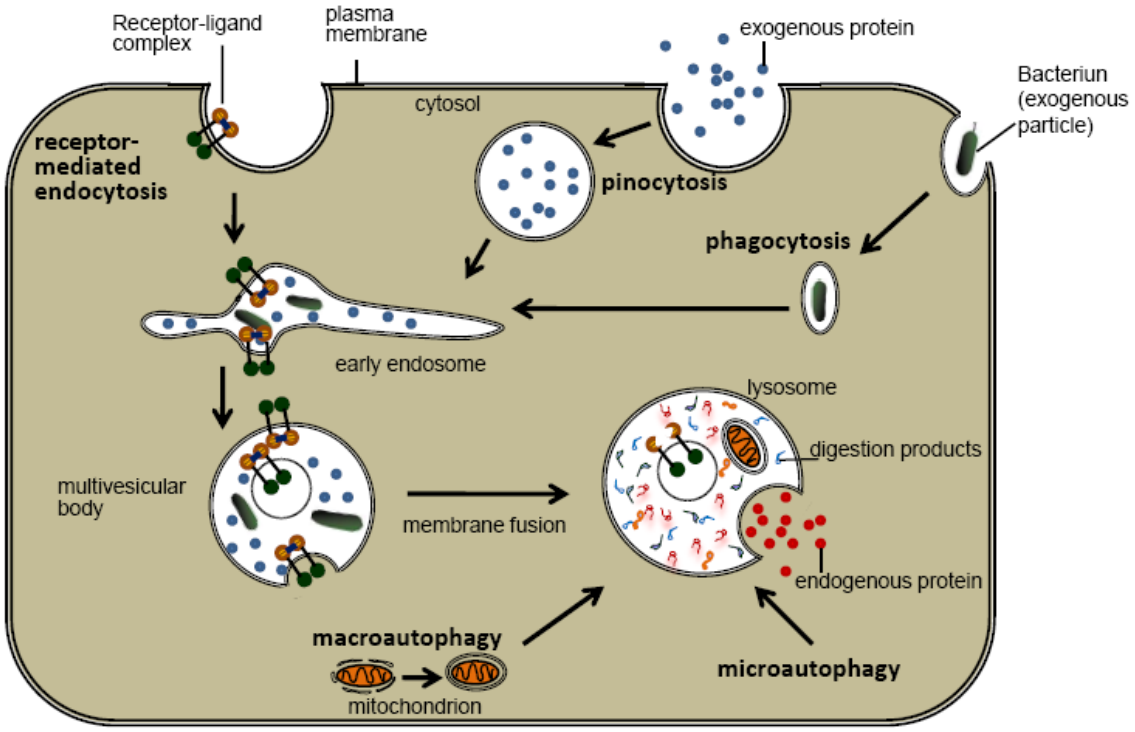

Figure 1.1. Schematic description of lysosomal system (modified from Ciechanover 2005).
Exogenous proteins are targeted to the lysosome through receptor-mediated endocytosis and pinocytosis. Exogenous particles or bacteria are targeted by phagocytosis. Endogenous proteins and cellular organelles are targeted by microaoutophagy and macroautophagy, respectively.

The majority of lysosomal hydrolases are tagged by mannose-6-phosphate during transport through the Golgi complex (Sleat et al 2005), which are later recognized by mannose-6-phosphate receptors (MPRs) in the *trans*-golgi network (TGN) (Kornfeld and Mellman 1989, von Figura and Hasilik 1986). These ubiquitiously expressed receptors could either be the cation-dependent MPR of 46 kD (MPR46 or CD-MPR) or the cation-independent MPR of 300 kD (MPR300 or CI-MPR) (Gosh et al 2003, Braulke and Bonifacino 2009). The MPR-ligand complexes form a membranic intermediate with clathrin. The later complex exits the TGN and fuses with early endosomes. In this mildly acidic compartment (pH 6), the MPR-ligand is dissociated to release the cargo, and the MPR is

transported back to the TGN for further cycles of transport (Figure 1.2). The acid hydrolases follow subsequent maturation steps of early endosomes, which involve several fusion evens, and are finally contained in mature lysosomes (Figure 1.2). A minor amount of MPRs (up to 10%), exclusively of the CI-MPR/MPR300 type, are also found at the plasma membrane and reported to be involved in the endocytosis of exogenous ligands (Braulke et al 1987, Breuer et al 1997, Braulke and Bonifacino 2009).

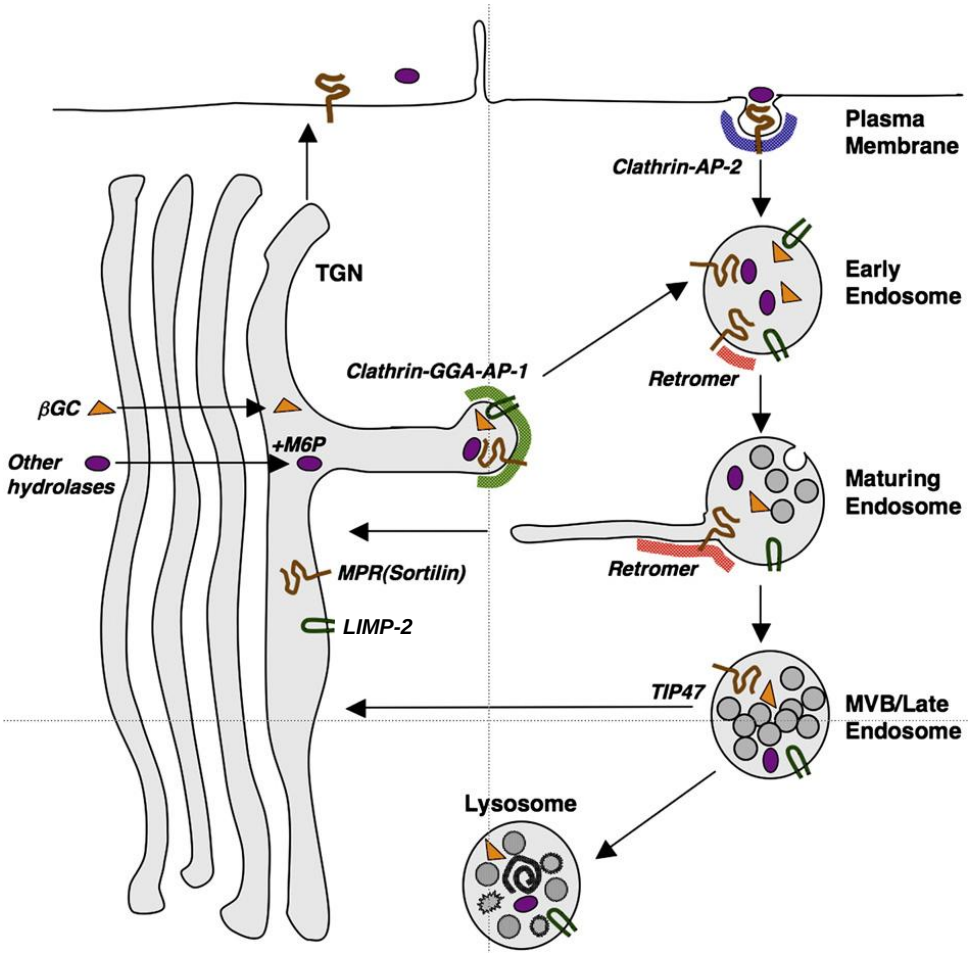

Figure 1.2 Targeting of lysosomal proteins (taken from Braulke and Bonifacino 2009).
All mannose-6-phosphate modified hydrolases bind to mannose-6-phosphate receptor or to sortilin in the TGN, whereas beta-glucocerebrosidase binds to LIMP-2. The enzyme-receptor complex concentrates in the clathrin/GGA/AP-1-coated areas of the TGN followed by transport to endosomes. In this acidic compartment, hydrolases are released from their receptors and follow subsequent maturation steps. MPR and sortilin are transported back to the TGN by a set of retrograde transport machinery, which includes retromer and TIP47, whereas LIMP-2 resides in the limiting membrane of lysosomes. MPR and other receptor may also act as a receptor for extracellular proteins. TGN, *trans*-Golgi network; βGC, beta-glucocerebrosidase; LIMP-2, lysosome integral membrane protein 2; MVB, multivesicular body; GGA, golgi-localized γ-ear containing adenosine diphosphate ribosylation factor-binding protein; AP, adaptor protein; TIP47, tail interacting protein of 47 kDa.

Study of patients with I-cells disease (mucolipidosis type II) demonstrated that they, despite the lack of mannose-6-phosphate tagged lysosomal hydrolases due to defective GlcNAc-1-phosphotransferase, do have normal lysosomal enzyme levels in many organs (Waheed et al 1982, Kornfeld and Sly 2001). Further studies on either GlcNAc-1-phosphotransferase-knockout mice (Gelfman et al 2007) or mice deficient for both type sof MPR46 and MPR300 (Dittmer et al 1999) have also revealed similar observations. This led to the unravelling of the existence of MPR-independent route(s) for the transport of lysosomal hydrolases. To date, however, very limited information is known about the MPR-independent pathway. Among these alternative receptor proteins sortilin has been described to mediate lysosomal trafficking of prosaposin and acid sphingomyelinase (Lefrancois et al 2003, Ni and Morales 2006), and more recently the lysosomal integral membrane protein type 2 (LIMP-2) has been identified as a specific receptor for lysosomal transport of β-glucocerebrosidase (βGC, Figure 1.2) (Reczek et al 2007).

In contrast to most soluble lysosomal proteins, lysosomal membrane proteins are not modified with mannose-6-phosphate and their transport from TGN to the lysosome is mostly independent of MPRs. The transport of lysosomal membrane proteins is achieved either by direct intracellular route or by indirect route through plasma membrane followed by subsequent endocytic evens (Janvier and Bonifacino 2005). The signals for lysosomal targeting of lysosomal membrane proteins are mostly contained in their cytosolic tails (Bonifacino and Traub 2003). The best characterized lysosomal targeting signals for lysosomal membrane proteins are the tyrosine motif YXXØ (Peters et al 1990, Williams and Fukuda 1990) and the dileucine motif [DE]XXXL[LI], where X represents any amino acid and Ø represents hydrophobic amino acid (Letourneur and Klausner 1992). Additionally, it has also been known that the mannose-6-phosphate receptor proteins have their own sorting signals (Gosh 2003). This signal consists of a cluster of acidic residues followed by a dileucine motif (DDSDEDLL in the MPR300 and EESEERDDHLL in the MPR46, or simply DXXLL motif) (Braulke and Bonifacino 2009). Some examples of lysosomal membrane proteins with their respective lysosomal targeting signals are listed in Table 1.1. The role of LIMP-2 as a receptor for βGC and the fact that this protein itself is a lysosomal membrane protein, which is not recycled back to the TGN after releasing of βGC, has shown that the lysosomal targeting pathways of membrane protein and soluble lysosomal protein can overlap (Saftig and Klumperman 2009).

DXXLL signals are also known as the minimal motif, since alteration of either aspartic acid or any of the two leucines to small amino acid such alanine leads to inactivation of the signals and causes mis-targeting of protein to the cells surface membrane. Most DXXLL signals are located nearly at the end of carboxy termini of cytosolic tail of lysosomal membrane proteins. DXXLL signals are recruited by the mammalian GGAs through their VHS domain (domain present in Vps27p, Hrs, Stam protein; Bonifacino and Traub 2003). GGAs belong to the family of ADP-ribosylation factor (ARF)-dependent clathrin adaptors localized to the TGN and endosomes (Figure 1.2; Bonifacino and Traub 2003). It has also noticed that the interaction between GGAs and DXXLL is highly specific, as VHS domains from other proteins, such as Hrs, STAM1, TOM1 and TOM1L1 do not bind DXXLL signals. Accordingly, the VHS domains of the GGAs recruit neither [DE]XXXL[LI] nor YXXØ signals (Bonifacino and Traub 2003).

[DE]XXXL[LI] Signals are very important in sorting of many of type I, type II and multispanning transmembrane proteins (Table 1.1). As in the case of DXXLL signals, the [DE]XXXL[LI] signals commonly have acidic cluster preceding the dileucine motif. In addition, the first leucine of this signal is not interchangeable with isoleucine without loss of activity, whereas substitution of the second leucine with isoleucine retains signal activity (Letourneur and Klausner 1992). In contrast to the DXXLL signals, the [DE]XXXL[LI] signals of late endosomal or lysosomal proteins are commonly located close to transmembrane domains (typically 6-11 residues apart). Additionally, these signals can be either at the carboxy termini (e.g. NPC1, LIMP-2) or at the amino termini (e.g. Ii) (Bonifacino and Traub 2003). These signals are recruited by adaptor proteins (APs) which later form complex with clathrin (Figure 1.2).

Also known as tyrosine-based sorting signals, the YXXØ motifs interact with the μ subunits of adaptor protein which later form complexes with clathrin. These signals also require that they are located close to transmembrane domains (6-11 residues) to be effectively recruited by the adaptor proteins.

Table 1.1 Examples of dileucine-based and tyrosine-based sorting signals (adapted from Braulke and Bonifacino 2009).

Protein	Motif Sequence
Type DXXLL	
MPR300/Cl-MPR	SFHDDS**D**ED**LL**
MPR46/CD-MPR	EESEER**D**DH**LL**
Sortilin	GYHDDS**D**ED**LL**
SorLA/SORL1	ITGFSD**D**VP**MV**
GGA1 (1)	ASVSLL**D**DE**LM**
GGA1 (2)	ASSGLD**D**LD**LL**
GGA2	VQNPSA**D**RN**LL**
GGA3	NALSWL**D**EE**LL**
Type [DE]XXXL[LI]	
LIMP-2	DEGTAD**E**RAP**LI**
NPC1	EERYKGT**E**RER**LL**
Mucolipin-1	PAGPRGS**E**TER**LL**
Sialin	DGEEST**D**RTP**LL**
GLUT8	PEDPE**E**TQP**LL**
Invariant chain (Ii)	EDQKPVMD**D**QRD**L**
Type YXXØ	
LAMP-1	G**Y**QT**I**
LAMP-2A	G**Y**EQ**F**
LAMP-2B	G**Y**QT**L**
LAMP-2C	G**Y**QS**V**
CD63	G**Y**EV**M**
CD68	A**Y**QA**L**
Endolyn	A**Y**QA**L**
DC-LAMP	G**Y**QR**I**
Cystinosin	G**Y**DQ**L**
Sugar phosphate exchanger 2	G**Y**KE**I**
Acid phosphatase	G**Y**RH**V**

1.3 Soluble Lysosomal Proteins

Degradative function of lysosomes are carried out by hydrolytic enzymes which are, according to their substrates, classified as proteases, glycosidases, lipases, nucleases, phosphatases and sulfatases (Journet et al 2002, Kollmann et al 2005, Sleat et al 2005). Lysosomal proteases include three subgroups which represent their active site amino acids: cysteine, aspartic and serine proteases (Brix 2005, Siintola 2008). Although they are contained within the lumen of lysosomes and protected by the lysosomal membrane, the proteases are usually detected within all vesicles of the endocytic pathway, i.e. early endosomes, late endosomes, autophagic vacuoles, and lysosomes. Several lysosomal proteases such as the aspartic proteinase cathepsin D or cysteine proteases cathepsin B, H and L, were reported to be ubiquitiously expressed, while others tend to be tissue-specific (Brix 2005).

Among lysosomal proteases, lysosomal cysteine proteases have long been subject of many studies. Lysosomal cysteine proteases, also known as cathepsins, are optimally active in the acidic and reducing condition found in lysosomes. Nevertheless, recent studies emphasize that cathepsins are not only active in the acidic milieu of endosomes/lysosomes. A nuclear isoform of cathepsin B has been reported to be involved in the development of thyroid malignancies (Tedelind et al 2010). Similarly, a cathepsin L isoform devoid of a signal peptide has also been reported to be localized in the mammalian cell nucleus (Goulet et al 2004). Cathepsin cysteine proteases share similar amino acid sequences and folds, and comprise a group of papain-related enzymes (Turk 2001).

Table 1.2 Human lysosomal cysteine proteases: Nomenclature and properties (taken from Turk et al 2001).

Name	**Synonyms**	**Endopeptidase**	**Exopeptidase**		**Chromosome localization**
			Carboxypeptidase	Aminopeptidase	
cathepsin L	-	+	-	-	9q21
cathepsin V	cathepsin L2 cathepsin U	+	-	-	9q21
cathepsin S	-	+	-	-	1q21
cathepsin K	cathepsin O cathepsin O2 cathepsin X	+	-	-	1q21
cathepsin W	Lymphopain	n.d.	n.d.	n.d.	11q13
cathepsin F	-	+	-	-	11q13
cathepsin O	-	n.d.	n.d.	n.d.	4q31-32
cathepsin B	cathepsin B1	+	+ dipeptidase	-	8p22-23
cathepsin X	cathepsin Z cathepsin P cathepsin Y	-	+ monopeptidase also dipeptidase	-	20q13
cathepsin H	cathepsin I	+	-	+ monopeptidase	15q24-25
cathepsin C	dipeptidyl peptidase I cathepsin J	-	-	+ dipeptidase	11q14

The majority of cathepsins are endopeptidases with exception of cathepsin C (aminopeptidase, Barret et al 1998), cathepsin X (carboxy mono- or dipeptidase, Klemencic et al 2000). Cathepsin B and H, which are endopeptidases, also show carboxypeptidase and

aminopeptidase activity, respectively (Turk et al 2001). Cathepsins are synthesized as proenzymes which require activation step(s). *In vivo* activation of procathepsins of the endopeptidase subgroup can be achieved by autoactivation in acidic environment or by glycosaminoglycans (Turk et al 2000). In contrast, the true exopeptidases, cathepsin X and cathepsin C, need to be activated by the activity of endopeptidases, such as cathepsin L and S (Nägler et al 1999, Dahl et al 2001, Turk et al 2001). Table 1.2 summarizes the nomenclature and properties of lysosomal cathepsins.

An example of a well described cathepsin cysteine protease is given by the cathepsin B. It is the first cathepsin being crystallized (Musil et al 1991, Turk 2001) and the first cathepsin being knocked out (Deussing et al 1998, Foghsgaard et al 2001, Brix 2005). However, cathepsin B knockout mice have shown no overall alteration in their phenotype (Deussing et al 1998), but a reduction in premature intrapancreatic trypsinogen activation, and increased resistance to tumor necrosis factor-alpha mediated hepatocyte apoptosis (Foghsgaard et al 2001, Guicciardi et al 2001). Its activity is inhibited by cysteine protease inhibitor such as leupeptin, cystatin B and E-64.

Cathepsin L represents one of the most potent lysosomal cysteine protease. It is 10 to 15 times more active than cathepsin B (Gordon et al 1995). It is involved in the processing of the spike (S) protein of severe acute respiratory syndrome coronavirus (SARS-CoV) (Bosch et al 2008) and in the perforin processing (Konjar et al 2010). However, as in the case of cathepsin B, cathepsin L deficient mice show only a mild phenotype, i.e. a reduction in CD^+ T cells (Nakagawa et al 1998) and recurrent hair loss (Roth et al 2000) and in the turnover of autophagolysosomes (Dennemaerker et al 2010). This suggests that lysosomal cysteine proteases are likely to be redundant (Nagler and Menard 2003, Brix 2005). On the other hand, a severe phenotype was reported in cathepsin B and L double deficient mice, which showed an early-onset brain atrophy which led to the death of animal four weeks after birth (Felbor 2002).

The above description of cathepsins, represented by cathepsin B and L, highlights the challenges in the understanding of the specific roles and natural substrates of individual lysosomal proteases.

1.4 Lysosomal Membrane Proteins

The limiting membrane of lysosomes contains a set of highly glycosylated lysosomal-associated membrane proteins (LAMPs) such as LAMP-1 and LAMP-2, and lysosomal integral membrane proteins such as LIMP-1 (CD63/LAMP-3) and LIMP-2. The limiting membrane has multiple functions including acidification of the lysosomal matrix, sequestration of the lysosomal enzymes from the rest of the cytoplasm, mediation of fusion events between lysosomes and other organelles, and transport of degradation products back to the cytosol (Eskelinen et al 2003).

Lysosomes were initially thought to be non-specifically permeable to small molecules, allowing the degraded materials within the lysosomes to be transported out of lysosomes for further use. This view was changed after the identification of protein-mediated pathway for cystine across the lysosome membrane (Gahl et al 1982, Jonas et al 1982). Further studies have also revealed the existence of transport pathways for amino acids, di- or tripeptides, sugars, inorganic ions and nutrients in purified lysosomal fractions (Pisoni and Thoene 1991, reviewed by Sagné and Gasnier 2008). Thereafter, many studies have been carried out to unravel the composition and the dynamic of lysosomal membrane.

1.4.1 Proteomic study of lysosomal membrane proteins

The study of lysosomal membrane proteins relies mostly on the availability of a highly pure lysosomal fraction. A comprehensive study of lysosomal membrane composition has been performed by Bagshaw and colleagues (Bagshaw et al 2005). This study has taken advantage of shifting the buoyant density of rat lysosomes by treating the rat with Triton WR1339, which provides a comfortable fractionation step in a sucrose gradient. In this way, the Triton WR1339-filled lysosomes (Tritosomes) retain their lysosomal enzymes activities, as well as their ability to fuse with endosomes/phagosomes. The subsequent tandem MS analysis of the fraction enriched in lysosomes has revealed over 200 proteins, with many of which were previously associated with lysosomes/endosomes (Bagshaw et al 2005). However, copurification of endoplasmic reticulum, golgi, cytosol, plasma membrane and lipid raft proteins in the lysosome enriched fraction could not be avoided.

Subsequent advance in the proteomics study of lysosomal membrane protein has been reported by Schroeder et al (Schroeder et al 2007). In this study, lysosomal membrane proteins were isolated from human placenta and statistical analysis was introduced to significantly exclude co-purified proteins. A lysosome enriched fraction was initially produced by percoll gradient centrifugation, followed by selective disruption of lysosomes of the lysosome enriched fraction by applying osmotic stress during incubation with methionine methyl ester. The co-purified mitochondria and lipofuscin were then removed in the sucrose and iodixanol gradient centrifugation, consecutively. LC-MS/MS data of the lysosomal membrane enriched fraction were compared to the data from material after the first density gradient centrifugation. By using this strategy, Schroeder et al were able to exclude the majority of known mitochondrial, ER, plasma membrane and peroxisomal membrane proteins. 58 proteins previously known to reside at least partially in lysosomes were confirmed, and additional 86 proteins were significantly enriched in the lysosomal membrane fraction, 12 of which were novel proteins with unknown function (Schroeder et al 2007, reviewed in Lübke et al 2009).

1.4.2 Lysosomal transporter proteins

The significance of the lysosome is underlined by the fact that around 50 diseases are related to lysosomal storage dysfunction. The majority of the diseases are caused by defects in soluble lysosomal proteins, whereas only few are related to defect in lysosomal membrane proteins. With the sole exception in the Mucopolysaccharidosis IIIC disorder (MPS IIIC, or Sanfilippo C syndrome, Hrebicek et al 2006), all of the known diseases related to the defect in the lysosomal membrane proteins are caused by defects in non-enzymatic membrane proteins, i.e. lysosomal transporter, channel or receptor proteins (Ruivo et al 2009). Table 1.3 lists a number of lysosomal transport proteins, which includes those related to lysosomal storage diseases.

The first characterized lysosomal storage disorder caused by failure of the transport of catabolism products across lysosomal membrane is cystinosis. In this disease, Cystinosin, a 7-transmembrane-domain transporter, is defective and result in the failure to export cystine out of lysosomes. Clinical pathology of this disease are found in the kidney, eye, liver, muscles, pancreas, brain and white blood cells and are manifested in growth retardation, diabetes

mellitus, hypothyroidism, myopathy and neurological deterioration (Kalatzis 2001, Ruivo et al 2009, Saftig and Klumperman 2009). In the Salla disease, transport of free sialic acid from lysosome is impaired, due to the mutation in Sialin, a 12 transmembrane-domains lysosomal transporter protein (Morin et al 2004, Wreden et al 2005). By the progress in the proteomics study of lysosomal membrane proteins, it is anticipated that more lysosomal transporters will be unveiled (Schroeder et al 2007, Ruivo et al 2009).

Table 1.3 Lysosomal transport activities and proteins from the lysosomal membrane with demonstrated or putative transport function (modified from Sagné and Gasnier, 2008).

Substrates transported	Transport protein (human gene)	Mechanism	Associated inherited disorder (OMIM no)	References
Protein catabolites				
Lys, Arg (system c)	?			Pisoni et al (1985, 1987b)
Glu, Asp (system d)	?			Collarini et al (1989)
Ala, Ser, Thr (system e)	?			Pisoni et al (1987a)
Pro, Ala, Ser, Thr (system f)	?			Pisoni et al (1987a)
Pro (system p)	?			Pisoni et al (1987a)
Pro, Ala, Gly	LYAAT1 (*SLC36A1*)	H^+ symport		Sagné et al (2001)
Leu, Phe, Thr (system t)	?			Stewart et al (1989)
Ile, Leu, Phe, Trp, Tyr (system h)	?			Bernar et al (1986)
Leu, Ile, Val, Met, Phe (system l)	?			Stewart et al (1986)
Cystine	Cystinosin (CTNS)	H^+ symport	Cystinosis (219800)	Town et al (1998), Kalatzis et al (2001)
Cystine, glutamate	xCT	Cystine/glutamate antiporter		Sakakura et al 2007
Cysteine*, cysteamine*	?			Pisoni et al (1990)
Di- and tripeptides	?			Thamotharan et al (1997)
His, dipeptides	PHT2 (*SLC15A3*)	H^+ symport		Sakata et al (2001)
Carbohydrate catabolites				
Neutral hexoses	GLUT8 (*SLC2A8)*?	Uniport or H^+ symport		Doere et al (2000), Ibberson et al (2000), Augustin et al (2005), Schroeder et al (2007)
GlcNAc, GalNAc	?			Jonas et al (1989)
Sialic acids, acidic hexoses	Sialin (*SLC17A5*)	H^+ symport	Salla disease (604369) ISSD (269920)	Verheijen et al (1999), Morin et al (2004)
Myo-inositol	HMIT (*SLC2A13*)			Uldry et al (2001), Schroeder et al (2007)
Inorganic ions				
H^+*	V-ATPase (ATP6Vxxx)	ATP driven	Infantile malignant osteopetrosis (ATP6VA3, 259700)	Forgac (2007)
PO^{4-}	?			Pisoni (1991)
SO^{4-}	*SLC26A11?*			Jonas and Jobe (1990), Schroeder et al (2007)
Ca^{2+}	?			Lemons and Thoene (1991)
Ag^{2+}, Cu^{2+}, Cd^{2+}	?			Havelaar et al (1998)
Monovalent cations	Mucolipin (*MCOLN1*)	Channel	Mucolipidosis type IV (252650)	Bach (2005)

Fe^{2+} and other divalent metal ions	DMT1 (SLC11A2), IRE + splicing isoform	H^+ symport		Gunshin et al (1997), Tabuchi et al (2002)
K^+, Cl^-	KCC1 (*SLC12A4*)	K^+, Cl^- symport		Schroeder et al (2007)
Zn^{2+}*	ZnT2 (*SLC30A2*)			Palmiter et al (1996), Schroeder et al (2007)
Cl^-	CLC-7 (CLCN7) + Ostm1 (*OSTM1*)	H^-, Cl^- antiporter	Infantile malignant osteopetrosis (259700)	Kornak et at (2001), Lange et al (2006), Weinert et al (2010)
Other				
Polymannose*	?			Saint-Pol et al (1997, 1999)
Nucleosides	ENT3 (*SLC29A3*)	Uniport or H^+ symport		Baldwin et al (2005)
Folylpolyglutamate	?			Barrueco and Sirotnak (1991), Barrueco et al (1992)
Vitamin B_{12}	LMBD1 (*LMBRD1*)			Rutsch et al (2009)
≥6-mer peptides*	TAP-like (*ABCB9*)	ATP-driven		Wolters et al (2005)
Unknown				
Arg, Lys?	CLN3		Juvenil neuronal ceroid-lipofuscinosis (204200)	Consortium (1995), Kim et al (2006), Ramirez-Montealegre and Pearce (2005)
?	CLN7 (*MFSD8*)		Late infantile neuronal ceroid-lipofuscinosis (610951)	Bagshaw et al (2005), Schroeder et al (2007), Siintola et al (2007)
Fatty acids?	NPC1		Niemann-Pick disease type C1 (257220)	Carstea et al (1997), but see Passeggio and Liscum (2005)
?	P40			Boonen et al (2006)
?	Spinster-like protein 1			Bagshaw et al (2005), Schroeder et al (2007)
Choline?	CTL2 (*SLC44A2*)			Schroeder et al (2007)
?	C19orf28			Schroeder et al (2007)

Asterisks (*) indicate the substrates which are imported into the lysosomes under physiological conditions. Transport proteins underlying these activities are indicated in the second column. Most known proteins are secondary active transporters indirectly driven by the lysosomal ATPase through an H^+ coupling mechanism. The table also lists primary transporters which are directly coupled to ATP hydrolysis and ion channels. Inherited diseases resulting from mutations of the corresponding genes are indicated in the fourth column.

1.4.3 Disrupted in Renal Carcinoma 2 (DIRC2)

The DIRC2 gene was initially reported in the context of renal carcinoma as this gene spans the breakpoint of a chromosomal translocation observed in a few cases of familial renal cancer (Bodmer et al 2002). *DIRC2* gene is expressed in various tissues, including kidney. *DIRC2* encodes a predicted protein of 478 amino acids residues with a high homology to the

human feline leukaemia virus subgroup C receptor, FLVCR (Bodmer et al 2002). FLVCR involves in the transport of free heme out of cytoplasm, which is other ways toxic for the cells (Keel et al 2008). DIRC2 shows also similarity to various putative transporters of major facilitator superfamily (MFS, section 1.5) transporter proteins. Transcript of the DIRC2 shows a high homology (>80%) to the transcripts from different species, including monkey, pig, dog and mouse (Bodmer et al 2002). A significant degree of homology (>30-45%) of human DIRC2 to different proteins from *Leishmania major* and *Arabidopsis thaliana* has also emphasized the conservation of this protein (Bodmer et al 2002).

DIRC2 is predicted to have 12 transmembrane spanning domains, which is the basic characteristic of MFS. Additionally, it has a conserved MFS-specific signature sequence which lays between transmembrane domain 2 and 3 (Maiden et al 1987, Law et al 2008, Bodmer et al 2002). DIRC2 is one of putative lysosomal membrane proteins identified in a recent proteomics study of lysosomes purified from human placenta (Schroeder et al 2007). Bioinformatic analysis of this DIRC2 suggests that it contains one glycosylation site and several phosphorylation sites. Additionally, DIRC2 has a proline rich region (P-x-x-P) between transmembrane domain 6 and 7, which is known to be a potential interaction site with Src homology 3 (SH3) domains from several proteins (Rickles et al 1994, Bodmer et al 2002). Apart from this genetic description of DIRC2, there is currently no further report about the biochemical and molecular aspects of DIRC2.

1.5 Major Facilitator Superfamily

Transport of biomolecules and inorganic materials across cytoplasmic and vesicular membranes is very important for the life of cells. The transport across membranes can be driven by the energy released by hydrolysis of ATP (primary transporters), or by the use of energy stored in the ion or solute gradients generated by primary transporters (so-called secondary transporters). In the group translocation system commonly found in bacteria, chemical modification of substrate results in transport of substrate onto the opposite side of membrane (Law et al 2008). The MFS proteins transport their substrate by uniport (translocation of a single species), symport (translocation of substrate and an ion in the same direction) or antiport (translocation of substrate and an ion or another substrate in opposite directions) (Kaback et al 2001).

Major facilitator superfamily (MFS) represents a group of secondary transporter proteins with thousands of members from all kingdoms of life and all living cells (Law et al 2008). In prokaryotes, around 25% of all known membrane transport proteins belong to the MFS (Saier et al 2003). This large superfamily is subgrouped into tenth of families on the base of both their functionality and phylogenic data (Saier et al 1999).With exception of only three families among 58 families known to date, all proteins belonging to MFS are characterized by twelve α-helices transmembrane domains (TMDs) connected by hydrophilic loops, and both their N- and C-termini reside in the cytoplasm (Pao et al 1998, Saier 2003).

The difficulty to purify, crystallize and resolve the structure of MFS protein has long kept the gap between structural and functional study of MFS proteins. Despite the lack of structural evidence, a growing list of human diseases has been related to the mutation of transporter proteins (Kaback et al 2001). Nevertheless, the current understanding of MFS transporter protein was boosted by the high-resolution structures of two proteins from this superfamily: the lactose permease symporter (LacY; Abramson et al 2003) and the glycerol-3-phosphate antiporter (GlpT; Huang et al 2003) from *Escherichia coli*. An intriguing fact of the two MFS proteins of different family is that they have very similar structure, although they share only 21% sequence identity. Significant sequence similarities are only identified among MFS proteins within the same family (Pao et al 1998). This leads to the hypothesis that all members of the MFS share a common structure (Vardy et al 2004).

The above hypothesis is further strengthened after the high-resolution structure of *E. coli* multidrug transporter emrD (Yin et al 2006) and the lower-resolution structure of *O. formigenes* OxlT (Hirai and Subramaniam 2004) have been resolved. Structural analysis of MFS has also revealed that the 12 transmembrane domains of MFS protein are clustered into two halves of 6 transmembrane-domains, and that the two halves are pseudo-symmetric to each other with a pore between the clusters which is essential for substrate binding (Law et al 2008). In accordance with this view, the only MFS protein consisting of 6 transmembrane domains likely functions as a homodimer, whereas the MFS family with 24 transmembrane domains is likely to be a result of gene fusion event (Pao et al 1998, Saier 2003). Additionally, the two transmembrane domain clusters are separated by a long central loop, typically more than 30 residues, which is very important for efficient insertion of MFS protein

into biological membranes. It has also noted that the central loop is unlikely to be involved in transport activity, as the two clusters can be expressed separately and demonstrate similar transport activity as the wild type (Weinglass and Kaback 2000).

1.6 Objectives

Since its first genetic description on 2002 (Bodmer et al 2002), followed by confirmation of its putative lysosomal residence by a proteomics approach (Schroeder et al 2007), there is no further study reported about the DIRC2. Hence, this study aims at the characterization of biochemical properties of the DIRC2 protein. This includes verification of its lysosomal localization, trafficking, post-translational modification, processing of the protein and downregulation of its expression.

This study takes an advantage from bioinformatic tools which help in the modelling of the topology of DIRC2, as well as in the designing of several DIRC2 mutants aimed at elaborating possible motifs, such as lysosomal targeting motif and glycosylation motif. Subcellular colocalization and trafficking of DIRC2 and DIRC2 mutants were investigated by using organelles immunostaining. In the course of this study, an intriguing fact was revealed that the DIRC2 is proteolytically processed. Efforts have been made to investigate the protease account for the DIRC2 processing. This involves the use of several protease inhibitors, from wide range protease inhibitors to specific protease inhibitors, to analyze the processing of DIRC2. Some mouse embryonic fibroblasts (MEFs) cells deficient in several proteases were also used to investigate the protease responsible for the processing of DIRC2.

The results of this study are expected to be the first biochemical characterization of DIRC2, as well as an advance for further studies of other lysosomal transporter proteins.

2 Materials and Methods

2.1 Materials

2.1.1 Equipments

Table 2.1.1 below lists the equipments used in this study

Table 2.1.1 Equipments.

Equipment	Model	Company
Autoclave	Tecnomara	Integra Bioscience, Fernwald
Agarose gel electrophoresis chamber	(Mini) Sub-Cell GT	BioRad, Hercules, USA
Analytical balance	Model 770-60	Kern and Sohn, Duerwangen
	Sartorius	Sartorius, Goettingen
Binocular	CKX41	Olympus, Tokyo, Japan
Centrifuges	Biofuge fresco	Heraeus, Hanau
	J6-HC	Beckman, California, USA
	J2-HS	Beckman, California, USA
	Centrifuge 5418	Eppendorf, Hamburg
	Multifuge 3SR+	Heraeus, Hanau
	Optima™ TLX Ultracentrifuge	Beckman, California, USA
	Optima™ LE-80K Ultracentrifuge	Beckman, California, USA
Density gradient fractionator	Auto Densi Flow	Labconco, Missouri, USA
Fluorescence microscope	Axiovert 200M	Carl Zeiss, Jena
Ice machine	AF30	Scotsman, Illinois, USA
Imager	LAS-3000 mini	Fujifilm, Carrolton, USA
Electric pipette	Accu-jet®*pro*	Brand, Wertheim
Electroporator	Gene Pulse	BioRad, Hercules, USA
Freezer -20^{o}C	Liebherr	Liebherr, Bulle, Switzerland
Freezer -80^{o}C	Hera Freeze	Heraeus, Hanau
Horizontal shaker	KL2	Edmund Buehler, Hechingen
	Swip	Edmund Buehler, Hechingen
Incubator	Certomat®H	B. Braun Biotech International, Melsungen
	Modell 200	Memmert, Schwabach
	Orbital incubator	Gallenkamp, Loughborough, UK

Liquid nitrogen tank	Consartic	Consartic, Schoellkippen
Magnetic stirrer	IKAMAG®REO	ScienceLab, Houston, USA
Microplate reader	Sunrise™	Tecan, Männedorf, Switzerland
	Synergi™ 4	BioTek, USA
	Take 3Modul	BioTek, USA
Microwave	NN-E245W	China Panasonic
pH- Electrode	Digital-pH-Meter 646	Krick, Langenselbold
Photometer	GeneQuant pro	Biochrom, Cambridge, UK
	Nanodrop ND-1000	Peqlab Biotech, Erlangen
Power supply	PowerPac 200/300/HC	BioRad, Munich
Roller shaker	RM 5	Assistent, Sondheim
Refrigerator	GKS 500	Wolfram Ungermann, Wetter
SDS-PAGE electrophoresis chamber	Mini-Protean 3	BioRad, Hercules, USA
Semi dry protein transfer	Twin Model L Trans-Blot® SD-Cell	Peqlab Biotech, Erlangen BioRad, Hercules, USA
Thermobloc	Thermomixer 5436	Eppendorf, Hamburg
Thermocycler	GeneAmp	Perkin Elmer, USA
	PCR System 2400	
	Biometra® Tpersonal	Analytik Jena
	Biometra® $T_{GRADIENT}$	Analytik Jena
Ultrasonicator	Micro Ultrasonic Cell	Kimble/Kontes
	Disrupter KT-50	Vineland, USA
UV-Documentation device	Gel Jet Imager	Intas, Goettingen
UV light	Reprostar	CAMAG, Berlin
Ultracentrifuge rotor	JA 17	Beckman, California, USA
	TLA55	Beckman, California, USA
Vortex	minivortex	Heidolph, Kelheim
Water purification	Mili-Q Plus Ultra Pure Water System	Milipore, Massachusetts, USA

2.1.2 Disposable materials

Table 2.1.1 lists the materials used in this study

Table 2.1.2 Materials.

Material	Type	Company
96-Well Microplate	Flat bottom	Sarstedt, Nuembrecht
Blot paper	Whatman	Roth, Karlsruhe
Culture dishes	Ø 3.5, 6, 10 cm	Sarstedt, Nuembrecht
Gloves	Rotiprotect-LATEX	Roth, Karlsruhe
	Rotiprotect-NITRIL	Roth, Karlsruhe
Lens paper	No. 1019	Assistant, Sondheim
Microscope cover glasses	Ø 13 mm	Assistent, Sondheim
Microscope slides	Menzel-Glaeser	Thermo Scientific, Braunschweig
Mini tubes	1.5 mL, 2.0 mL	Sarstedt, Nuembrecht
Conical tubes	15 mL, 50 mL	Sarstedt, Nuembrecht
Nitrocellulose membrane	Protran	Whatman, UK
Parafilm	Grösse M	Pechiney Plastic Packaging, Chicago, USA
Pipette tips	Different sizes	Sarstedt, Nuembrecht
Serological pipettes	5, 10, 25 mL	Sarstedt, Nuembrecht

2.1.3 Cells

2.1.3.1 Bacteria:

Escherichia coli XL1-Blue (Stratagene, La Jolla, California, USA) [endA1 gyrA96(nal^R) thi-1 recA1 relA1 lac glnV44 F'[::Tn10 $proAB^+$ $lacI^q$ Δ(lacZ)M15] hsdR17(r_K^- m_K^+)]

2.1.3.2 Mammalian cells:

Table 2.1.3 Mammalian cells used in this study.

Cell	Source/Reference
HeLa	(DSMZ, Deutsche Sammlung von Mikroorganismen und Zellkulturen/German Collection of Microorganisms and Cell Cultures, Braunschweig)
Cos7	DMSZ, Braunschweig
$PS1^{+/+}$ wild type MEF	De Strooper et al 1999

CathB$^{-/-}$ MEF	Halangk et al 2000; Reinheckel et al 2001
Cath BL$^{-/-}$ MEF	Sevenich et al 2006
Cath L$^{-/-}$ MEF	Roth et al 2000; Reinheckel et al 2001
Cath D$^{-/-}$ MEF	Saftig et al 1995

2.1.4 Chemicals

Below is list of chemicals used. Common chemicals used for buffers and solutions are given separately in the section 2.1.11.

Table 2.1.4 Chemicals used in this study.

Chemical	Company
β-D-glucopyranoside	Sigma-Aldrich, Taufkirchen
Acrylamide/bis-acrylamide solution	Roth, Karlsruhe
Agarose	Roth, Karlsruhe
Ammonium persulfate	Roth, Karlsruhe
Bacto agar	Roth, Karlsruhe
Bacto pepton	Roth, Karlsruhe
Bafilomycin A1	Sigma-Aldrich, Taufkirchen
Brefeldin A	Sigma-Aldrich, Taufkirchen
CA-074-Me cathepsin B inhibitor	Biomol, Pennsylvania, USA
Complete Protease Inhibitor	Roche, Mannheim
Dabco	Sigma-Aldrich, Taufkirchen
DMEM with L-Glutamine	PAA, Pasching, Austria
DMSO	Roth, Karlsruhe
dNTPs 2 mM	Fermentas, St. Leon-Rot
E-64 cysteine protease inhibitor	Merck, Darmstadt
Ethidium bromide 1% solution	Roth, Karlsruhe
Fetal calf albumin (FCS)	PAA, Pasching, Austria
FuGENE HD transfection reagent	Roche, Mannheim
Leupeptin	Sigma-Aldrich, Taufkirchen
Mowiol®4-88	Sigma-Aldrich, Taufkirchen
NH_4Cl	Roth, Karlsruhe
Non-fat milk powder	Roth, Karlsruhe

Pefabloc	Roth, Karlsruhe
Penicillin-Streptomycin	PAA, Pasching, Austria
Pepstatin A	Sigma-Aldrich, Taufkirchen
Percoll®	GE Healthcare, UK
PMSF	Sigma-Aldrich, Taufkirchen
TEMED	Roth, Karlsruhe
TRANSFERin siRNA trasnfection	Polyplus, Strasbourg, French
Turbofect transfection reagent	Fermentas, St. Leon-Rot
Vinblastine	Lilly, Indiana, USA
Yeast extract	Roth, Karlsruhe
Z-FY-CHO cathepsin L inhibitor II	Calbiochem, San Diego, USA

2.1.5 Plasmids

1. pEGFP-N1 (Clontech)

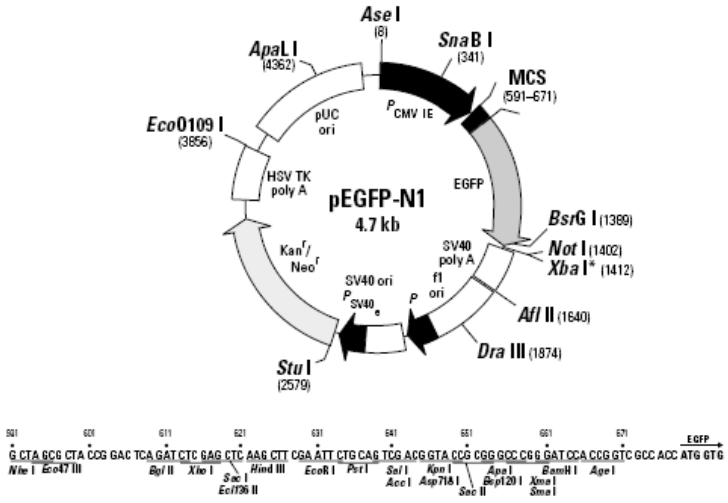

Figure 2.1 pEGFP-N1.

pEGFP-N1 vector encodes a red-shifted variant of wild-type GFP which has been optimized for brighter fluorescence (excitation maximum 488 nm and emission maximum 507 nm) and higher expression in mammalian cells. It has a classical pUC origin of replication (ori) for propagation in *E. coli*, and SV40 ori for replication in mammalian cells. The multi cloning site (MCS) of pEGFP-N1 is located between the pCMV promoter and the N-terminus of EGFP, which allows the EGFP tag to be conjugated at the C-terminus of the protein of interest. Cloning marker is provided by a neomycin-resistance cassette (Neo_r), consisting of the SV40 early promoter, and the neomycin/kanamycin resistance gene of Tn5).

2. pEGFP-C1(Clontech)

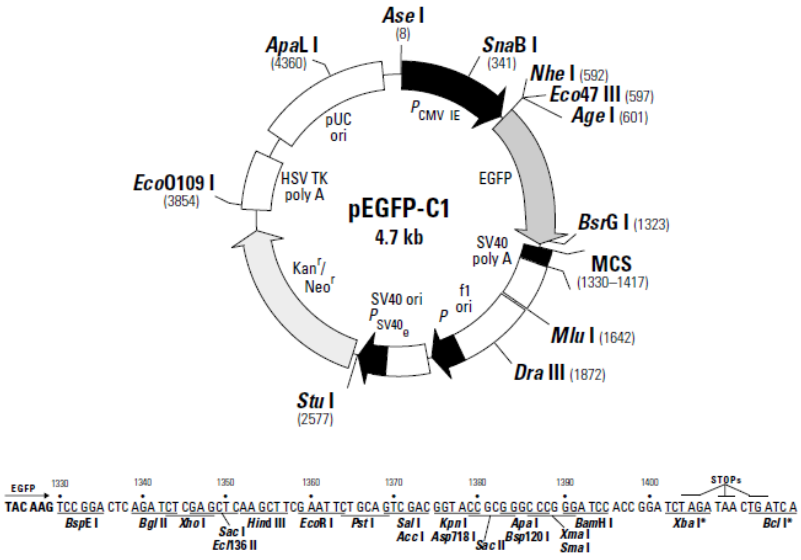

Figure 2.2 pEGFP-C1.
The vector pEGFP-C1 is similar to the pEGFP-N1, except that the genes cloned into the MCS will be expressed as a fusion protein to the C-terminus of EGFP.

3. pcDNA™3.1/Hygro(+) (Invitrogen)

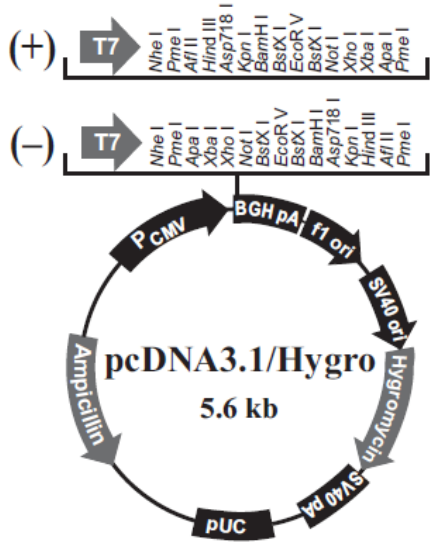

Figure 2.3 pcDNA3.1/Hygro+.
The pcDNA3.1/Hygro+ vector is a mammalian expression vector. It has a CMV promoter and a hygromycin resistance coding gene and allows high level transient and stable expression in mammalian cells

2.1.6 Primers and Oligonucleotides

Table 2.1.5 primers used to generate constructs in this study.

Name of primer	Oligonucleotide sequence 5'→ 3'	Construct nr
pEGFP.C1_DIRC2 Fw	CATGCAAGATCTATGGGCTCTCGCTGGAGCA	2
pEGFP.C1_DIRC2 Rv	TAGAATTCTTAAACGGAGACAACCACAT	2
CLN7_3xMyc_XhoI_Rev	CCGCTCGAGTTACAGATCCTCTTCTGAGATGAGTTTTT GTTCCAGATCCTCTTCTGAGATGAGTTTTTGTTCCAGA TCTTCTTCAGAAATAAGTTTTTGTTCGGATCCTTCCTG AATCCT	All, except GFP construct
CLN7_HindIII_Fw	GCTTAAGCTTGCCACCATGGCCGGCCTGCGG	All, except GFP construct
DL5A1.Ext.F	TCCCAATGGGACAGCCGCAGCTGCAGCTGCG GAGAGCAG	9
DL5A1.Ext.R	CGCAGCTGCAGCTGCGGCTGTCCCATTGGGAGCTGG	9
DL5A2.Ext.F	CTCTTCTTGCTGCAGCGGCTGCAGCTGCAGCCATTAAA GATC	10
DL5A2.Ext.R	TGCTGCTGCTGCTGCTGCTGCAGCAAGAAGAGGTGAT G	10
DL5A3.Ext.F	AGCAGGGCGCATGCAGCGGCCGCAGCTGCGGCTGTGT TA TAT	11
DL5A3.Ext.R	TGCTGCTGCTGCTGCTGCATGCGCCCTGCTGCTCTCTG C	11
mCtsB_HindIII_Fw	CTAGAAGCTTATGTGGTGGTCCTTG	12
mCtsB_XhoI_Rv	CAGTCTCGAGTTAGAATCTTCCCCAG	12
mCtsL_HindIII_Fw	CTAGAAGCTTATGAATCTTTTACTC	13
mCtsL_XhoI_Rv	CAGTGAGCTCTCAATTCACGACAGGATAGC	13

Table 2.1.6 DIRC2 siRNA (Stealth Select RNAi™, Invitrogen, CA, USA).

Nr	siRNA	Oligonucleotide sequence 5'→ 3'
1	HSS131473	GGA GGC UGU GUU GUU GGA AUA GCU A
2	HSS131474	UCU UGA AUA GCA GCG UGC CUA UAU U
3	HSS131475	GCA GAA UUU GGA GUU GUC UGC UUA A

2.1.7 Constructs

Except otherwise indicated, all constructs below are placed in the multicloning site of pcDNA3.1 mammalian expressing vector

Table 2.1.7 Constructs used in this study.

No	Construct	Constructor
1	pEGFP-N1.DIRC2	Dr. B. Schroeder, Kiel
2	pEGFP-C1.DIRC2	LRT Savalas, Kiel
3	DIRC2-3xmyc	Dr. B. Schroeder, Kiel
4	DIRC2-N_{209}A-3xmyc	Dr. B. Schroeder, Kiel
5	DIRC2-Ha_{214}-3xmyc	Dr. B. Schroeder, Kiel
6	DIRC2-Ha_{261}-3xmyc	Dr. B. Schroeder, Kiel
7	DIRC2-3xmyc-ERret	Dr. B. Schroeder, Kiel
8	DIRC2-LL/AA-3xmyc	Dr. B. Schroeder, Kiel
9	DIRC2-(Loop5 A1)-3xmyc	LRT Savalas
10	DIRC2-(Loop5 A2)-3xmyc	LRT Savalas
11	DIRC2-(Loop5 A3)-3xmyc	LRT Savalas
12	mCtsB	LRT Savalas
13	mCtsL	LRT Savalas

2.1.8 Antibodies

2.1.8.1 Primary antibody

Table 2.1.8 Primary antibodies used in Western blot or immunofluorescence.

Antibody	Source	Company/Source
α-Actin	Rabbit	Sigma-Aldrich, Taufkirchen
α-mCtsB AF965*	Goat	RD Systems, Wisconsin, USA
α-mCtsL AF1515*	Goat	RD Systems, Wisconsin, USA
α-hCtsB AF953*	Goat	RD Systems, Wisconsin, USA
α-hCathepsin D	Mouse	Prof. Dr. A. Hasilik, Marburg
α-mCathepsin D	Rabbit	University of Goettingen
α-hCtsL AF952*	Goat	RD Systems, Wisconsin, USA
α-hDIRC2 (epitope: GSRWSS EEERQPLLGPGLGPGLG)	Rabbit	Pineda, Berlin
α-h-β glucocerebrosidase	Mouse	Hans Aerts, Amsterdam
α-GFP	Mouse	Roche, Mannheim
α-HA-biotin 3F10	Rat	Roche, Mannhein

α-KDEL clon 10C3	Mouse	Stressgen, San Diego, USA
α-KDEL receptor clon KR10	Mouse	Stressgen, San Diego, USA
α-hLAMP-2	Mouse	Prof. Dr. A. Hasilik, Marburg
α-mLAMP-2 ABL93	Rat	DSHB, Univ of Iowa, USA
α-LBPA	Mouse	J. Gruenberg, Geneva
α-myc	Rabbit	Santa Cruz, California, USA
α-myc 9B11	Mouse	Cell signaling, Danvers, MA, USA
α-PDI	Rabbit	Santa Cruz, California, USA
α-Tubulin-E7-beta	Mouse	DSHB, University of Iowa, USA

*) Catalog numbering system of the RnD Systems

2.1.8.2 Secondary antibody

Table 2.1.9 Secondary antibodies used in Western blot or immunofluorescence.

Antibody	Source	Company
α-Rabbit-IgG AF350[#], AF488[#], AF594[#]	Goat	Molecular Probes, Oregon, USA
α-Mouse-IgG AF350[#], AF488[#], AF594[#]	Goat	Molecular Probes, Oregon, USA
α-Rat-IgG AF350[#], AF488[#], AF594[#]	Goat	Molecular Probes, Oregon, USA
α-Rabbit-IgG HRP	Donkey	Santa Cruz, California, USA
α-Mouse-IgG HRP	Sheep	Dianova, Hamburg
α-Rat-IgG HRP	Donkey	Santa Cruz, California, USA

[#]) AF: Alexa Fluor, refers to the synthetic fluorescent dyes developed by the Molecular Probes, Oregon, USA (currently part of Invitrogen)

2.1.9 Media

Bacterial culture:

Lysogeny Broth (LB) liquid media:

1% (w/v) tryptone

1% (w/v) NaCl

0.5% (w/v) yeast extract

Autoclaved at 121^{o}C

LB plate

1% (w/v) tryptone

1% w/v) NaCl

0.5% (w/v) yeast extract

2% (w/v) bacto agar

Autoclaved at 121^{o}C

Optional: for clone selection, appropriate antibiotic was added to the final concentration of 50 μg/mL of ampicillin or kanamycin.

Cell culture

Dulbecco's Modified Eagle Medium (DMEM) with L-Glutamine

10% (v/v) fetal calf albumin (FCS)

100 I.U. Penicillin

100 μg/mL Streptomycin

2.1.10 Kits

Table 2.1.10 Kits used in this study.

Kit	Product	Company
DNA recovery	High Pure PCR Purification Kit	Roche, Mannheim
Plasmid isolation	PureYield™ Plasmid Midiprep System	Promega, Madison, WI, USA
	Gen JET™ Plasmid Miniprep Kit	Fermentas, St. Leon-Rot
Protein determination	BCA Protein Assay Kit	Pierce, USA
Reverse transcription kit	RevertAid™	Fermentas, St. Leon-Rot
RNA isolation	NucleoSpin® RNA II	Macherey Nagel, Dueren
Western blot detection	ECL™ Advance	GE Healthcare, UK

2.1.11 Buffers

Below are the buffer used in this study. Except otherwise stated, chemicals are obtained from Merck (Darmstadt), Roche (Mannheim), Roth (Karlsruhe), Serva (Heidelberg) or Sigma Aldrich (Taufkirchen) with "p.a." grades

6 x Agarose gel electrophoresis loading buffer (Fermentas)

- 10 mM Tris-Cl, pH 7.6
- 0.03% Bromphenol blue
- 0.03% Xylene cyanol FF
- 60% Glycerol
- 60 mM EDTA

5 x Cathepsin L buffer

- 400 mM NaOAc pH 5.5
- 4 mM EDTA
- 8 mM DTT

5 x Endoglycosidase H buffer

- 0.5% SDS
- 5% NP-40
- 125 mM EDTA
- 250 mM Natrium acetat pH 5.5

Iso-osmotic buffer

- 250 mM Sucrose
- 10 mM Tris-Cl pH 7.4

Lysis buffer

- 50 mM Tris-Cl pH 7.4
- 150 mM NaCl
- 1% Triton X-100
- 0.1% SDS
- 1 x Complete protease inhibitor
- 4 mM Pefabloc
- Pepstatin A
- 4 mM EDTA

1 x PBS

137 mM NaCl

2.7 mM KCl

1.5 mM KH_2PO4

8.1 mM Na_2HPO4

pH adjusted to 7.4 with HCl or NaOH

4 x SDS-PAGE loading buffer (reductive)

4 mL of 20% SDS

2.4 mL of 1 M Tris-Cl (pH 6.8)

400 µL of 1% Bromphenol blue

1.2 mL H_2O

2 mL of 2 M DTT (freshly prepared)

SDS Resolving gel buffer

1.5 M Tris-Cl

0.4 % SDS

pH brought up to 8.8 with HCl

10 x SDS Running buffer

1.92 M Glycerol

250 mM Tris-Cl

35 mM SDS

Volume adjusted to 1000 mL with dH_2O

SDS Stacking gel buffer

0.5 M Tris-Cl

0.4 % SDS

pH brought up to 6.8 with dilute HCl

Stripping buffer

2 % SDS

62.5 mM Tris-Cl

pH brought up to 6.7 with HCl

100 mM β-Mercaptoethanol (freshly prepared)

Stripping buffer (mild stripping, Abcam)

15 g glycine

1 g SDS

10 mL Tween 20

pH adjusted to 2.2 with HCl

Volume brought up to 1 L with dH_2O

50 x TAE buffer

2 M Tris-Cl

2 M Acetic acid

100 mL 0.5 M EDTA

Adjust pH to 8.0

Volume brought up to 1000 mL with dH_2O

10 x TBS

150 mM NaCl

25 mM Tris-Cl

pH brought up to 7.4 with HCl

TBS-Tween

1 mL Tween-20

1000 mL 1 x TBS

Western-Blot blocking solution

5 % Non-fat milk powder in TBS-Tween

2.1.12 Enzymes

Table 2.1.11 List of enzymes used in this study.

Enzymes	Function	Company
BglII	Restriction (A^G A T C T)	Fermentas, St. Leon-Rot
Dream *Taq*	Polymerase	Fermentas, St. Leon-Rot
EcoRI	Restriction G^A A T T C	Fermentas, St. Leon-Rot
Endoglycosidase H	Hydrolysis of N-linked oligosaccharides	Roche, Mannheim
PNGase F	Hydrolysis of N-glycan chains	Roche, Mannheim
Hind III	Restriction (A^A G C T T)	Fermentas, St. Leon-Rot
Pfu polymerase	Polymerase	Fermentas, St. Leon-Rot
*Pfu*Ultra™	Polymerase	Agilent/Stratagene, USA
Recombinan human cathepsin L	Cysteine protease	Biozol, Massachusetts, USA
Reverse transcriptase	Synthesis of DNA from RNA	Fermentas, St. Leon-Rot
T_4DNA ligase	Ligase	Fermentas, St. Leon-Rot
XhoI	Restriction (C^T C G A G)	Fermentas, St. Leon-Rot

2.1.13 Softwares and web-based tools

Table 2.1.12 Softwares and web-based tools aided the analysis in this study.

Software	Product	Company/Resource
DNA analysis	Lasergene	DNASTAR, Madison, Wisconsin, USA
Image processing	Photoshop	Adobe, California, USA
	AxioVision Release 4.8	Carl Zeiss MicroImaging, Jena
	Image-Reader LAS-3000	Fujifilm, Carrolton, USA
Protein topology	TMHMM	http://www.cbs.dtu.dk/services/TMHMM/ (Krogh et al 2001)
	I-TASSER	http://zhanglab.ccmb.med.umich.edu/ (Zhang 2008, Roy et al 2010)
N-glycosylation site prediction	NetNGlyc 1.0 Server	http://www.cbs.dtu.dk/services/NetNGlyc/ (Gupta et al 2004)

2.2 Methods

2.2.1 Molecular biology

2.2.1.1 Basic PCR

Polymerase chain reaction (PCR) is a method to specifically amplify a certain fragment of DNA. This reaction mimics the polymerase reaction *in vivo*, in that it uses the DNA polymerase enzyme to synthesize a single strand DNA from nucleic acid precursors, complement to a single strand DNA template. It differs however, in that the DNA replication in living cells requires the activity of helicase to unwind the double helix DNA and the single-strand DNA binding (SSB) protein to stabilize single strand DNA, whereas in PCR reaction the double stranded DNAs are unwinded by applying high temperature (94^{o}C or higher), followed by a cooling process to faciliate the pairing of the targeted DNA fragment with primers (annealing step, 50^{o}C to 56^{o}C). Finally, by using DNA polymerase from the *Thermus aquaticus* (*Taq* polymerase) which is active at high temperature (72^{o}C), the amplification process is taken placed. The primers in an *in vivo* reaction are of ribonucleic acid, snythesized by the primase, whereas in PCR reaction, the pimers are short double stranded DNAs which are chemically snyhtesized.

Belows are the typical PCR mixture and the PCR program used:

Table 2.2.1 Standard PCR Reaction mixture for 50 μL volume PCR.

Component	Volume
DMSO	2.5 μL
dNTPs (2mM)	5.0 μL
10 x DNA polymerase buffer	5.0 μL
Forward primer (10 μM)	2.0 μL
Reverse primer (10 μM)	2.0 μL
Template DNA (10 ngμL)	5.0 μL
H_2O	27.5 μL
Taq DNA polymerase (2.5 U/μL)	1.0 μL

Table 2.2.2 Standard PCR program.

Temperature	Time (minute)	
94°C	5	
94°C	1	25-40 cycles
56°C	1	
72°C	Varies	
72°C	10	
10°C	~	

2.2.1.2. Fusion PCR

Substitutions of a certain sequence of a gene with other sequence were carried out by fusion PCR. It involves several steps of PCR reaction to obtain the sequence of interest (schematically described in Figure 2.4). To minimize the systemic error which may be produced in an individual PCR reaction, the *Pfu* DNA polymerase was used in fusion PCR, instead of the standard *Taq* DNA polymerase. *Pfu* DNApolymerase has been engineered from the hyperthermophilic archaeum *Pyrococcus furiosus* (Fermantas,St. Leon-Rot), and it has an advantage that it possesses 3'=>5' exonuclease (proofreading) activity, which enables the polymerase to correct nucleotide incorporation errors, with an overall fidelity 8 times as high as those performed by the standard *Taq* DNA polymerase. It has, however, a slower overall activity (around 2 minutes to synthesize 1 kb single strand DNA), so that a longer elongation time is required for each PCR cycle.

Table 2.2.3 PCR mixture for fusion PCR.

Fusion PCR mixture (PCR 1 and 2)		Elongation PCR mixture (PCR 3)	
DMSO	2.5 μL	DMSO	2.5 μL
dNTPs (2mM)	5.0 μL	dNTPs (2mM)	5.0 μL
10 x *Pfu* polymerase buffer	5.0 μL	10 x *Pfu* polymerase buffer	5.0 μL
Forward primer (10 μM)	2.0 μL	Forward primer (10 μM)	2.0 μL
Reverse primer (10 μM)	2.0 μL	Reverse primer (10 μM)	2.0 μL
Template DNA (10 ng/μL)	5.0 μL	Template DNA (10 ngμL)	0.0 μL
H_2O	27.5 μL	H_2O	32.5 μL
Pfu polymerase (2.5 U/μL)	1.0 μL	*Pfu* polymerase (2.5 U/μL)	1.0 μL

Table 2.2.4 PCR program for fusion PCR.

Temperature	Time (minute)	
94°C	5	
94°C	1	35-40 cycles
56°C	1	
72°C	3-5	
72°C	10	
10°C	~	

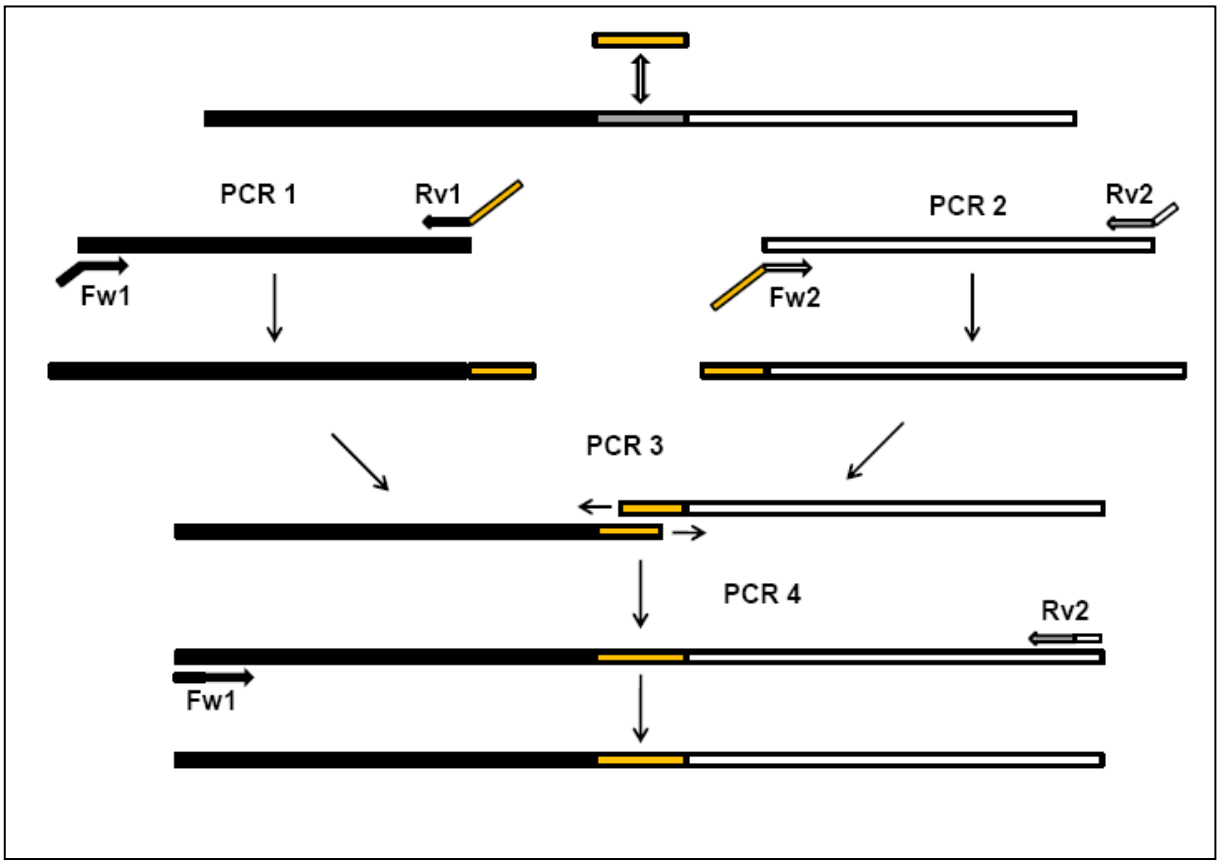

Figure 2.4 Fusion PCR strategy.

The sequence depicted in grey will be replaced by the yellow sequence. Two primer pairs (Fw1 and Rv1; Fw2 and Rv2) are used in the PCR 1 and PCR 2 to amplify the left and the right region of the targeted gene, respectively. Rv1 and Fw2 contain an overlap region (20 to 25 base pairs) which is required as a "self template" for the fusion PCR (PCR 3). The resulted fusion product was reamplified by using Fw1 and Rv2 primer pair (PCR 4) to ensure that the both ends contain the intended restriction sites which are important in the cloning step of the chimeric gene with an expression vector.

2.2.1.3 Reverse transcription-PCR

The analysis of gene expression at mRNA level was carried out by reverse transcription PCR. This reaction used mRNA as a template to synthesize its respective double strand DNA. mRNA expression analysis is important, for example, to observe to which extend the expression of a gene is downregulated by siRNA. RNA from mammalian cell was isolated according to the protocol on 2.2.1.9 and its concentration was determined by Nanodrop ND-1000 (Peqlab, Erlangen). The reverse transcription reaction was carried out according to the RevertAid™ manufacterer´s instruction (Fermentas, St. Leon-Rot) and summarized in the table below.

Table 2.2.5 Reverse transcriptase reaction.

Component	Quantity	Treatment
RNA	x μL (= 2.5 μg)	
DEPC treated H_2O	(11-x) μL	
Oligo dT	1 μL	Mixed and briefly centrifuged
		Incubated at 70°C for 5 minutes
		Placed on ice and briefly centrifuged
5X Reaction buffer	4 μL	
RNAse inhibitor	1 μL	
dNTP	2 μL	Mixed and centrifuged
		37°C for 5 minutes
Reverse transcriptase	1 μL	Reaction at 42°C for 60 minutes
	(Total volume 20 μL)	Reaction stopped by heating at 70°C for 10 minutes
		Sample kept on ice

To analyze the result of the reverse transcription reaction, 2 μL of reaction mixture was used as the template in a standard PCR reaction (2.2.1.1) and the PCR result was visualized on an agarose gel (2.2.1.5).

2.2.1.4 DNA Isolation

Isolation of DNA from living cells was undertaken either by the mini or midi DNA preparation procedures. They differ from each other in their scale and objective of the

preparation. Additionally, in a gel elution procedure, DNA is recovered after electrophoretic separation in an agarose gel (Gel elution 2.2.1.5).

Mini DNA preparation (Gene JET™ Plasmid Miniprep Kit, Fermentas, St. Leon-Rot)

Mini DNA preparation is used for the screening of *E. coli* colonies bearing plasmid DNA of interest. Following the transformation of *E. coli*, bacterial colonies spread out on an agar plate containing an antibiotic marker. Only *E. coli* colonies bearing recombinant plasmid DNA are expected to grow on a selective media. However, in false positive cases, linear vector are recircularized and regain their ability to grow on a selective media despite the lack of gene of interest. Several colonies of *E. coli* were picked up with sterile tooth picks and transferred into 3 to 5 mL LB medium containing an appropriate antibiotic. Bacteria were grown overnight (14 to 18 hours) at 37^{o}C. On the second day, cells from individual colonies were harvested by centrifugation.

A typical volume or 1.0 to 1.5 mL of culture was pelleted in a microcentrifuge (~7.000 x g for 5 minute at room temperature). The rest of medium was decanted, and cell pellet was resuspended by 250 μL resuspension solution containing RNAse. Cells were lysed by 250 μL of lysis solution containing SDS/alkaline and suspension was mixed by inverting microcentrifuge tube for 4-6 times. Plasmid DNA was neutralized by the addition of 350 μL neutralization solution (mixed by inverting the microcentrifuge tube for 4-6 times). Cell debris and chromosomal DNA are pelleted in the next centrifugation step (12.000 x g, 5 minutes) and lysate containing plasmid DNA is transferred into the spin column. Plasmid DNA will bind to the silica membrane in a spin column in the next centrifugation step. Plasmid DNA was washed twice with 500 μL of wash solution containing ethanol followed by an empty centrifugation to ensure the removal of washing solution. Plasmid DNA was finally eluted by 50 μL ultrapure H_2O.

An enzymatic restriction was usually performed to check whether the gene of interest is present in the plasmid DNA (Restriction assay 2.2.1.10). Plasmid DNA which was positive in the restriction assay was then sequenced to proof the correct sequence and framing of the gene of interest (2.2.1.8).

Midi DNA preparation (PureYield™ Plasmid Midiprep System, Promega, Madison, WI, USA)

Expression study of a certain construct requires a substantially amount of plasmid DNA. This has been mostly achieved by the midi preparation of plasmid DNA. Individual clone of *E. coli* with sequence-proofed plasmid DNA was cultured in 50 to 100 mL LB media supplemented with an appropriate antibiotic. Culture was cultivated in 50 mL conical tubes and centrifuged at 3.500 x g for 15 minutes (room temperature). Cell pellet was resuspended with 3 mL resuspension solution and lysed with 3 mL lysis solution. The mixture was homogenized by inverting the tube 3-5 times. To this mixture, 6 mL neutralization solution was added and the mixture was centrifuged at 15.000 x g for 15 minutes at room temperature. The resulted lysate was filtered through a filtering column (blue column) and the plasmid DNA in the overflow was trap in a binding column. The plasmid DNA was washed first with 5 mL detoxification solution and followed by 20 mL ethanol-containing washing solution. The DNA was left air-dried prior to elution with 600 µL ultra pure H_2O. The concentration of the isolated plasmid DNA was determined by Take 3 Modul of BioTek Multiplate Reader.

2.2.1.5 Agarose gel electrophoresis

Following the PCR reaction or enzymatic cleavage, DNA needs to be purified from the unwanted products or contaminants. This is achieved by first performing electrophoresis in an agarose gel, which separated the DNA according to the molecular weight, followed by the elution of DNA fragment from the agarose gel (see 2.2.1.6 below).

Agarose gel electrophoresis is a simple way to separate DNA samples from their contaminants or undesired products. In this method samples DNA are separated according to their molecular weight. The supporting matrix through which the DNA samples were separated is made of a network of polysaccharide derived from seaweed powder (agarose). The typical concentration of agarose used to make the agarose gel lies between 1% to 2% (w/v) agarose in TAE buffer. Agarose powder was boiled in TAE buffer and cooled down to around 50^{o}C. At this point, chelating dye ethidium bromide was added, which later aided the visualization of the DNA. The mixture was poured into a casting tray with a comb to provide sample pockets and let hardened. DNA samples were diluted with water and 6x loading dye and loaded into sample pockets. Separation of samples was achieved by applying 5V current per electrodes distance (cm).

2.2.1.6 Gel elution (High Pure PCR Purification Kit, Roche, Mannheim)

DNA fragments resulted from PCR reaction or restriction enzyme digestions were eluted from agarose gel by High Pure Purification Kit (Roche, Mannheim). DNA band of interest was cut from the agarose gel and placed in a 1.5 mL microtube. 150 μL isopropanol and 350 μL of binding solution were added to the DNA fragment. The Mixture was incubated in Thermo bloc at 62^{o}C until the gel was dissolved. The lysate was then transferred into spin column and centrifuged at 12.000 x g for 1 minute. DNA will bind to the silica matrix at the bottom of spin column. DNA was washed twice with 500 μL and 200 μL washing solution, sequentially, and finally eluted with 50 μL ultrapure H_2O. The purified PCR fragment can further be digested with restriction enzyme, or used in the fusion PCR, whereas the purified DNA from restriction reaction can be used in the ligation reaction (2.2.1.11).

2.2.1.7 Determination of nucleic acid concentration

The DNA concentrations of each plasmid DNA preparation were determined spectrophotometrically by GeneQuant Pro spectrophotometer (Biochrom, Cambridge, UK) or by the Take 3 Modul of BioTek Multiplate Reader (BioTek, USA). The RNA concentration was determined by the Nanodrop ND-1000 (Peqlab, Erlangen). The devices basically measured the absorption of the nucleic acids at 260 nm. Close to that wavelength, contaminant proteins also show a peak at 280 nm, so that the ratio of A_{260} to A_{280} nm indicated the purity of nucleic acid samples. For most application, the ratio $A_{260/280}$ of 1.80 or higher met the requirement for further use of samples (plasmid DNA for cell line transfection 2.2.3.3 or reverse transcriptase reaction 2.2.1.3).

2.2.1.8 DNA sequencing

The critical step in the molecular cloning is confirmation of the sequence of the gene of interest. Following the *E. coli* transformation by the ligation mixture and screening of *E. coli* colonies bearing the intended plasmid DNA and restriction digestion assay of the isolated plasmid DNA, the sequence of DNA needs to be determined. The DNA sequencing throughout this study was done by MWG Biotech (Martinsried) or GATC Biotech (Konstanz).

2.2.1.9 RNA isolation

The total RNA isolation protocol referred to the NucleoSpin RNA® II User Manual (Macherey Nagel, Dueren) optimized for mammalian cell culture. The basic principle of RNA purification using this kit resembles the isolation of DNA by the majority of commercial DNA isolation kits, except that a measure needs to be taken to prevent the degradation of RNA, and that there is an additional on-column DNA digestion by DNAse to allow only RNA is left in a spin column prior to elution step.

The RNA isolation steps are described as follow: Cell pellet was lysed by chaotropic ions within the lysis buffer and filtered by the NucloeSpin® Filter column. The lysate was homogenized with 70% Ethanol and transferred into the NucleoSpin® RNA II Column. Upon centrifugation, nucleic acids (RNA dan DNA) were bound to the silica matrix in the column. The high salt concentration which facilitates the nucleic acid binding in previous step was reduced by the membrane desalting buffer. On-membrane digestion of DNA was achieved by adding RNase-free rDNase for 15 minutes. The salt removal is important for the activity of the rDNase. Three washing steps were the carried out, and the RNA was finally eluted with RNase free H_2O. RNA samples were stored in -80^oC prior to further use.

2.2.1.10 DNA digestion by restriction enzyme

Restriction enzymes have the ability to cut a specific sequence of DNA. They are frequently used in molecular cloning to produce overhang at both 5' and 3' end of DNA fragment, which can later be fused with a linearized plasmid cut by the same restriction enzyme. The fusion of a DNA fragment with a vector is termed ligation reaction (2.2.1.11).

In a typical cloning procedure, a certain sequence of DNA or a gene was amplified in a PCR reaction (2.2.1.1) by using a pair of primers with known restriction recognition sites. These recognition sites were included in the primers. The primers in this study were ordered from Sigma-Aldrich Genosys (Steinheim). The choice of the restriction enzyme recognition sites in the design of PCR primers took into account the recognition sites available in the multi cloning sites (MCS) of the plasmid vector, i.e. that the overhang ends of both DNA fragment and vector were compatible to each other, to ensure that the DNA fragment can be ligated to the vector. The restriction reactions were carried out overnight at 37^oC.

Table 2.2.6 Digestion of DNA by restriction enzymes.

Digestion of PCR fragment		Digestion of plasmid DNA (vector)	
Component	Quantity	Component	Quantity
PCR fragment*	44 μL	Plasmid DNA	1 μg
10 x buffer[#]	5 μL	10 x buffer[#]	5 μL
RE 1	1 μL (10 U)	RE 1	1 μL (10 U)
RE 2	1 μL (10 U)	RE 2	1 μL (10 U)
H_2O	→ 50 μL	H_2O	→ 50μL

*) eluted from agarose gel (2.2.1.6)

[#]) referred to the Fermentas buffers system (Fermentas, St. Leon-Rot). The buffer should be compatible to both restriction enzymes (RE) 1 and RE 2.

2.2.1.11 Ligation

The fusion of a DNA fragment with a linearized vector plasmid was carried out by the aid of T4-DNA ligase (Fermentas, ST. Leon-Rot). The prerequisite for a successful ligation reaction is that both DNA fragment and the linearized vector have to be compatible to each other, which is achieved by restriction reaction of both parts. The table below shows a typical ligation reaction of DNA fragment (PCR product, digested with restriction enzymes, and eluted from an agarose gel) with a vector plasmid (originally from 1 μg plasmid DNA, linearized with the same restriction enzymes and eluted from an agarose gel).

Table 2.2.7 Ligation reaction mixture.

Component	Ligation	Control
DNA fragment	6 μL	-
Vector	2 μL	2 μL
10 x Ligation buffer	1 μL	1 μL
T4 DNA Ligase	1 μL	1 μL
H_2O	-	6 μL

Ligation reactions were undertaken by incubating the ligation mixture in a water bath of 17^{o}C overnight. Reactions were terminated by incubation at 62^{o}C for 10 minutes and the ligation reaction mixtures were used in *E. coli* transformation (Section 2.2.3.2) followed by the screening of bacterial colonies.

2.2.1.12 Dephosphorylation

In a ligation reaction, the linearized plasmid vector can recircularize and result in false positive identification in the screening of positive clones. This may be reduced or prevented by the use of alkaline phosphatase enzyme which cleaves the phosphate group either at the 5' or at the 3' end of DNA, prior to the ligation reaction. In this study, FastAP™ Thermosensitive Alkaline Phosphatase (Fermentas, St. Leon-Rot) was used. It has an advantage that it is compatible to all of Fermentas buffer system of the restriction enzymes which were used to produce overhang for ligation reaction. Hence, an electrophoresis and gel elution step is not necessary to perform. 1 μg plasmid DNA was initially digested with appropriate restriction enzymes and recovered from an agarose gel. The linearized plasmid DNA was digested with 1 U FastAP™ Alkaline Phosphatase in a thermobloc of 37^{o}C for 5 minutes. The alkaline phosphatase was then inactivated by incubation at 75^{o}C for 10 minutes, and the reaction mixture was finally ready to use in a ligation reaction.

2.2.2 Biochemistry

2.2.2.1 Total lysate preparation

Proteins from transfected cells were isolated to analyze the expression of different DIRC2 constructs or effect of the use of siRNA. In a standard preparation, cells were harvested 32 hours to 48 hours post-transfection. In another application, cells were harvested earlier, for example in the investigation of effect of proteolysis inhibitors administration.

To isolate the proteins, cells on a 10 cm Ø culture dishes were washed twice with ice cold PBS buffers, and then scrapped with 1 mL PBS containing 1 x complete protease inhibitor and 4 mM EDTA (accordingly, cells in a 3.5 Ø cm dishes were scrapped with 0.5 mL such buffer). Cells were centrifuged at 1000 x g for 5 minutes at 4^{o}C. At this stage, cells can be stored for further analysis or directly resuspended in the lysis buffer (2.1.11). Prior to disruption, the cells suspension was placed on ice for 1 hour. Disruption of the cells was

achieved by ultrasonication (2 x 10 seconds by a micro-ultrasonic cell disruptor Kimble/Kontes, Vineland, NJ). Lysate containing protein was separated from the cell debris by centrifugation at 13.000 x g for 10 minutes.

2.2.2.2 Membrane protein preparation

The membranic fraction of transfected cells was prepared as follows: cells were seeded in 4 dishes (10 cm), transfected by plasmid DNA (2.2.6.1) and harvested two days after transfection. Cells were washed two times with ice cold PBS, then scrapped in 1 mL iso-osmotic buffer for each dish. Cells were centrifuged at 1.000 x g for 5 minutes (4^{o}C). Cell pellet from individual tubes were pooled and resuspended in 1 mL iso-osmotic buffer. Cells were disrupted by pipetting through a 27G cannula (30x up and down) and the lysate was centrifuged at 1.500 x g for 10 minutes (4^{o}C). The membranic fraction was gained by centrifugation of the resulted post nuclear supernatant (PNS) at 100.000 x g for 30 minutes.

2.2.2.3 Protein determination

Protein determination of the lysate was carried out according to the manual of the BCA Protein Assay Kit (Pierce, USA). The basic of this protein determination lies on the reduction of Cu^{2+} to Cu^{1+} in an alkaline environment by protein (known as biuret reaction). In the second reaction step, two molecules of bicinchoninic acid (BCA) within the assay kit react one Cu^{1+} ion which produces an intense purple color complex. Bovine serum albumin (BSA) proteins of different concentration were used as the standard in this protein determination. The color intensities of both sample and standards were determined by measuring their absorbance at 562 nm, after incubation of the reaction mixture at 37^{o}C for 15 to 30 minutes. The sample protein concentration was calculated from the linear regression path produced by a set of standard BSA proteins.

2.2.2.4 Percoll® fractionation

To analyze the cellular distribution of a certain protein, subcellular fractionation has been carried out. This was done by the Percoll® fractionation which separated cellular components according to their density. Percoll® consists of silica particles (15-30 nm in diameter) coated with non-dialyzable polyvinylpyrrolidone (PVP). Percoll® is non-toxic, almost chemically inert and does not adhere to membranes. Upon centrifugation, it produces a

self-formed gradient from 1.0 to 1.3 g/mL, which makes it is highly versatile for many applications in the separation of biological samples. It has been long time used in the fractionation of many biological materials, such as sperma from semen, blood components, bacteria, viruses and subcellular components.

In this study, subcellular distribution of the DIRC2 has been analyzed. HeLa cells were transfected with pcDNA3.1 DIRC2-3xmyc (4 x 10 cm dishes, each transfected with 2.5 μg plasmid DNA). Cells were harvested 32 hours after transfection. Cells were washed two times with ice cold PBS buffer, then with homogenization buffer (250 mM sucrose, 10 mM HEPES pH 7.4, 1 mM EDTA, Complete protease inhibitor). Cells were scrapped from the dish in homogenization buffer. After centrifugation, cells were pooled in one microtube and resuspended in homogenization buffer. The lysis of cells was done by 10-12 up and down pipetting by a 27G cannula. PNS was separated from cells debris and nuclear by centrifugation at 1.000 x g for 5 minutes. PNS lysate was layered on the top of ultracentrifuge tube previously filled with 0.5 mL 2.5 M sucrose and 5.8 mL 17% Percoll® (w/v). Gradient centrifuge was performed at 40.000 x g, 47 minutes (70.i.Ti rotor). Fractionation was carried out by pumping the sample using a density gradient fractionator (Labcono, USA). Sample was pumped out from the lightest fraction and aliqouted in a volume of 0.5 mL.

Percoll® fractions of DIRC2 transfected HeLa cells were subjected to SDS-PAGE and Western blot. DIRC2 was detected by an anti-myc antibody, and the Western blot results of percoll fractions were aligned with several organelle markers, such as cathepsin D and βGC for the lysosomes, and PDI for the endoplasmic reticulum. The Western blot of Percoll® fraction was also aligned with the enzymatic activity assays of each fraction (Section 2.2.13).

2.2.2.5 SDS-PAGE

Sodium dodecyl sulfate polyacrylamide gel electrophoresis (SDS-PAGE) is an analytical method to separate protein samples in a polyacrylamide matrix. It offers an advantage that the protein samples can be separated according to their molecular weight. It, hence, enables an estimation of molecular weight of a certain protein, as well as the expression level of a protein of interest. This is especially true if further analysis by Western blot is performed (2.2.3.6), since overexpression of a protein in mammalian cell culture is not readily observable in a polyacrylamide gel. The use of SDS from the sample buffer (Laemmli buffer) in this method facilitates the formation of artificial molecular charges of proteins. As

almost all proteins are covered by SDS molecules, a total negative charge of protein is produced, and they move toward the anode during the progress of electrophoresis.

In a standard sample treatment with Laemmli buffer, protein samples and Laemmli buffer are boiled for 5 to 10 minutes. However, in order to maintain the stability of the DIRC2 protein structure, in most application the DIRC2 protein were incubated with Laemmli buffer at 37^{o}C for 10 minutes. Electrophoresis was undertaken at 100 V to 140 Volt in a Mini Protean 3 electrophoresis chamber (BioRad, Hercules, USA) or Twin Model L (Peqlab Biotechnology, Erlangen). Throughout this study, 10% resolving gels and 4.5% stacking gels were used and prepared according to the chart below.

Table 2.2.8 Recipe for polyacrylamide gel.

Component	10% Resolving gel	4.5% Stacking gel
Resolving buffer	2.6 mL	-
Stacking buffer	-	1.35 mL
30% acrylamide solution	3.3	1.75 mL
H_2O	4.0	6.85 mL
TEMED	30 µL	30 µL
10% Ammonium persulfate	60 µL	60 µL
Total Volume	~10 mL	~10 mL

2.2.2.6 Western blot

The immobilization of protein on a membrane before detection using antibody refers to protein blotting. The most popular application of this method is the Western blot. Practically, it is an analytical method which involves the separation of protein samples in a polyacrylamide gel (protein electrophoresis) followed by the transfer of protein from polyacrylamide gel onto a membrane surface. The membrane can either be a polyvinylidene fluoride or nitrocellulose membrane.

In this study, proteins were separated by SDS-PAGE (2.2.3.5) and they were transferred onto a nitrocellulose membrane in a semi-dry transfer set up. The transfer process is schematically depicted in the Figure 2.5. Following the transfer, the nitrocellulose can be considered as the replica of the gel. Membrane was blocked overnight by 5% non-fat milk (in

TBS Tween buffer) in cold room. To detect the protein band of interest, incubation with the primary antibody specifically recognizes the protein or tag of protein of interest was undertaken. The primary antibody was diluted in 5% non-fat milk (in PBS Tween buffer) according to the manufacturer´s instruction (for commercial antibody). Alternatively, optimation of the dilution factor for the primary antibody was undertaken.

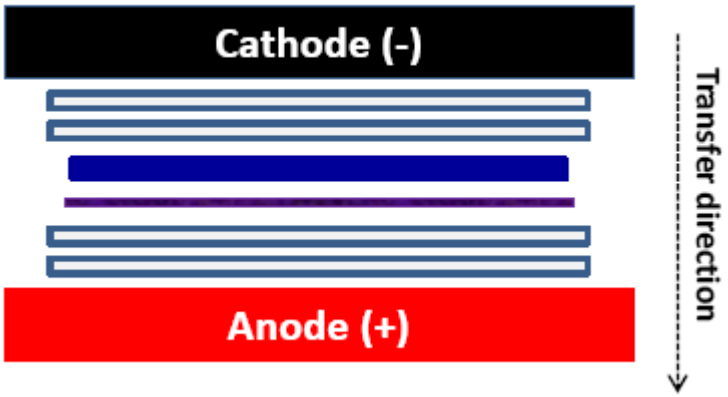

Figure 2.5 Semi-dry transfer of protein.

Proteins to be transferred were subjected into SDS-PAGE separation. Transfer onto membrane was done by semi-dry transblot (BioRad, Hercules, USA). 4 filter papers and nitrocellulose membrane were pre wet with semi-dry transfer buffer. Two filter papers were placed directly on the anode plate, followed by the nitrocellulose membrane and polyacrylamide gel. Two filter papers covered the gel, and cathode was connected on the top. Transfer of protein was achieved by applying electric current of 1 mA/cm^2 membrane surface for 2 hours.

After 3 x 10 minutes washing steps, the membrane was incubated with a second ary antibody which specifically recognizes the primary antibody. Finally, the membrane was washed 3 x 10 minutes with PBS Tween buffer, and luminogen reaction was carried out with ECL Advance solution (GE Healthcare, UK), and the bands on the membrane was photographed in LAS-3000 Imager.

For further analysis with an alternative primary antibody, the membrane can be stripped to get rid of the previous primary antibody and the secondary antibody attached to it. The stripping process can either be undertaken by a harsh stripping or mild stripping solution (2.1.11). A harsh stripping solution was used if it is known that sufficient proteins are blotted on the membrane. The membrane was incubated in the harsh stripping buffer at 55^{o}C with occasional shaking. The membrane was then washed with PBS Tween buffer. An alternative

stripping procedure provided by the mild stripping process. In this case, the membrane was incubated with mild stripping buffer for 5 to 10 minutes at room temperature, washed two times with PBS (10 minutes each) and two times with PBS Tween buffer (5 minutes each). After the stripping process, the blocking step was carried out again, followed by the primary and the secondary antibody incubations, and detection the protein of interest by luminogen reagents.

2.2.2.7 Enzyme assays

This section compiles the enzymatic reaction performed in this study. Enzymatic reactions related to molecular cloning (PCR, restriction, dephosphorylation and ligation) are described in 2.2.1.

PNGase F digestion

Sample protein was incubated with denaturing buffer (containing β-mercaptoethanol) at 56^{o}C for 5 minutes. Triton buffer was added as well as 1 x Complete protease inhibitor (Roche, Mannheim) and H_2O to the sample to the total volume of 70 μL. The sample was divided into two parts, the undigested control and the test. 2 μL of PNGase F or steril H_2O were loaded to the test and undigested control tubes, respectively, and both were incubated at 37^{o}C for at least 4 hours or overnight. Laemmli buffer was added to both sample and control tubes, and the sample was further analysis by SDS-PAGE and Western blot.

Endoglycosidase H

Sample protein of 20 to 100 μg was mixed with 5 x Endoglycosidase H buffer and 25 x Complete protease inhibitor (Roche, Mannheim). To that mixture, β-mercaptoethanol was added to final concentration of 50 mM. Sample was digested with 2 μL recombinant *Streptomyces plicatus* Endoglycosidase H (5mU/μL, Roche, Mannheim) and H_2O was added to undigested control. Incubation was completed overnight at 37^{o}C.

Lysosomal enzyme: β-hexosaminidase activity

Lysosomal enzyme activities were determined for the DIRC2 siRNA downregulated HeLa cell extracts or percoll fractions. 10 μL of cell extract or percoll fractions was added to

100 μL substrate solution (10 mM p-Nitrophenyl-2-acetoamido-2-deoxy-β-D-glucopyranoside in citrate buffer). Reaction was carried out by incubation at 37°C for 15 minute. The reaction was stopped by the addition of 261 μL stop solution (0.4 M Glycin/NaOH, pH 10.4) and the extinction of the solution was measured at 405 nm.

The activity of β-hexosaminidase was formulated by the following equation:

$$\text{Activity (mU/mL)} = \frac{\text{dE x Total volume (μL) x 1000}}{\text{Extinction coefficient x Sample volume x Incubation time}}$$

The specific activity of sample was determined by dividing the activity with the protein content of the respective sample.

Lysosomal enzyme: β-galactosidase

The β-galactosidase activity of cell extract was determined as follows: 10 μL of cell extract was added to 100 μL of β-galactosidase substrate solution (o-nitrophenyl-β-D-galactopyranoside in citrate buffer). The reaction was stopped after 30 minutes incubation at 37°C by the addition of 250 μL stop solution. The extinction of solution was determined at 405 nm, and the activity of β-galactosidase was calculated similarly to the calculation of β-hexosaminidase activity.

Lysosomal enzyme: α-mannosidase

The α-mannosidase activities of cell extract was determinted as follows: 20 μL of cell extract was added to 100 μL α-mannosidase substrate solution (10 mM p-Nitrophenyl-β-D-mannopyranoside in citrate buffer). The reaction was stopped after 120 minutes incubation at 37°C by the addition of 261 μL of stop solution. The extinction of solution was determined at 405 nm, and the α-mannosidase activity of each sample were calculated similarly to the calculation of the β-hexosaminidase activity.

2.2.2.8 Immunofluorescence

Subcellular analysis by visualization of target molecule to locate the occurrence or distribution of target molecule was carried out by immunofluorescence. This technique

mostly relies on a specific interaction between the molecules of interest with its respective (primary) antibody. The molecules of interest can be either an endogenous protein/molecules or an overexpressed protein achieved by cell transfection. To locate the subcellular distribution of the targeted molecule, a secondary antibody, tagged with a fluorescent dye, was used. The secondary antibody interacts specifically with the first antibody, and hence gives a hint where the interaction takes place.

Cells were seeded on coverslips. On the second day, cells were transfected with an appropriate plasmid DNA and TurboFect transfection reagent (Fermentas, St. Leon-Rot). Cells were fixed with 4% paraformyldehyde on the next day and stored in PBS buffer in refrigerator. If the incubation time needs to be prolonged, the cells were washed and new medium was added, and the cells were further incubated prior to fixation.

Cells were permeabilized by incubation with 0.8% saponin (Roth) in PBS buffer for 5 minutes, followed by incubation in 0.12% glycine fo 10 minutes. Cells were then washed with 0.8% saponin and incubated for at least 15 min in 3% bovine serum albumin (BSA)/PBS buffer containing 0.8% saponin. Incubation with the first antibody was undertaken in a humid-chamber. Antibodies were diluted in 3% BSA/PBS/0.8% saponin solution to appropriate dilutions and applied for 1 hour. The secondary antibodies, chromophore conjugated antibodies recognizing the primary antibodies, were applied after the primary antibody incubation, with several washing steps of the coverslips in between. The used antibodies are listed in the section 2.1. Cells were then washed 5 times in 0.8% saponin/PBS and 2 times in water. Coverslips were placed on a glass plate and finally mounted with moviol. Moviol contains DAPI for nuclear straining. Coverslips were protected from light exposure. Immunofluorescence analysis was carried out on an Axiovert 200M Zeiss fluorescence microscope.

2.2.3 Cell biology

The introduction of foreign plasmid DNA into bacterial cells is known as transformation, so called because the transformed bacteria acquire new properties which are determined by the new genetic information carried by the plasmid DNA. The purpose of this technique can either be the amplification of plasmid DNA, or employing bacteria as a production platform of protein encoded by genetic information within the plasmid DNA. Both

objectives can be achieved because the plasmid DNA is able to replicate within the bacterial host, and can be transferred from parental bacteria to their daughter cells. In this study, the objective of bacterial transformation is limited to the amplification of plasmid DNA.

2.2.3.1 Preparation of electro-competent *E. coli*

Bacterial cell walls are normally impermeable to the hydrophilic plasmid DNA. In order to permeabilize the bacterial cell walls, the bacteria have to be competent of taking up plasmid DNA when they are treated under electrical or heat shock. Bacteria used in this study are of the XL1-Blue strain of *Escherichia coli* (Stratagene) which have tetracycline resistance. Bacteria competent of taking up plasmid DNA under electrical shock (electro-competent cells) are prepared by inoculating a single colony of *E. coli* XL1-Blue in 50 mL Lysogeny Broth (LB) liquid media, followed by an overnight incubation in a shaking incubation chamber of 37^{o}C. All LB media in the preparation of XL1-Blue electro-competent cells contain 50 μg/mL tetracycline. On the next day, two aliquots of 25 mL of the preculture were transferred into 1 L LB medium in a 2 L flask. Incubation was continued until the optical density at 600 nm (OD_{600}) of the cultures reaches 0.5 - 0.6, monitored by OD_{600} measurement with GeneQuant spectrophotometer. Once this point was reached, cells were cooled on ice with occasional shaking to ensure the homogenous cooling. Cells were divided into 4 x 250 mL, each in a centrifuge tube, and then collected by cold centrifugation at 2.400 x g for 15 minutes (JA14-Rotor, J2-HS centrifuge, Beckman). Cells were washed two times with ice cold sterile distilled H_2O and centrifuged at 2.400 x g for 15 minutes. Cells were then washed with 20 mL ice cold 10% glycerol prior to centrifugation at 1.000 x g for 20 minutes. The resulted electro-competent cells were finally resuspended in 4 mL 10% (v/v) glycerol and aliquoted each in 50 μL volume in a 1.5 mL microtube, frozen immediately with dry ice and stored in -80^{o}C for further use.

2.2.3.2 *E. coli* transformation

Transformation of *E. coli* by means of electrical shock is called electroporation. In this process, ~ 100 ng of plasmid DNA of known identity or 1 μL of ligation product (section 2.2.1.11) is mixed with 50 μL electro-competent *E. coli* on ice. The mixture was transferred into a pre-chilled electroporation cuvette, and an electrical shock of 2.5 kV, 400 Ω and 25 μF of electroporator (BioRad, Hercules, USA) was applied. Transformation mixture was

immediately resuspended in 1 mL LB medium, and shaked in a thermobloc of 37°C for 45 minutes. For retransformation of known plasmid DNA, 1 mL of transformation mixture was directly transferred into 50 mL LB medium containing an appropriate antibiotic (50 μg/mL kanamycin or ampicillin), followed by an overnight incubation in a shaking incubator of 37°C. The plasmid DNA from the retransformation process was isolated according to the DNA midi preparation protocol (section 2.2.1.4). For screening of ligation reaction, 200 μL of transformation mixture was spread out on an LB agar plate containing an appropriate antibiotic, followed by an overnight incubation at 37°C. Several colonies from the screening LB agar plate were isolated according to the mini DNA preparation (section 2.2.1.4), and subjected to restriction assay to check whether they contain an intended DNA insert.

2.2.3.3 DNA transfection

The introduction of foreign DNA into a mammalian cell-line is called transfection. TurboFect™ transfection reagent (Fermentas, ST. Leon-Rot) was used in this study. It consists of cathionic polymer which complexes the DNA, and facilitates the up take up DNA through cell membrane.

Cells were seeded on a culture dish in DMEM medium. On the second days, cells of around 70% confluency were transfected by DNA construct of interest. For HeLa cells in a Ø 10 cm dish, 2.5 μg DNA was added into 250 μL pre-warmed DMEM medium (without penicillin/streptomycin). The DNA was mixed thoroughly, and 5 μL TurboFect transfection reagent was added and placed in room temperature for 15 minutes. The tranfection mixture was added into the cells and the culture was incubated in a humid incubator of 37°C conditioned with 5% CO_2. If the incubation time should be more than one day, the medium was changed 24 hours after the transfection, since the transfection reagent is commonly toxic to the cells when applied for a longer time. For transfection of cells in a 3.5 cm dish or for one well of 6-wells plate, 1 μg plasmid DNA was diluted in 100 μL DMEM medium, followed by the addition 2 μL transfection reagent.

2.2.3.4 siRNA transfection

Transfection of mammalian cells by siRNA was carried out similarly to the transfection with DNA. A certain amount of siRNA was diluted in DMEM medium (without FCS or antibiotics penicillin/streptomycin). To that mixture, INTERFERin transfection

reagent (Polyplus, Strasbourg, French) was added and the mixture was incubated in room temperature for 15 minutes to allow the formation of complex of siRNA with the transfection reagent. The mixture was then added to 1-2 days old mammalian cells. The transfection scheme is summarized in the following table.

Table 2.2.9 siRNA transfection mixture.

Dish diameter (cm)	20 μM siRNA	Plain DMEM	INTERFERin Reagent	Vol DMEM (10% FCS + Pen/Strep)
3.5	1 μL	200 μL	4 μL	2.0 mL
10.0	3.15 μL	300 μL	24 μL	6.0 mL

2.2.3.5 Protease inhibition *in vivo*

In order to investigate whether a specific protease inhibitor has an ability to prevent the processing of the DIRC2 protein, inhibitory profiling of DIRC2 with several protease inhibitors have been tested. HeLa cells were initially transfected with DIRC2-3xmyc. Medium was changed 6 hours after transfection and inhibitors or relevant solvents were added into the cells. Cells were harvested 10 hours after the addition of protease inhibitors. Lysates were prepared and subjected into SDS-PAGE separation and further analyzed by Western blot.

The following table list the protease inhibitor used in this study.

Table 2.2.10 Concentrations of protease inhibitors in cells media. Sources of inhibitors are included in Table 2.1.4.

Inhibitor (solvent)	Function	Concentration
Brefeldin A1 (methanol)	Inhibits protein transport out of ER	5 μg/mL
NH_4HCl (H_2O)	Lysosomes acidification inhibitor	25 mM
Leupeptin (H_2O)	Serine and Cysteine protease inhibitor	100 μM
Pepstatin A (DMSO)	Aspartyl protease inhibitor	1 μg/mL
E-64 (H_2O)	Cysteine protease inhibitor	40 μM
CA-074-Me (DMSO)	Cathepsin B inhibitor	40 μM
Z-FY-CHO (ethanol)	Cathepsin L inhibitor	40 μM

3. Results

3.1 Analysis of DIRC2 sequence

The 1434 bps long open reading frame of human *DIRC2* gene corresponds to a protein of 478 amino acids. The sequence of DIRC2 protein shows a high degree of homology to known members of Major facilitator superfamily (MFS) proteins, such as human feline leukemia virus type C receptor (FLVCR) with 43% similarity within the amino acid region 69-427, as well as homology to a number of putative MFS members, e.g. 50% similarity in amino acids 156-215 to inorganic phosphate cotransporter in *Arabidopsis thaliana*, 44% similarity in amino acids 278-433 to a putative transporter in *Leishmania major* (Bodmer et al 2002). *In silico* analysis of DIRC2 sequence by TMHMM program (http://www.cbs.dtu.dk/services/TMHMM/, Krogh et al 2001) suggests a protein consisting of twelve transmembrane domains (Figure 3.1 A and B, transmembrane domains shaded in grey). The hydrophilic amino acids sequence between TM2 and TM3 also fits well to the signature sequence of proteins belonging to the MFS superfamily. Individual transmembrane domains consist of 20-23 amino acid residues (Figure 3.1 B). Furthermore, whereas the length of individual loops can vary and may contain post-translational modifications, the central loop between TM6 and TM7 (Figure 3.1 A, B) is predicted to be around 30 amino acid residues which represents the loop size usually found in members of MFS proteins. It is thought that this length is required for an efficient insertion of MFS protein into a membrane (Weinglass and Kaback 2000).

It has been described in the introduction (Section 1.2) that at least three motifs are involved in lysosomal targeting of membrane proteins, i.e. DXXLL, [DE]XXXL[LI] and YXXØ motifs. The first two are referred to as dileucine motifs, whereas the latter are known as tyrosine-based motifs. Cation dependent and independent MPRs are examples of lysosomal proteins utilizing DXXLL motifs. The [DE]XXXL[LI] type sorting motifs are found e.g. in LIMP-2, sialin and GLUT8 proteins. The tyrosine-based motif YXXØ is present in LAMP-1, LAMP-2 and CD63 proteins. Sequence analysis of the DIRC2 protein revealed a potential dileucine lysosomal targeting motif –E_9**E**RQP**LL**$_{15}$-, which is located at the N-terminal end (Figure 3.1 A) and two putative tyrosine-based lysosomal targeting motifs at its C-terminal end (-Y_{467}-D-RL_{470}- and Y_{471}-L-D-V_{474}-).

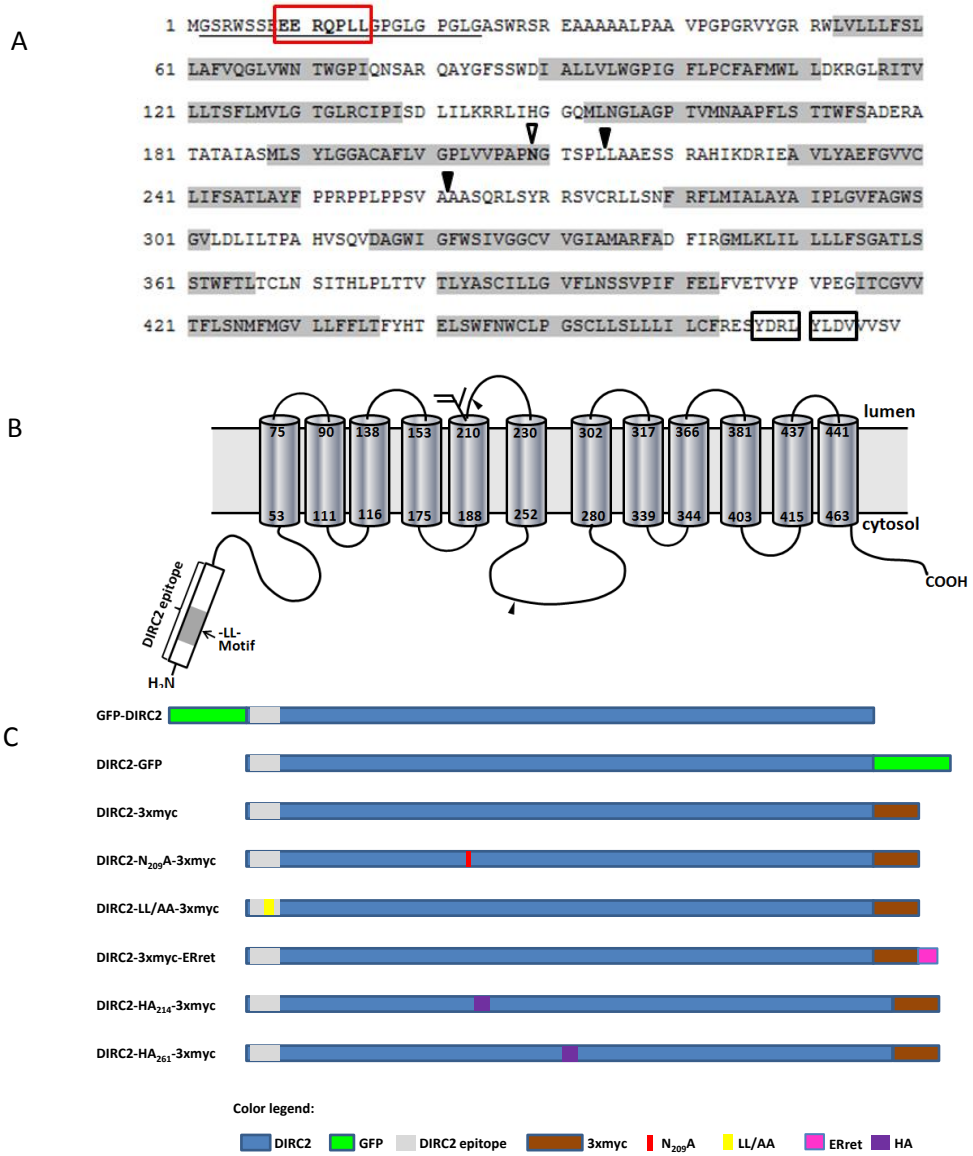

Figure 3.1 Proposed topology of human DIRC2.

(A) Human DIRC2 consists of 478 amino acid residues. It is proposed to have 12 transmembrane spanning domains (highlighted in grey). The sequence shown in the box represents a dileucine lysosomal targeting motif (red box) and two potential tyrosine-based motifs (black box). Asn_{209} is part of a putative N-glycosylation site (open head arrow). A synthetic peptide (underlined sequence) was used to generate a rabbit anti hDIRC2 antiserum.

(B) Topology prediction of DIRC2 generated by TMHMM server (http://www.cbs.dtu.dk/services/TMHMM/, Krogh et al 2001). According to this model, DIRC2 consists of twelve transmembrane spanning domains, with both termini facing the cytosol and a putative glycosylation site in the lumen of lysosomes (N_{209}). Two sites of internal HA tags are shown by arrow heads. The epitope used to raise an anti human DIRC2 antiserum in rabbit is depicted along with a dileucine motif close to the N-terminal end of DIRC2.

(C) Schematic representation of DIRC2 constructs.

N-glycosylation modification is a common post-translational modification of proteins exhibiting a consensus sequence of Asn-X-Ser/Thr (X represents any amino acid residue, except proline), although not all such sequences are used for N-glycosylation (Medzihradszky 2008; Brooks et al 2006). The DIRC2 sequence shows two such consensus sequences, i.e. -N_{209}-G-T_{211}- and -N_{394}-S-S_{396}-. The first putative N-glycosylation site was analyzed whether it is used (Section 3.4), whereas the second N-glycosylation motif was not explored, since it is located within a predicted transmembrane region and is unlikely to be used.

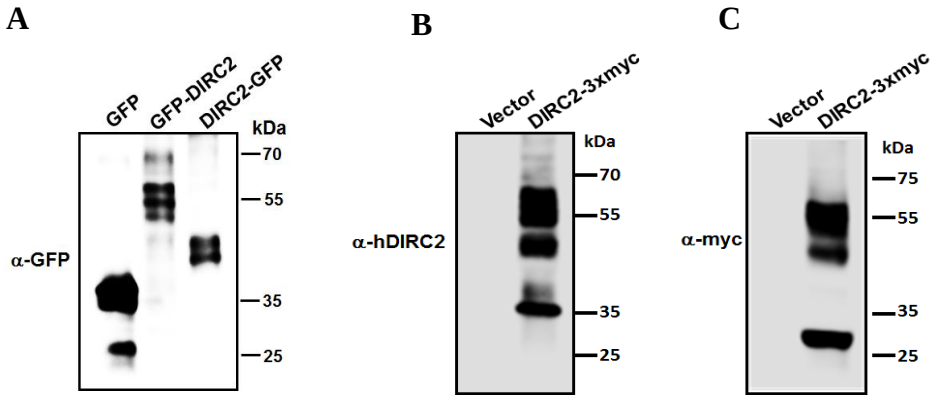

Figure 3.2 Expression of GFP and 3xmyc-tagged DIRC2 analyzed by Western blot.

Two GFP-tagged constructs of DIRC2, pEGFP.C1-DIRC2 and pEGFP.N1-DIRC2 (GFP-DIRC2 and DIRC2-GFP, respectively), as well as DIRC2-3xmyc and empty vectors were expressed in HeLa cells. Cells were harvested 24 hours after transfection. Lysates were prepared as described in the Materials and Methods. Aliquots of total lysates (10 µg and 15 µg for GFP-tagged and -3xmyc tagged DIRC2, respectively) were subjected to SDS-PAGE and Western blot analysis.

(A) Detection of GFP-tagged DIRC2 proteins was carried out by an anti-GFP primary antibody followed by HRP-conjugated secondary antibody. GFP-DIRC2 fusion shows an apparent molecular weight of about 55 kDa, whereas DIRC2-GFP fusion appears at about 45 kDa.

(B) DIRC2-3xmyc expression detected with anti-DIRC2 recognizing the N-terminal part of DIRC2. The uppermost bands of about 55 kDa and a slightly smaller band of around 50 kDa may represent the modified and unmodified form of full length DIRC2, respectively. The band of about 35 kDa is presumably the N-terminal fragment of DIRC2 which contains its sugar rest

(C) The nitrocellulose membrane in (B) was reprobed with anti-myc antibody recognizing the 3xmyc tag at the C-terminal end of DIRC2. The bands of about 55 kDa and 50 kDa represent the modified and unmodified full length DIRC2, respectively. The band of about 26 kDa is likely the C-terminal fragment of DIRC2.

3.2 DIRC2 is proteolytically processed

Expression analysis of DIRC2 was carried out in transiently transfected HeLa cells with either GFP or 3xmyc tagged DIRC2 constructs (Figure 3.1 C). Cell lysates were analyzed by Western blot. Interestingly, different bands were observed for overexpressed DIRC2 when it was tagged with GFP at the N- and C-terminus, respectively (Figure 3.2 A). GFP-DIRC2 showed a band of about 55 kDa, whereas DIRC2-GFP appeared at molecular weight of about 45 kDa. Both fusion proteins were detected at a lower apparent molecular weight as predicted (from the fusion of DIRC2 with GFP), which is expected to be about 75-80 kDa. This suggests that DIRC2 protein is likely to be proteolytically processed.

The expression of 3xmyc tagged DIRC2 provides substantiation that DIRC2 is proteolyzed. Figure 3.2 B and C show the expression of DIRC2-3xmyc detected with an antibody against the N-terminal epitope and 3xmyc tag at the C-terminus of DIRC2, respectively. In both cases, full length DIRC2 appears at a molecular weight of about 55 kDa, and a slightly lower band whose apparent size is approximately close to the calculated molecular weight of 52.1 kDa of the core polypeptide of DIRC2. However, detection with the anti DIRC2 antibody shows an additional band at a molecular weight of about 35 kDa, whereas detection with anti-myc antibody reveals a band at a molecular weight of about 26 kDa. Both smaller bands are likely to represent proteolytic products of DIRC2, which may correspond to the bands at about 55 kDa and 45 kDa when DIRC2 was fused to GFP (Figure 3.2 A).

3.3 DIRC2 is a lysosomal membrane protein

DIRC2 has been identified in a sub-proteomic study as a putative lysosomal membrane protein (Schroeder et al 2007). In order to experimentally confirm the lysosomal localization of DIRC2, DIRC2-3xmyc was expressed in HeLa cells and detected with antibodies against the N-terminal epitope and 3xmyc tag at the C-terminus by indirect immunofluorescence. Figure 3.3 shows that signals for both the N-terminal epitope and C-terminal 3xmyc tag colocalize with the lysosomal membrane protein LAMP-2 (A-C and D-F, respectively). As expected, DIRC2 detected by antibody against the 3xmyc also colocalizes with another lysosomal marker protein β-glucocerebrosidase, βGC (G-I) and with a late endosomal lipid Lysobiphsosphatidic acid, LBPA (J-L). This result suggests that DIRC2 is a lysosomal membrane protein.

Lysosomal localization of DIRC2 could also be demonstrated by subcellular fractionation of HeLa cells transiently transfected with DIRC2-3xmyc. Cells were disrupted mechanically by passage through a 27G cannula in an iso-osmotic buffer. Post nuclear fraction (PNS) was obtained by centrifugation at lower speed (1.000 x g). PNS was separated by density gradient centrifugation employing a self-forming Percoll® gradient, with a starting concentration of 17% (w/v) Percoll® and centrifugation at 40.000 x g for 47 minutes. Fractions were collected from the resulting gradient from top to bottom.

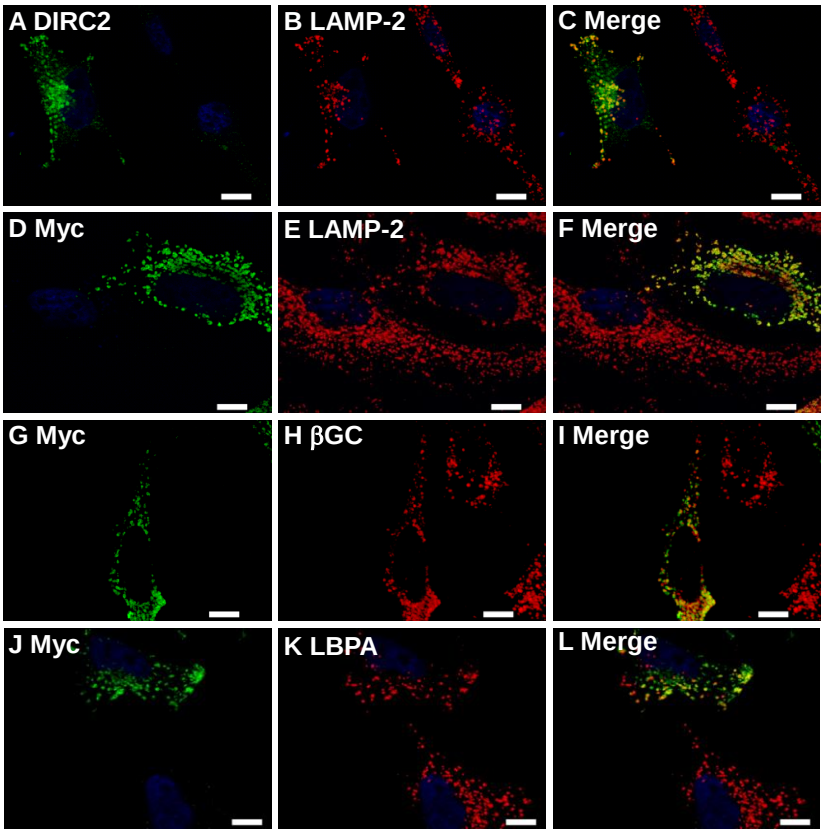

Figure 3.3 Localization of DIRC2.

HeLa cells were transfected with DIRC2 constructs tagged with 3xmyc at the C-terminus. Cells were fixed and double stained with primary antibodies recognizing the N-terminus of DIRC2 and the lysosomal marker protein LAMP-2 (A-C) or with primary antibody recognizing the C-terminal 3xmyc tag and lysosomal markers LAMP-2 (D-E), βGC (G-I), and late endosomal lipid LBPA (J-L). Both N- and C-terminal detection of DIRC2 colocalizes with the lysosomal/late endosomal markers. Of note, the primary antibody against the N-terminus of DIRC2 does not detect endogenous DIRC2 (A). Bars represent 10 μm.

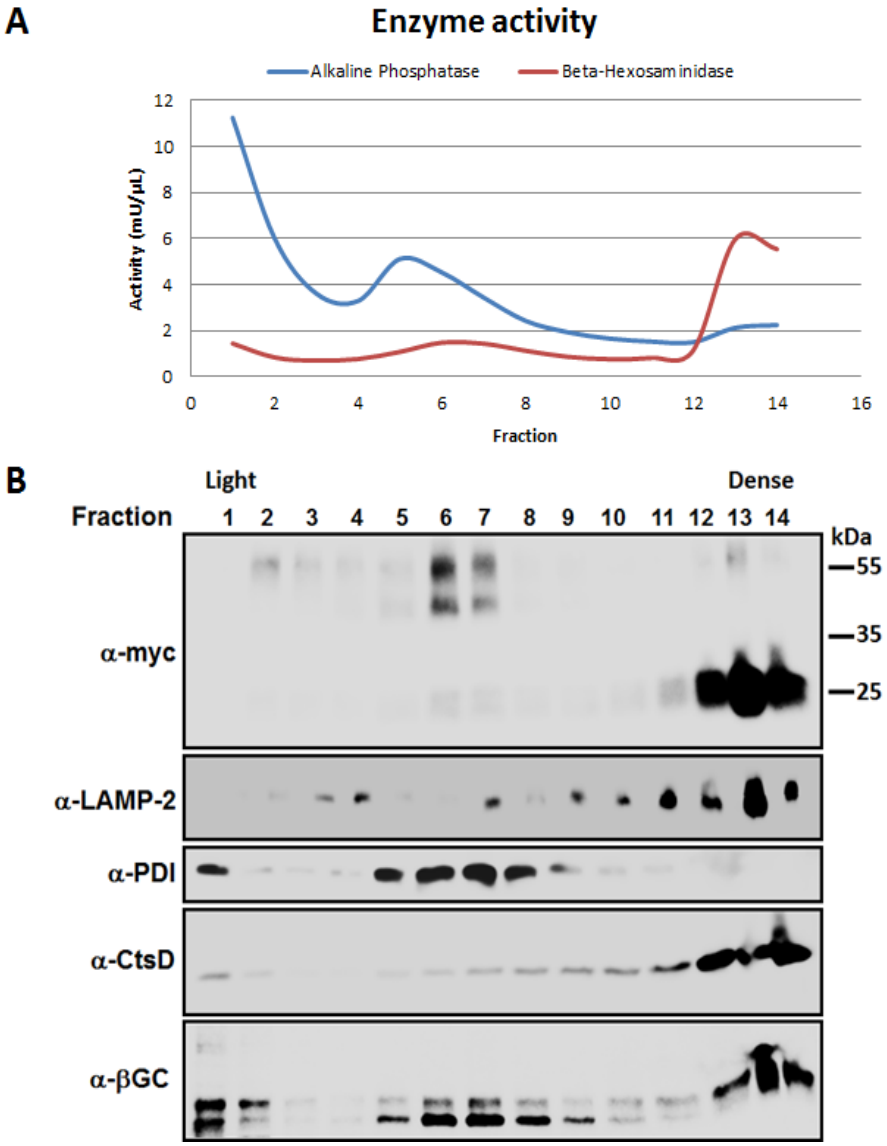

Figure legend: LAMP-2: lysosomal associated membrane protein type 2; PDI: protein disulfide isomerase; CtsD: cathepsin D; βGC: beta-glucocerebrosidase.

Figure 3.4 Percoll® fractionation of the extract of HeLa cells transiently transfected with DIRC2-3xmyc.

HeLa cells were transfected with DIRC2-3xmyc and harvested 48 hours after transfection. Cells were disrupted and suspended in iso-osmotic buffer. Cell homogenate was fractionated in a self-forming Percoll® gradient (17% w/v) upon centrifugation at 40.000 x g for 47 minutes.

(A) Enzymes activities of β-hexosaminidase and alkaline phosphatase were determined in each fraction using spectrophotometric methods as described in Materials and Methods.

(B) Equal volumes of each fraction were subjected to SDS-PAGE and Western blot analysis. Western blot detection of each fraction was undertaken with several subcellular markers. DIRC2, as detected by anti-myc, is shown to be co-sedimenting with lysosomes. It is recovered in the dense fractions (12-14), as shown by lysosomal markers LAMP-2, cathepsin D and βGC. A minor amount of DIRC2 is distributed in fraction 6 and 7 where the signal of ER marker PDI appears.

Figure 3.4 A shows the distribution of lysosomal enzyme β-hexosaminidase, which is found in the dense fractions (fraction 12-14). In contrast, activity of alkaline phosphatase, an enzyme of the plasma membrane, was recovered in two peaks in fractions 1-2 and fractions 4-5, respectively. Parallel to this observation, the immunoblot analysis of individual fractions of HeLa cells transfected with DIRC2-3xmyc is depicted in Figure 3.4 B. It is revealed that proteolytically processed DIRC2 with a molecular weight of 25 kDa is observed in fraction 12-14 co-sedimenting with lysosomes as indicated by the lysosomal markers LAMP-2, cathepsin D and β-glucocerebrosidase. The discrepancy between theoretical and apparent molecular weight of DIRC2 (55 kDa and 25 kDa, respectively) suggests that DIRC2 may have been proteolytically processed. Nevertheless, the rather weak signals that presumably represent full length DIRC2 are observed co-sedimenting with the endoplasmic reticulum (fraction 5-7, shown by ER marker PDI). Taken together, both immunofluorescence and subcellular data confirmed the lysosomal localization of DIRC2 protein. However, further evidence is required to validate whether the processing of DIRC2 first takes place when it reaches lysosomes.

3.4 DIRC2 is N-glycosylated at Asn-209

Bioinformatics analysis of the DIRC2 sequence (Section 3.1) highlighted the possibility that DIRC2 may undergo N-glycosylation. Expression of DIRC2 in HeLa cell analyzed by Western blot (Section 3.2) also indicated that DIRC2 is expressed at an apparent molecular weight higher than the calculated molecular weight. In order to confirm whether DIRC2 is N-glycosylated, the lysate of HeLa cells overexpressing DIRC2-3xmyc was treated with N-glycosidase F (PNGase F). PNGase F is an amidase isolated from *Flavobacterium meningosepticum* that cleaves between the innermost *N*-acetyl-D-glucosamine (GlcNAc) and asparagine residues of high mannose, hybrid, and complex oligosaccharides from N-linked glycoproteins (Maley et al 1989). It is shown that wild-type DIRC2 is sensitive to PNGase F digestion (lane 3 and 4, detected by anti-hDIRC2 and anti-myc in Figure 3.5 A and 3.5 B, respectively). This result suggests that DIRC2 is an N-linked glycosylated protein.

A closer view on the expression of wild-type, undigested, DIRC2 -upon detection with anti hDIRC2 antibody- (lane 3 Figure 3.5 A) revealed that wild-type DIRC appears in three forms: a band of about 55 kDa which represents the full length DIRC2 with its sugar moiety,

a band of about 35 kDa which represents the N-terminal half with a sugar moiety, and the small band slightly lower than the 25 kDa marker, which is supposed to be the deglycosylated N-terminal half of DIRC2. Incubation of wild-type DIRC2 in the presence of PNGase F (lane 4 Figure 3.5 A) confirmed the identity of the full length DIRC2 bands, as removal of sugar moiety by PNGase F allowed the identification of the core polypeptide of DIRC2 of about 50 kDa. Additionally, upon PNGase F digestion, the 35 kDa band completely disappeared and shifted to a band slightly below 25 kDa, thus confirming that the 35 kDa and 25 kDa bands are the glycosylated and the unglycosylated N-terminal half of DIRC2, respectively. This suggests that Asn-209 is used for N-glycosylation. On the other hand, redetection of the same blot with an anti-myc antibody revealed that the undigested DIRC2-3xmyc appears as two bands: the upper band of 55 kDa which fits the molecular weight of full length DIRC2 and a smaller band above 25 kDa protein marker, which is likely to be the C-teminus fragment of DIRC2 (Figure 3.5 B, lane 3). Upon PNGase F digestion, the full length DIRC2 was shifted to 50 kDa which represent the core polypeptide DIRC2, whereas the C-terminal fragment was not shifted (Figure 3.5 B, lane 4). This validates that Asn-394 in the C-terminal half of DIRC2 is not used for N-glycosylation.

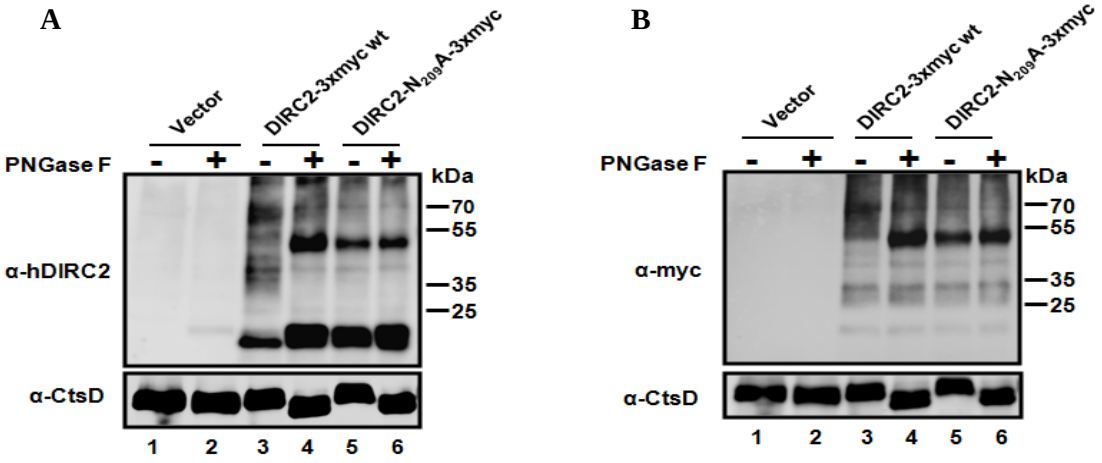

Figure 3.5 Deglycosylation of DIRC2 by PNGase F.

Wild-type DIRC2-3xmyc and DIRC2-N_{209}A-3xmyc were overexpressed in HeLa cells. Cells were harvested 2 days after transfection. Lysates were incubated in the presence or absence of PNGase F prior to SDS-PAGE separation and Western blot analysis as described in the Materials and Methods.

A) Immunodetection of the full-length DIRC2 and its N-terminal fragment of both wild-type and N_{209}A mutants of DIRC2 with antibody directed against N-terminal epitope.

(B) Immunodetection of the same blot with an anti-myc antibody. Loading controls as well as PNGase F digestion control are provided by immunodetection of cathepsin D.

Equal loading and control of PNGase F digestion were shown by cathepsin D detection (A and B).

A direct proof that the first N-glycosylation motif (-N_{209}-P-T_{211}-) is instead used for glycosylation was shown by analyzing the expression of DIRC2-N_{209}A-3xmyc mutant. In this mutant, Asn-209 is replaced by Ala-209 (construct provided by Dr. B. Schroeder). Lysate of HeLa cells expressing this mutant was incubated with PNGase F and analyzed by Western blot. Figure 3.5 A and B (Lane 5 and 6) revealed that both full length and fragments DIRC2 appear at the same molecular weight as that apparently shown by PNGase F digested wild-type DIRC2 (lane 4), irrespective of PNGase F digestion. These patterns are in agreement with the prediction that Asn-209 not Asn-394 is used for N-glycosylation. Moreover, validation of N-glycosylation site gave an indirect substantiation of the topology of DIRC2 (Figure 3.1). The DIRC2 topology suggests that the loop 5 (region between TM5 and TM6 where the N-glycosylation site located) resides on the luminal face of the membrane, whereas both N-terminal and C-terminal are facing the cytoplasmic environment.

3.5 Lysosomal targeting of DIRC2 depends on a lysosomal sorting motif at its N-terminus

3.5.1. Expression of dileucine and ER retention mutants of DIRC2

The targeting of proteins into lysosomes, as described in the Introduction (Section 1.2), is defined by several lysosomal sorting motifs. One subclass of lysosomal targeting motifs is the consensus sequence [DE]XXXL[LI] (Table 1.1). Sequence analysis of DIRC2 protein reveals that such a motif resides in its N-terminal region, namely –E_9**E**RQP**LL**$_{15}$-. In order to analyze whether this motif has a functional relevance for the lysosomal targeting of DIRC2, a DIRC2 mutant was constructed where the dileucine in the putative lysosomal targeting motif was replaced by alanines (LL/AA mutant, Figure 3.1 C). Expression of this mutant is shown in Figure 3.6 D-F. It is revealed that replacement of the dileucine motif with alanines resulted in surface expression of DIRC2. This mutant showed very few or no colocalization with the lysosomal marker LAMP-2 (Figure 3.6 D-F). On contrary, disruption of two tyrosine-based lysosomal targeting motifs close to C-terminal end of DIRC2 (Figure 3.1 B) had only minor effect on the lysosomal targeting of DIRC2 (data not shown). It is concluded that the dileucine motif is important for the lysosomal targeting of DIRC2. This observation underlines the critical importance of the dileucine motif of DIRC2 in the sorting of DIRC2 to the lysosomes.

Subcellular fractionation of HeLa lysate transfected with DIRC2 indicated that the majority of DIRC2 was distributed in lysosomal fraction in processed form, whereas only a small amount of DIRC2 co-sedimented with ER in full-length form (Section 3.3, Figure 3.4 B). In order to validate that the absence of processed form of DIRC2 in the ER fraction was not due to the minor distribution of DIRC2 in ER, a DIRC2 mutant appended with RR-based ER targeting motif (DIRC2-3xmyc-ERret, Figure 3.1. C) was generated and overexpressed in HeLa cells. Expression of this mutant in HeLa cells, analyzed by immunofluorescence, resulted in an ER localization (Figure 3.6 J-L). This mutant appeared as a full length form on Western blot (M). It was likely to be retained in the ER or transported back from Golgi to the ER, and was not able to reach lysosomes (G-I). This result suggests that the ER retention motif predominantly retains the DIRC2 in the ER, irrespective of the presence of functional dileucine lysosomal targeting motif. This observation along with the result of subcellular fractionation (Figure 3.4 B) underlined the fact that DIRC2 was not fragmented in the ER, and that the processing had to occur in a post ER compartment.

3.5.2 Stepwise post-translational modification of DIRC2

Analysis of DIRC2 expression or localization in the ER can also be achieved by addition of brefeldin A1 to cultured cells. Brefeldin A has long been known to have an ability to inhibit the transport of protein out of the ER, although the rate of protein biosynthesis itself is not affected (Misumi et al 1986). In agreement to the function of brefeldin A, expression of DIRC2 in the presence of brefeldin A1 prevents proteolysis of DIRC2. Hence, it is concluded that DIRC2 is not proteolytically processed in the ER (Figure 3.6 M lane 3). It is also shown that the full length DIRC2 expressed in ER had a lower molecular weight in comparison to the full length DIRC2 expressed in the lysosomes (Figure 3..6 M lane 2).

In order to analyse the glycosylation of DIRC2, wild-type and $N_{209}A$ mutant DIRC2 were overexpressed in HeLa cells in the presence and absence of brefeldin A1. The lysates were treated with either PNGase F or Endo-β-N-acetylglucosaminidase H (Endo H). The latter cleaves oligosaccharides directly linked to an asparagine residue but not of complex oligosaccharides form (Maley et al 1989). Figure 3.7 shows the expression of wild-type DIRC2-3xmyc and DIRC2-N_{209}A-3xmyc mutant in HeLa cells in the absence and the presence of brefeldin A1. As expected, addition of brefeldin A1 prevented the proteolytic of

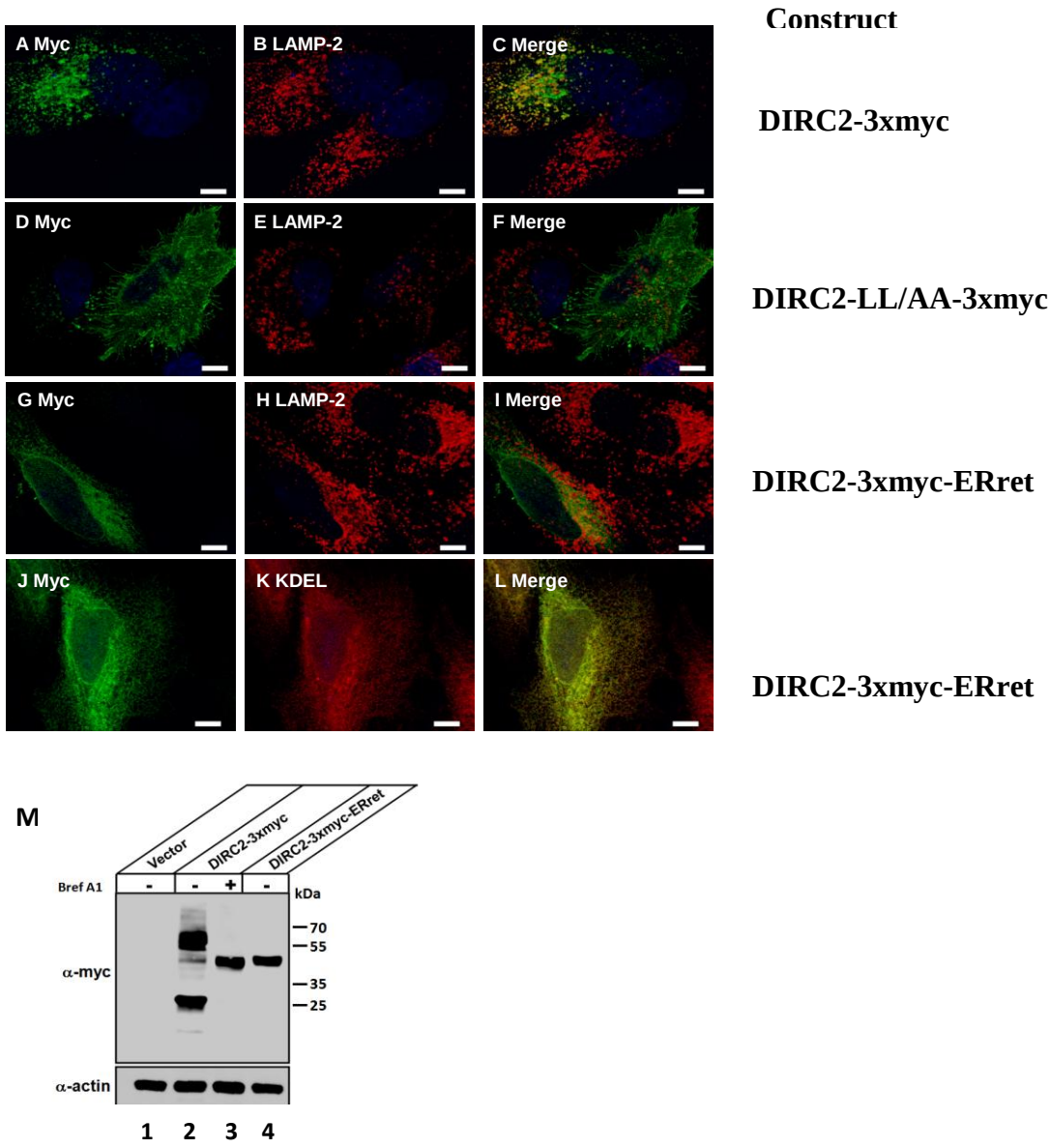

Figure 3.6 Immunofluorescence analyses of dileucine and ER retention mutants of DIRC2.

HeLa cells were transfected either with dileucine and ER retention mutants (DIRC2-LL/AA-3xmyc and DIRC2-3xmyc-ERret, respectively; Figure 3.1 C). For immunofluorescence assay, transfected cells were fixed two days after transfection. The DIRC2 LL/AA mutant was mainly expressed at the cell surface (D-F) and did not colocalize with the lysosomal marker LAMP-2. The DIRC2 ER retention mutant did also not colocalize with the lysosomal marker LAMP-2 (G-I). Instead, it colocalized with the endoplasmic reticulum marker KDEL (J-L). Figure A-C shows control of wild-type DIRC2-3xmyc overexpressed in HeLa cells. Bars represent 10 μm. For Western blot analysis (Figure M), DIRC2-3xmyc was expressed in HeLa cells in the presence of brefeldin A1, which was added 6 hours after transfection to a final concentration of 5 μg/mL. Cells were harvested 10 hours after brefeldin A1 addition. DIRC2 ER retention mutant as well as wild-type and empty vector were also used to transfect HeLa cells, and cells were harvested 16 hours after transfection. Aliquots of lysates (20 μg protein) were subjected to SDS-PAGE and Western blot analysis as described in the Materials and Methods. Blot was detected with anti-myc primary antibody followed by HRP-conjugated secondary antibody. Equal loading was shown by actin detection (Figure M, lower panel).

both wild-type and $N_{209}A$ mutant of DIRC2 (Figure 3.7 lane 12-19). On the opposite, both DIRC2 and $N_{209}A$ mutant of DIRC2 were processed in the absence of brefeldin A1 (Figure 3.7 lanes 1-10). In all cases, the full length form of DIRC2-$N_{209}A$-3xmyc mutant showed a molecular weight of about 50 kDa, irrespective of PNGase F and Endo H digestion (lane 3-4, 7-8, 14-15, and 18-19). In the absence of brefeldin A1, the glycosylated full length and the C-terminal fragment of wild-type of DIRC2 appeared as heterogeneous cluster of bands at molecular weight higher than 55 and a band of 25 kDa, respectively (Figure 3.7 lane 2, 6 and 9). The wild-type DIRC2 expressed in the absence of brefeldin A1 was sensitive to PNGase F digestion (lane 1), but hardly sensitive to Endo H digestion (lane 5), reflecting that only a minor amount of DIRC2 is retained in the ER (and hence sensitive to Endo H digestion). In the presence of brefeldin A1, the wild-type DIRC2 shows a molecular weight slightly lower than 55 kDa (lane 13 and 17). However, this band was clearly shifted upon digestion with both PNGase F and Endo H (lane 12 and 16, respectively). This was a hint that DIRC2 acquired its core glycans in the ER, and a further modification of its sugar is occurring in the post ER compartment.

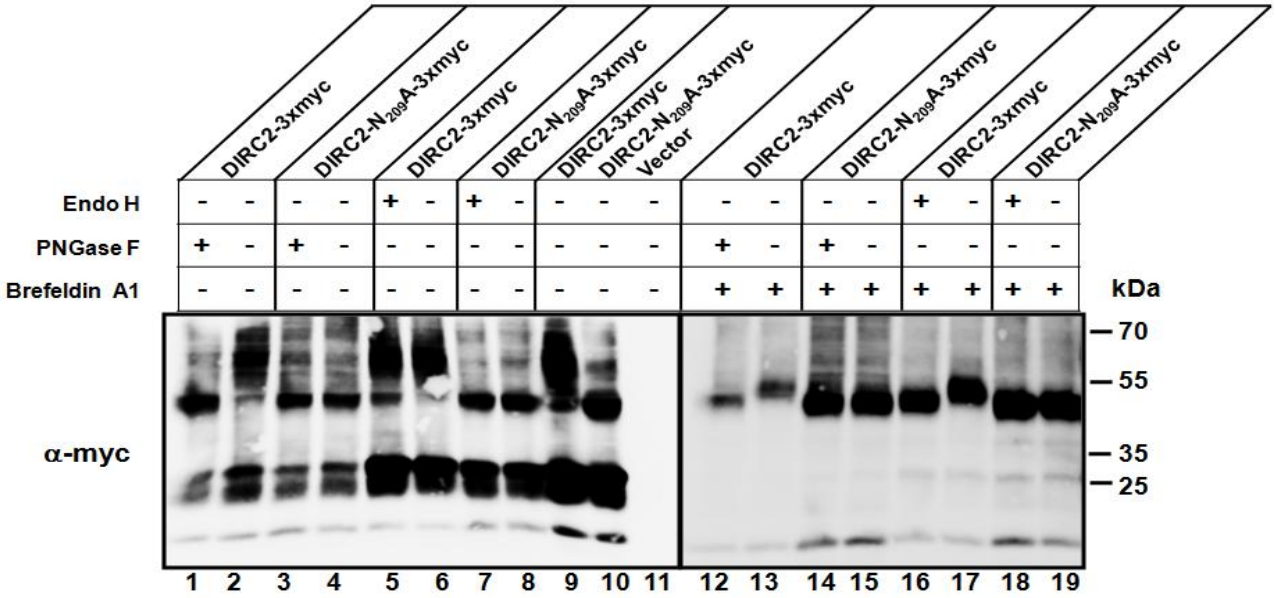

Figure 3.7 Post-translational modification of DIRC2 takes place in multiple steps.

HeLa cells were transfected with DIRC2-3xmyc wild-type and DIRC2-$N_{209}A$-3xmyc in the presence and absence of 5 μg/mL brefeldin A. Cells were washed 6 hours after transfection and brefeldin A1 was added into the new medium. Cells were harvested 10 hours after the addition of brefeldin A1. Cell lysates were digested with PNGase F and Endo H as described in the Materials and Methods. The digested samples and undigested controls were subjected to SDS-PAGE separation and Western blot detection with an anti-myc antibody recognizing the C-terminally appended epitope tag wild-type and $N_{209}A$ mutant of DIRC2.

3.6 Detection of endogenous DIRC2

It has been shown that overexpressed DIRC2 in HeLa cells can be detected by anti-hDIRC2 antibody recognizing an epitope at the N-terminus of DIRC2 (Figure 3.2. B). In order to validate whether anti-hDIRC2 antibody is able to detect DIRC2 at the endogenous level, anti-hDIRC2 antibody was used to detect DIRC2 from HeLa lysates transfected either by DIRC2 siRNAs or non-targeting siRNA. Control lane in Figure 3.8 B shows that endogenous DIRC2 from HeLa cell can be detected by the anti-hDIRC2 antibody. The endogenous DIRC2 appeared as a cluster of bands between 30 to 40 kDa. This cluster of bands resembles the N-terminal half of overexpressed DIRC2-3xmyc detected by an anti-hDIRC2 antibody (Figure 3.5 A lane 3). This result suggests that endogenous DIRC2 is glycosylated and proteolytically processed in a similar way as the overexpressed DIRC2.

By using three different DIRC2 siRNAs or combination of them, DIRC2 can be significantly downregulated as shown by the reduction of DIRC2 mRNA and protein level (Figure 3.8 A and B, respectively). Following DIRC2 downregulation, expression level of several lysosomal marker proteins (LAMP-2, β-glucocerebrosidase and cathepsin D) and activities of lysosomal enzymes (β-hexosaminidase, β-galactosidase and α-mannosidase) were tested. Both types of analyses could not reveal significant alterations of either lysosomal marker proteins or lysosomal enzymes activities following DIRC2 downregulation by siRNA (Figure 3.8 C and D, respectively). Immunofluorescence analysis of DIRC2 siRNAs transfected HeLa cells revealed no apparent morphological alteration of cells and lysosomes or alteration of lysosomal storage (e.g. cholesterol, tested by filipin staining) (data not shown).

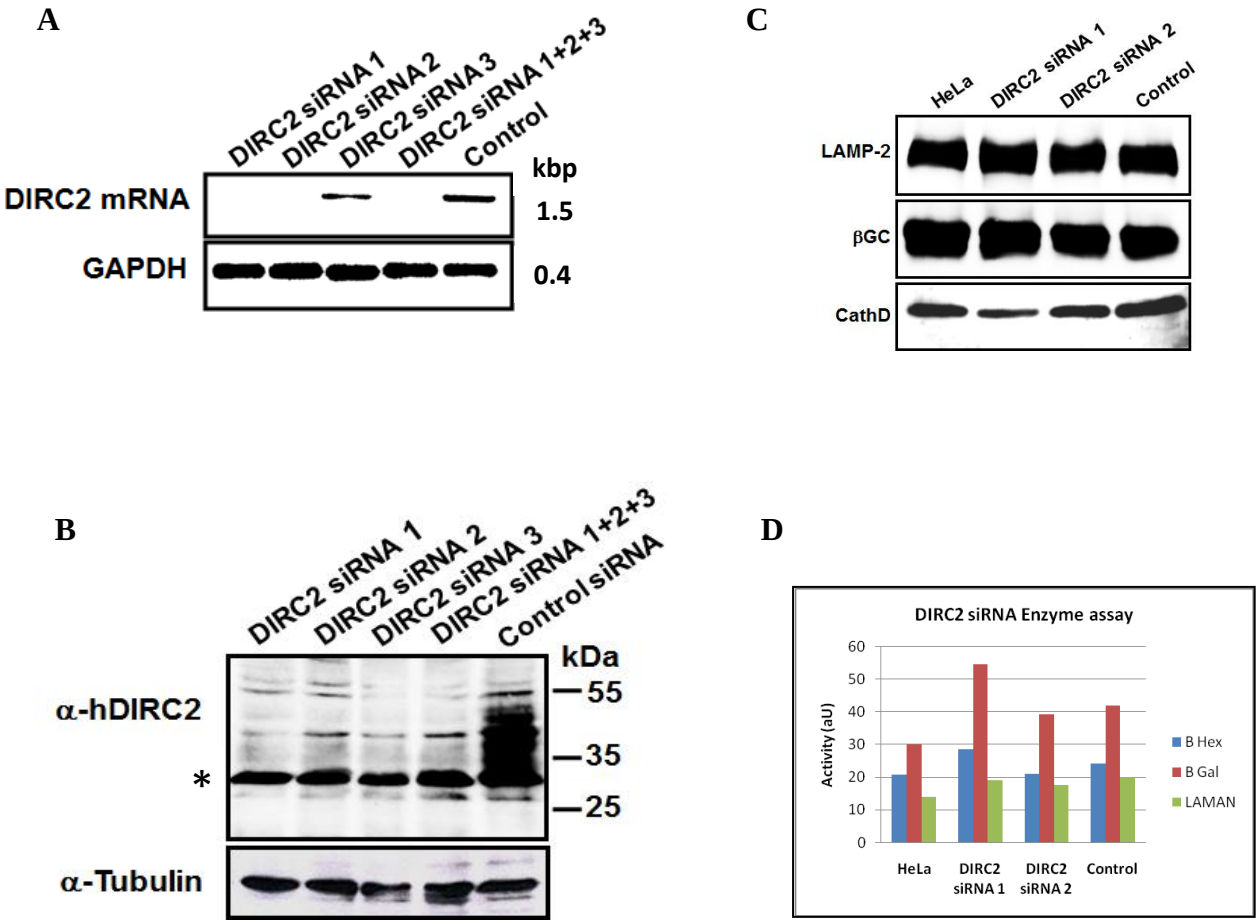

Figure 3.8 Downregulation of DIRC2 with siRNA.

HeLa cells were grown on 10 cm dishes and transfected with DIRC2 siRNA (Stealth pre-design oligo siRNA, Invitrogen) on the second day to the final concentration of 10 nM. Transfections were achieved by TRANFERin siRNA transfection reagent (PolyPlus, Strassbourg, French). Analysis of mRNA level of DIRC2 was undertaken by first isolating the total RNA of the transfected cells 48 hours after siRNA transfection, followed by reverse transcriptase reactions using aliquots of the isolated total RNA as templates (RevertAid, Fermentas, St. Leon-Rot).

(A) The relative amount of DIRC2 mRNA levels was then determined by PCR with a primer pair which amplifies full length DIRC2 sequence from the reverse transcriptase reaction mixture. Control for this analysis was provided by analyzing the mRNA level of a house-keeping gene GAPDH (exon7-8).

(B) siRNA transfected HeLa cells were harvested 48 hours after tranfection and the lysates were subjected to SDS-PAGE separation and Western blot analysis. Expression level of DIRC2 following DIRC2 siRNA transfection was detected by using anti-hDIRC2 antibody. The N-terminal fragment of DIRC2 is shown by the cluster of bands at 30 to 40 kDa in control, non-targeting, siRNA lane. Asterisk shows unspecific band.

(C) Expression of lysosomal proteins LAMP-2, βGC and Cathepsin D.

(D) Activities of lysosomal enzymes β-hexosaminidase (β-hex), β-galactosidase and α-mannosidase.

3.7 Inhibitory profiling indicates involvement of the lysosomal cysteine protease cathepsin L

In an attempt to unravel the identity of the protease(s) involved in DIRC2 proteolysis, DIRC2 was overexpressed in HeLa cells in the presence of several protease inhibitors. An initial screening with a broad panel of inhibitors excluded, for example, a role of proteosome, aspartyl peptidase and γ-secretase in the fragmentation of DIRC2 (tested by MG132, pepstatin A and inhibitor X, subsequently; data not shown). On the contrary, prevention of DIRC2 proteolysis was observed in DIRC2 transfected cells treated with NH_4Cl and leupeptin. Effects of these inhibitors are shown in the Figure 3.9 lane 3 and 4, respectively. NH_4Cl is known to interfere with the acidification of lysosomes (Gahl and Tietze 1985; Galbiati et al 2000), which implied that the fragmentation of DIRC2 takes place in the lysosomes, and acidic environment is a prerequisite for a successful proteolysis. Leupeptin is known as a competitive serine/cysteine protease inhibitor (Aoyagi et al 1969). Pepstatin A, an inhibitor for aspartyl protease (Umezawa et al 1970), did not inhibit the proteolysis of DIRC2 (lane 5). These observations opened the possibility that DIRC2 is proteolyzed by lysosomal acid hydrolases of serine or cysteine protease class.

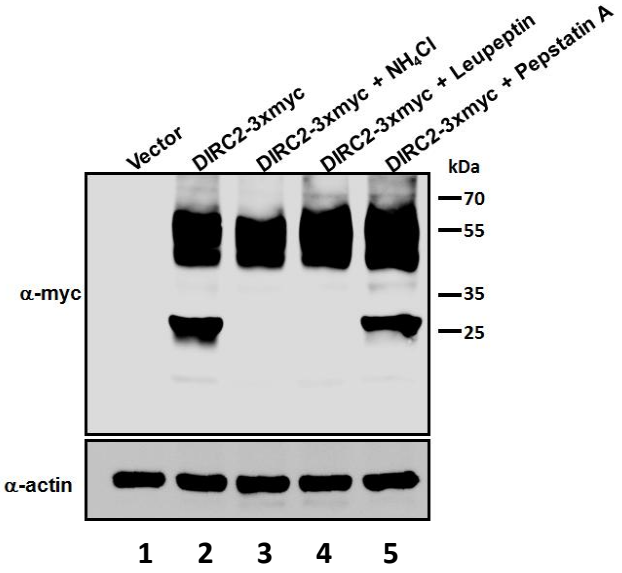

Figure 3.9 Inhibition of DIRC2 proteolysis.

HeLa cells were transfected with DIRC2-3xmyc in DMEM medium supplemented with 10% FCS and penicillin/streptomycin. Medium was refreshed six hour after transfection and inhibitors were added to final concentrations of 25 mM, 100 μM and 1 μg/mL for NH_4Cl, leupeptin and pepstatin A, respectively. Cells were harvested 10 hours after the addition of inhibitors. Cells lysates were subjected to SDS- PAGE followed by Western blot analysis. Expression of DIRC2 was detected by a mouse anti-myc antibody. Equal loading was confirmed by detection of actin.

Lysosomes are harbouring a variety of hydrolases, including serine/cysteine proteases. Most of them are known as cathepsins. Members of this group include cathepsin A and G (serine protease), cathepsin B, C, F, H, K, L, O, S, W, V and Z (cysteine protease). Additionally, there are also cathepsin D and E which are known as lysosomal aspartic proteases (Reiser et al 2010). Further refinement was attempted by the use of additional, more specific, inhibitors. It is shown in the Figure 3.10 lane 4 that E-64 was able to inhibit the proteolysis of DIRC2. E-64 was reported to inhibit mostly cysteine proteases (Barrett et al 1982, Katunuma and Kominami 1995). Hence, the result of proteolysis inhibition assay with E-64 ruled out the role of serine protease, and suggests a protease involved in the processing of DIRC2 which belongs to the cysteine protease group.

Cathepsin B and L are two prominent cysteine proteases in lysosomes. In order to investigate their possible role in the processing of DIRC2, an experiment by using CA-074-Me and Z-FY-CHO, inhibitors of cathepsin B and cathepsin L, respectively, was performed. Figure 3.10 lane 6 and 8 shows that both cysteine protease inhibitors were able to prevent the fragmentation of DIRC2. It suggests that cathepsin B and/or cathepsin L may be involved in the proteolysis of DIRC2.

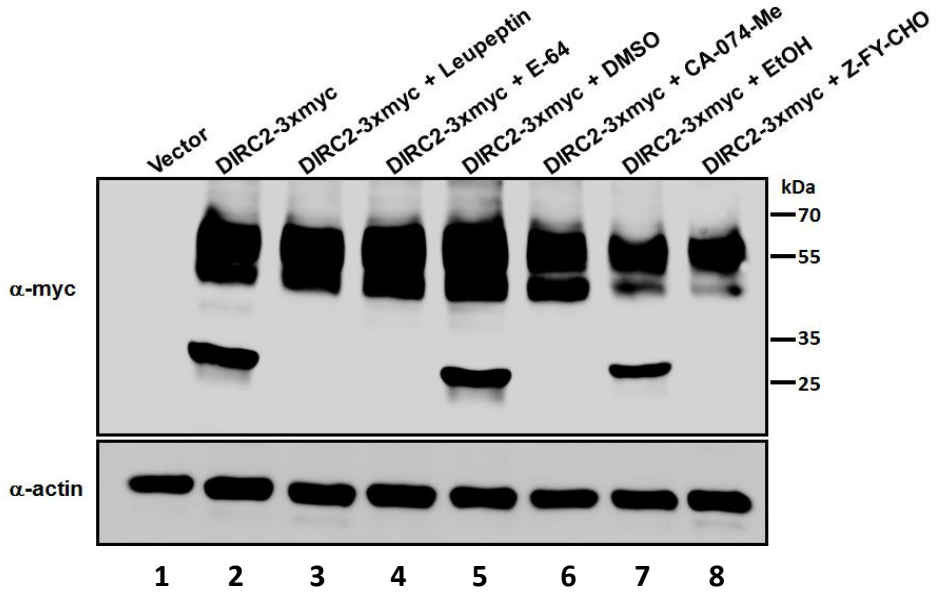

Figure 3.10 Inhibition of DIRC2 proteolysis by cysteine protease inhibitors.
HeLa cells were tranfected with DIRC2-3xmyc in DMEM medium supplemented with 10% FCS and penicillin/streptomycin. Medium was refreshed six hour after transfection and inhibitors were added into the cells to final concentrations of 100 μM for leupeptin, and 40 μM for E-64 (in H_2O), CA-074-Me (in DMSO) and Z-FY-CHO (in ethanol). The effects of the solvent of inhibitors were shown by the addition of equivalent volumes of solvents (DMSO and ethanol; lane 5 and 7, respectively) to the transfected cells. Cells were harvested 10 hours after the addition of inhibitors. Cells lysates were subjected to SDS-PAGE separation and analyzed by Western blot. Expression of DIRC2 was detected by anti-myc antibody. Equal loading was shown by detection of actin.

3.8 Processing of DIRC2 is abolished in Cathepsin L deficient fibroblasts

In order to dissect the contribution of different cathepsins, various murine embryonic fibroblast (MEF) cell-lines deficient in one or more cathepsins were utilized. Since lysosomal targeting is a prerequisite for proteolysis of DIRC2, an immunofluorescence analysis was first performed to ensure that the transected DIRC2-3xmyc localized in the lysosomes of cathepsin deficient MEFs. DIRC2-3xmyc construct was used to transiently transfect cathepsin $B^{-/-}$, cathepsin $L^{-/-}$, cathepsin $BL^{-/-}$ MEFs, as well as wild-type and cathepsin $D^{-/-}$ MEFs. It was revealed from figure 3.11 that human DIRC2 was localized in the lysosomes of all MEF cells tested. Therefore, these cells can be employed in the experimental set-up whether or not DIRC2 proteolysis was impaired in the absence of individual cathepsins.

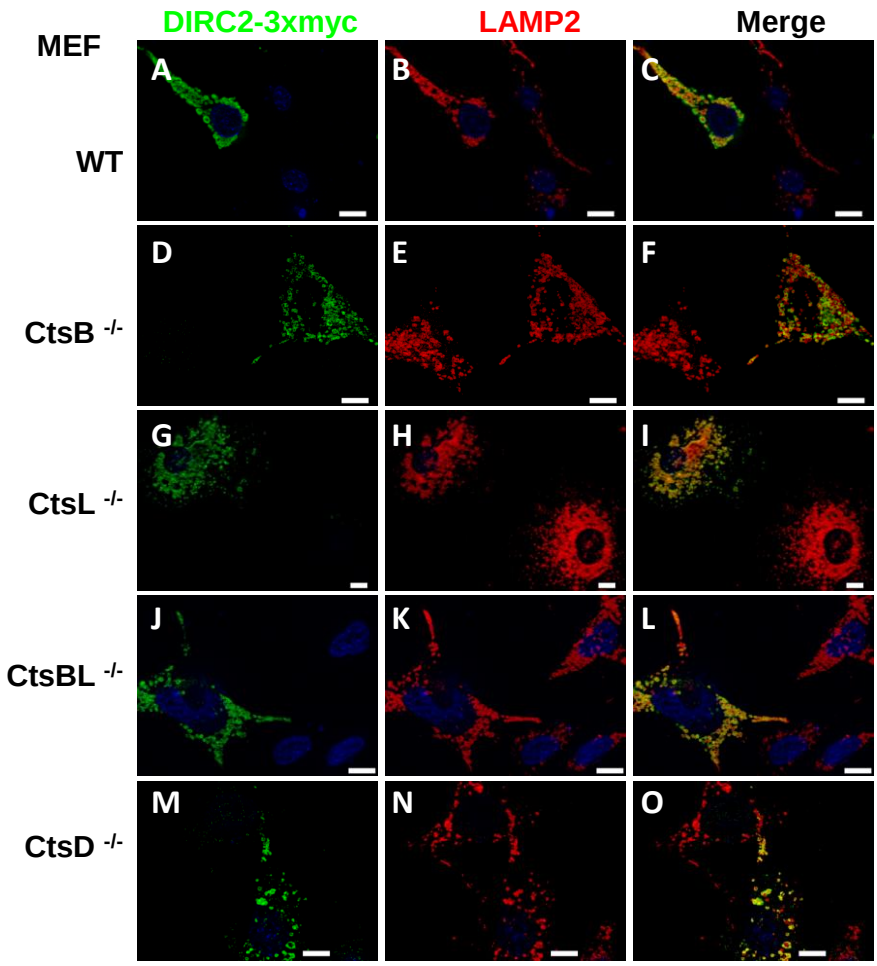

Figure 3.11 Localization of hDIRC2 in cathepsin deficient MEFs.

DIRC2-3xmyc was used to transfect different MEF cell-lines deficient in one or two cathepsins (cathepsin B, $CtsB^{-/-}$; cathepsin L, $CtsL^{-/-}$; cathepsin B and L, $CtsBL^{-/-}$, cathepsin D, $CtsD^{-/-}$) as well as wild-type MEF. Cells were fixed with 4% paraformaldehyde 24 hours after transfection, permeabilized with 0.2% saponin and blocked with 3% BSA. DIRC2 expressions were visualized by anti-myc antibody, whereas lysosomes were stained by anti-LAMP-2 antibody. Nuclei were stained by DAPI (blue). Bars represent 10 μm.

Figure 3.12 shows the expression of DIRC2-3xmyc in cathepsin deficient MEF cell-lines. DIRC2-3xmyc expressed in wild-type MEF cells (lane 4) showed a similar pattern to the DIRC2-3xmyc expressed in HeLa cells (lane 2): the full length DIRC2 appears at about 55 kDa and the C-terminal fragment appears at about 25 kDa. Among the cathepsin deficient MEF cells, it was revealed that DIRC2-3xmyc was not proteolyzed in the cathepsin L deficient and cathepsin B and L double deficient MEF cells (CtsL $^{-/-}$ in lane 8 and $CtsBL^{-/-}$

10, respectively). In contrast, DIRC2-3xmyc was proteolyzed similar to wild-type cells in cathepsin B single deficient MEF (lane 6) and cathepsin D deficient MEF (lane 12). This result ruled out a role of cathepsin B and D in the proteolysis of DIRC2 and showed that cathepsin L is indispensable for the proteolysis of DIRC2 in MEF cells.

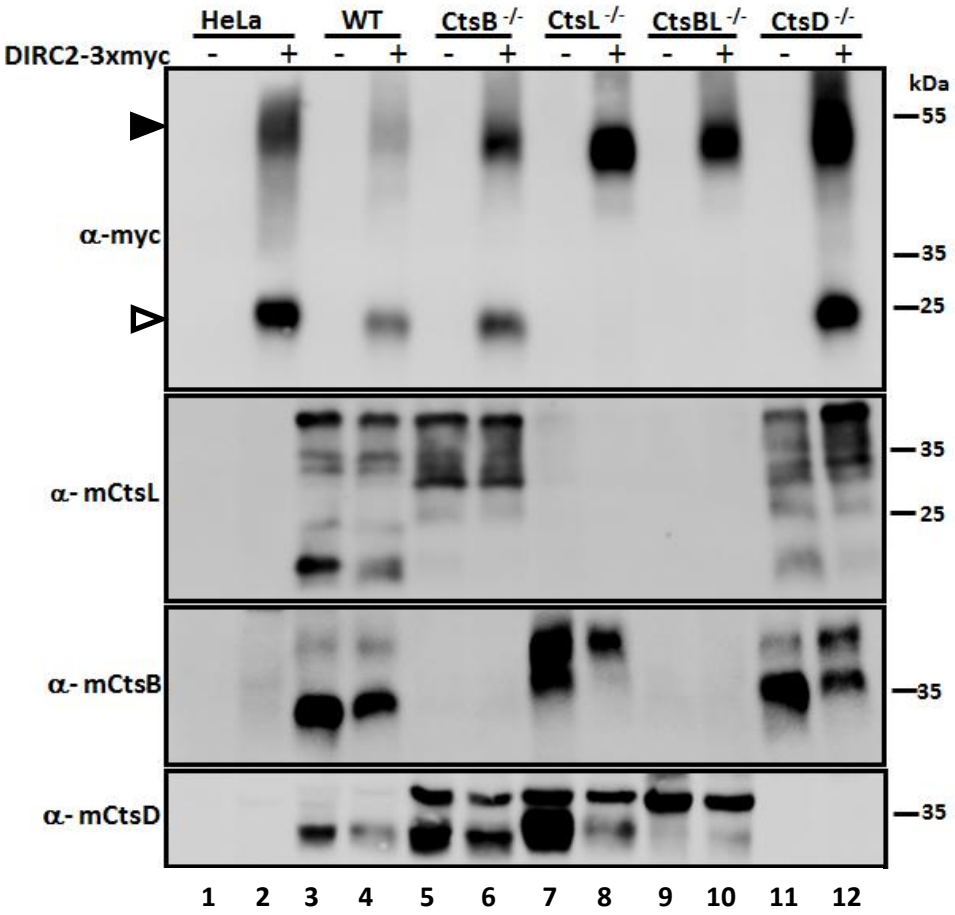

Figure 3.12 Expression of DIRC2 in cathepsin deficient MEFs.
Murine embryonic fibroblast (MEF) cells deficient in cathepsin B ($CtsB^{-/-}$), cathepsin L ($CtsL^{-/-}$), cathepsin B and L ($CtsBL^{-/-}$) and cathepsin D ($CtsD^{-/-}$) were transfected with DIRC2-3xmyc. Controls were DIRC2 expressed in HeLa and wild-type MEF. Cells were harvested 48 hours after transfection. Aliquots of cell lysates (20 µg protein) of each sample were subjected to SDS-PAGE followed by Western blot detection. The full length DIRC2 and its C-terminal fragment (detected by anti-myc antibody) are shown by closed and opened arrow heads, respectively. There was no proteolytic fragment of DIRC2 observed when DIRC2 was expressed in either cathepsin L single deficient or cathepsin B and L double deficient MEF (upper panel). Lower panels confirm the absence or presence of respective cathepsins in different cell-lines.

It has been described above that overexpression of human DIRC2 in cathepsin L deficient MEFs prevents the processing of DIRC2. It is to be expected that endogenous DIRC2 is not processed in murine tissue deficient in cathepsin L. Murine DIRC2 has a similar

sequence to human DIRC2 with about 95% identity. The sequence of synthetic oligopeptide used to generate anti human DIRC2 antibody in rabbit (-G_2SRWSSEEE RQPLLGPGLG PGLG$_{24}$-, Figure 3.1 A) was very similar to the N-terminal sequence of mouse DIRC2 (-G_2SGWSSEEE ERQPLLGPGL GPAP$_{24}$-) so that a cross-reactivity of the antibody against hDIRC2 with murine DIRC2 was expected. In order to investigate whether endogenous DIRC2 in cathepsin L knockout mouse was also proteolyzed, lysosome-enriched fractions from mouse liver was analyzed by Western blot. The lysosome-enriched samples (tritosomes) were obtained from Dr. Markus Damme (University of Goettingen) and were prepared by injecting tyloxapol (Triton WR1339) into mice 4 days prior to sacrifice. This treatment alters the density of mouse lysosomes and facilitates an easy separation of highly-enriched lysosomes from the lysates of mouse livers. Details of this preparation were recently published (Damme et al 2010).

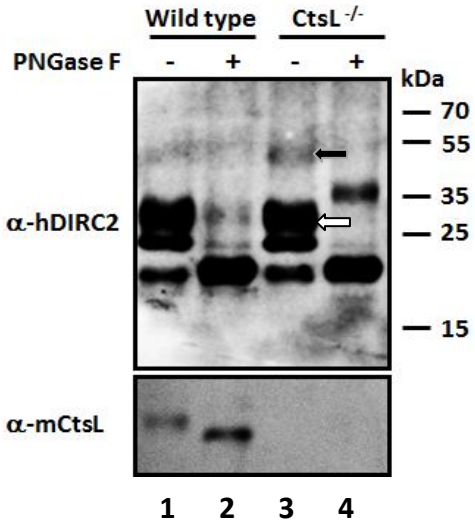

Figure 3.13 Expression of endogenous mouse DIRC2 in wild-type and CtsL$^{-/-}$ mouse liver.
Lysosome-enriched liver lysates (tritosomes) of wild-type mouse and mouse deficient in cathepsin L livers were provided by Dr. Markus Damme (University of Goettingen). Aliquots of untreated and PNGase F treated tritosomes (1.5 µg protein) were subjected to SDS-PAGE separation and Western blot analysis. Blot was detected by anti-hDIRC2 which also recognized murine DIRC2. Full length murine DIRC2 was hardly detected in wild-type mouse liver tritosomes (lane 1), whereas in CtsL$^{-/-}$ mouse liver tritosomes a small fraction of DIRC2 was detectable (lane 3, shown by a closed arrow). In both wild-type and CtsL$^{-/-}$ mouse liver, their bulk of DIRC2 was present at a cluster of bands with an apparent molecular weight of 30 kDa (open arrow) that shifted to a band of about 20 kDa upon PNGase F digestion (lane 2 and 4, respectively). The PNGase F digested full length DIRC2 from CtsL$^{-/-}$ mouse liver was represented in a band of about 40 kDa (lane 4). The presence and the absence of cathepsin L in the wild-type and knockout mouse liver, respectively, were shown by detection with anti-mouse cathepsin L (lower panel).

Unlike the result shown by overexpressing of human DIRC2 in MEF cells deficient in cathepsin L, DIRC2 was proteolyzed to a significant degree and only a small amount of full length DIRC2 appeared in endogenous CtsL$^{-/-}$ mouse liver (Figure 3.13 lane 3 shown by opened and closed arrows, respectively). Both full length and processed forms of mouse DIRC2 were shifted to bands of about 40 and 20 kDa upon PNGase digestion, respectively (lane 4). In contrary, lysosome-enriched fractions from wild-type mouse liver showed very few or no full length DIRC2 (lane 1). The bulk N-terminal fragment of DIRC2 from wild-type mouse was shifted from 30 kDa to 20 kDa upon PNGase F digestion (lane 1 and 2, respectively). There was no observable PNGase F digestion product of full length DIRC2. The fact that DIRC2 processing in CtsL$^{-/-}$ mouse liver is only slightly impaired indicates that the role of cathepsin L in the proteolysis of DIRC2 in CtsL$^{-/-}$ liver may be compensated by one or more unknown proteases.

3.9 Rescue of DIRC2 proteolysis by coexpression of cathepsin L in cathepsin deficient MEF

In order to substantiate the role of cathepsin L in the proteolysis of DIRC2, a rescue experiment was undertaken. Human DIRC2-3xmyc was co-expressed with mouse CtsL cDNA in CtsL$^{-/-}$ MEF. Mouse CtsL cDNA was cloned in the pcDNA3.1 vector and used in co-transfection experiment. Co-expression of DIRC2-3xmyc together with mCtsL in CtsL$^{-/-}$ MEF showed that mCtsL had the ability to rescue the proteolysis of DIRC2 (Figure 3.14 lane 2). The rescue of DIRC2-3myc proteolysis by co-expression of mCtsL was abolished in the presence of cathepsin L inhibitor Z-FY-CHO (Figure 3.14 lane 3), in spite of expression of mCtsL (lower panel).

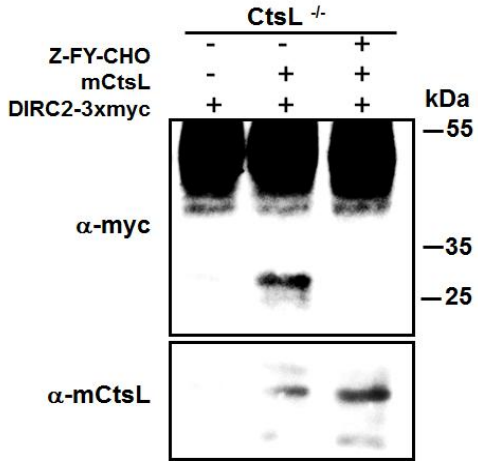

Figure 3.14 Rescue of DIRC2 processing in cathepsin L deficient MEF.

Murine cathepsin L cDNA was inserted in a mammalian expression vector pcDNA3.1/Hygro+. Cathepsin L deficient, $CtsL^{-/-}$ MEF cells were transfected with DIRC2-3xmyc; DIRC2-3xmyc and murine cathepsin L, mCtsL; DIRC2-3xmyc and mCtsL in the presence of 40 μM cathepsin L inhibitor Z-FY-CHO (lane 1, 2, and 3, respectively). Cells were harvested 48 hours after transfection. Aliquots of cell lysates (20 μg protein) were separated in 10% gel SDS PAGE and transferred onto nitrocellulose membrane. DIRC2 expression was detected by an anti-myc antibody. Rescue effect of co-expression of human DIRC2 and mouse cathepsin L was shown by presence of a DIRC2 C-terminal fragment of 25 kDa (lane 2). Transient mouse cathepsin L expression was detected by anti-mCtsL antibody (lower panel).

3.10 Determination of the DIRC2 cleavage site

The initial Western blot data showed that DIRC2 was fragmented into two-halves approximately in the middle region of the protein (Figure 3.2 and 3.5). It was also determined that the N-terminal fragment of DIRC2 contains a sugar moiety, reflecting that the proteolysis site must be located after N_{209} (Figure 3.1). In addition, Figure 3.5 showed that cleavage of DIRC2 was independent of its glycosylation. In order to identify the cleavage site within DIRC2, several DIRC2 mutants were constructed, overexpressed in HeLa cells and analyzed by immunofluorescence and Western blot. Two DIRC2-3xmyc constructs with internal hemagglutinin (HA) tags, DIRC2-HA_{214}-3xmyc and DIRC2-HA_{261}-3xmyc, respectively, were generated and expressed in HeLa cells. The HA tags were inserted in the down-stream position of N-glycosylation site (loop 5) and in the middle of loop 6 for DIRC2-HA_{214}-3xmyc and DIRC2-HA_{261}-3xmyc constructs, respectively (Figure 3.1. C). Expression of the both internal HA constructs revealed similar protein bands for both full length and processed form

of DIRC2, detected either with anti-hDIRC2 and anti-myc (Figure 3.15 A, left and right panels, respectively). These bands were also similar to the expression of wild-type DIRC2-3xmyc. However, detection of the same blot with anti-HA antibody shows that, additionally to the full length DIRC2, DIRC2-HA_{214}-3xmyc had a fragment of the same molecular weight as the N-terminal fragment of DIR2 (Figure 3.15, middle panel; N-terminal fragment is shown by asterisk), whereas DIRC2-HA_{261}-3xmyc had a fragment of the same molecular weight as the C-terminal fragment of DIRC2. This result suggests that the amino acid residues 214 and 261 are part of the N- and C-terminal fragment of DIRC2, respectively. Consequently, the fragmentation of DIRC2 seems to occur between amino acids 214 and 261.

According to the predicted topology of DIRC2 (Figure 3.1 B and shown in 3.15 B), the amino acid 214 is located in the loop 5 of DIRC2. Loop 5 and loop 6 of DIRC2 are located in the lumen of lysosomes and in the cytosol, respectively. It has been shown that lysosomal cysteine protease cathepsin L is critical for processing of DIRC2. It is therefore reasonable to consider that the processing of DIRC2 takes place in the loop 5 where lysosomal cathepsins are able to exert their function. To test this hypothesis, three alanine mutants were generated (DIRC2-6A1-3xmyc, DIRC2-6A2-3xmyc and DIRC2-6A3-3xmyc, Figure 3.15 B), expressed in HeLa cells and analyzed by Western blot and immunofluorescence. Whereas the first two mutants (DIRC2-6A1-3xmyc and DIRC2-6A2-3xmyc) showed similar band patterns to that shown for wild-type DIRC2 (Figure 3.15 C lane 1 and 2, respectively), the mutant with alanine substitution close to the TM6 segment (DIRC2-6A3-3xmyc mutant) was present mainly as full length precursor (lane 3). The appearance of this full length precursor suggests an ER-localization, since no cluster of band as in the case of fully glycosylated full length DIRC2 was observed. Figure 3.15 D confirmed that this mutant hardly localized to lysosomes, and instead localized to the ER (lysosomes and ER were detected by anti-LAMP-2 in the upper panel and anti-KDEL in the lower panel, respectively). This result suggests the critical role of the boundary region between loop 5 and the TM6 of DIRC2 for lysosomal targeting (and hence processing of DIRC2). The ER localization of this mutant may also be attributed to the significance of the boundary region of loop 5 and TM6 for proper folding of protein or to pass the quality control function of ER.

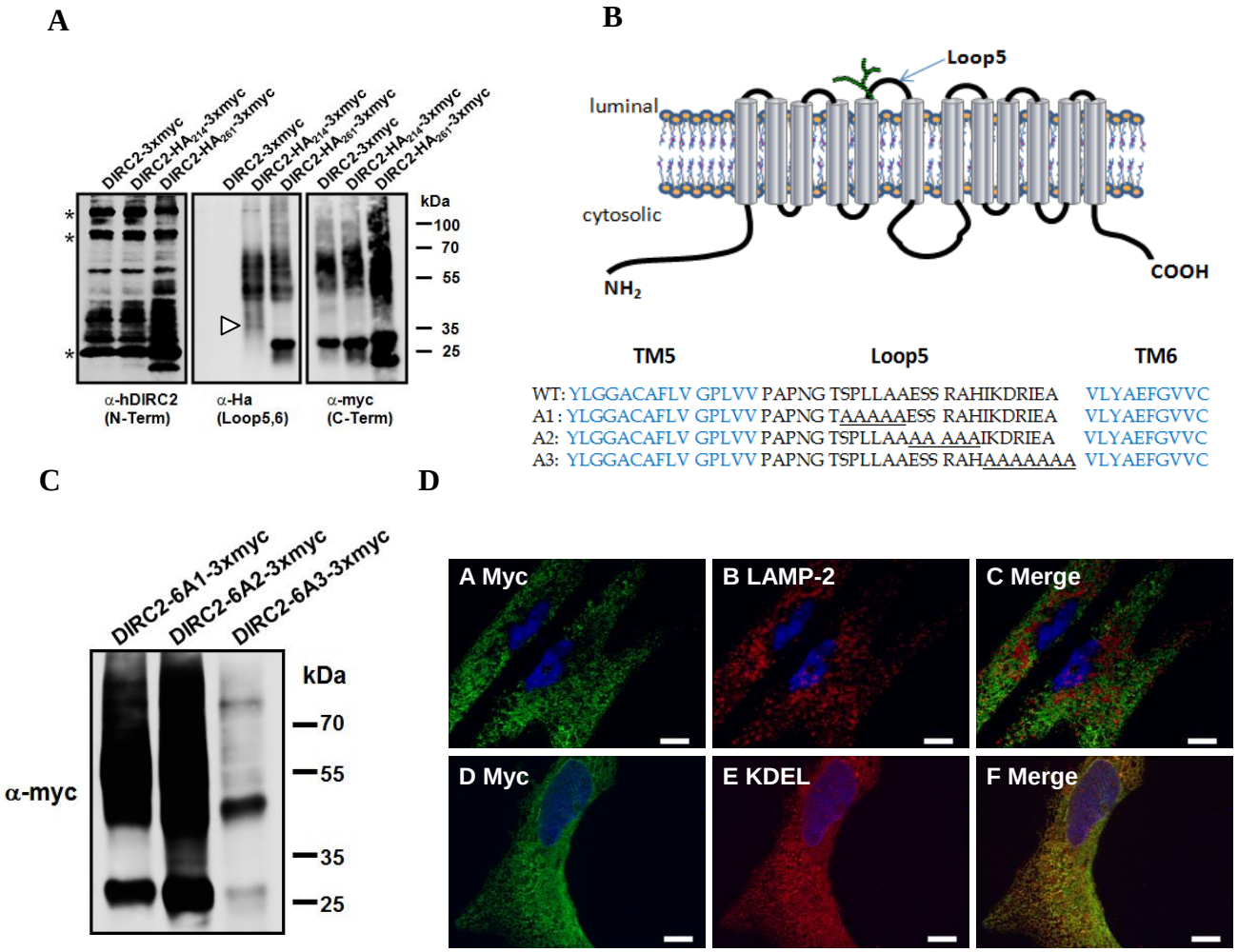

Figure 3.15 Expression of internal HA-tagged and alanine mutants of DIRC2.

(A) Two internally HA-tagged DIRC2 appended with 3xmyc constructs, DIRC2-HA_{214}-3xmyc and DIRC2-HA_{261}-3xmyc were expressed in HeLa cells. Cells were harvested 24 hours after transfection and lysates (20 µg protein) were subjected to SDS-PAGE separation and Western blot analysis. Blot was detected with anti-hDIRC2, anti-HA, and anti-myc. Arrow head (middle figure) shows the N-terminal fragment of DIRC2 whereas cluster of bands in the left figure show N-terminal half of DIRC2 detected by anti-hDIRC2. Asterisks show unspecific bands.

(B) Amino acids in the loop 5 of DIRC2 were replaced by three short alanines sequences designated as DIRC2-6A1-3xmyc, DIRC2-6A2-3xmyc and DIRC2-6A3-3xmyc.

(C) The three alanines mutants were transfected into HeLa cells. Cells were harvested 24 hours after transfection. Lysates (20 µg protein) were subjected to SDS-PAGE and Western blot analysis. Blot was detected with anti-myc antibody. The full length DIRC2 forms of DIRC2-6A1-3xmyc and DIRC2-6A2-3xmyc appear as strong and difused bands at about 55 kDa (lane 1 and 2). The full length, ER-form of DIRC2-6A3-3xmyc shown by a band at about 50 kDa was the predominant form over they processed form.

(D) DIRC2-6A3-3xmyc mutant analyzed by immunofluorescence. In the majority of transfected cells, DIRC2 localized to ER as shown by detection of KDEL (lower panel) and not localized to lysosomes as shown by detection of LAMP-2 (upper panel). Bars represent 10 µm.

3.11 Overexpression of GFP-tagged DIRC2 and formation of enlarged/clustered lysosomes

3.11.1 Overexpression of DIRC2 in mammalian cells lead to the formation of enlarged and/or clustered of acidic compartments

In an initial attempt to reveal a possible function of DIRC2, GFP-tagged constructs of DIRC2 were overexpressed in different cell-lines and analyzed by immunofluorescence. It was revealed that expression of C-terminally GFP-tagged DIRC2 (DIRC2-GFP, Figure 3.1) led to formation of enlarged or clustered acidic organelles in Cos7, HeLa and HEK293 cells, as detected by lysotracker (Figure 3.16, shown by arrow heads). Similar effect was also revealed by N-terminally GFP-tagged DIRC2 (GFP-DIRC2). This result underlines that enlargement or clustering of acidic organelles induced by overexpression of GFP-tagged DIRC2 does not depend on the position of the GFP tag.

3.11.2 Effects of bafilomycin A1, vinblastine and Rab5 on the DIRC2-GFP driven enlargement of acidic organelles

To investigate whether acidification of organelles is a prerequisite for the enlargement or clustering of organelles, Cos7 cells transfected with DIRC2 were treated with 20 nM bafilomycin A1, an inhibitor of vacuolar-type H^+-ATPase (V-ATPase) (Droese and Altendorf 1997). V-ATPase is the proton pump protein responsible for the proton transport into lysosomes and inhibition of V-ATPase prevents the acidification of lysosomes. It is shown in Figure 3.1.3 (A-F) that the formation of large organelles or cluster of organelles is apparently not affected by the administration of bafilomycin A1. Prolonged treatment with bafilomycin A1 up to more than 24 hours or increased concentration of bafilomycin up to 200 μM did not change the enlarged vacuole formation (data not shown). This result suggests that lysosome acidification is not required for the vacuolation or organelle clustering.

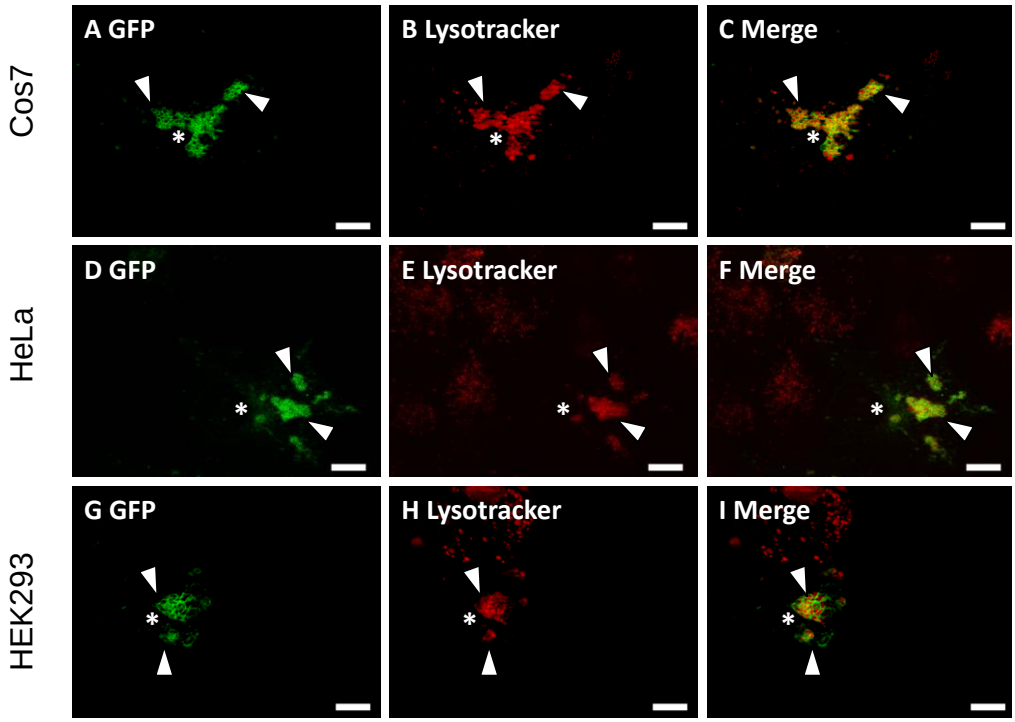

Figure 3.16 Overexpression of DIRC2-GFP.

Cos7, HeLa and HEK293 cells were transfected with DIRC2-GFP and fixed after 24 to 36 hours. Prior to fixation, cells were incubated with lysotracker (in plain DMEM). Distribution of DIRC2-GFP and acidic organelles as indicated by the accumulation of lysosomes was visualized by fluorescence microscopy. Figure A-C, D-F and G-I show the overexpression of DIRC2-GFP in Cos7, HeLa and HEK293 cells, respectively. Arrow heads show the clustered organelles. Transfected cells are marked with asterisks. Bars represent 10 µm.

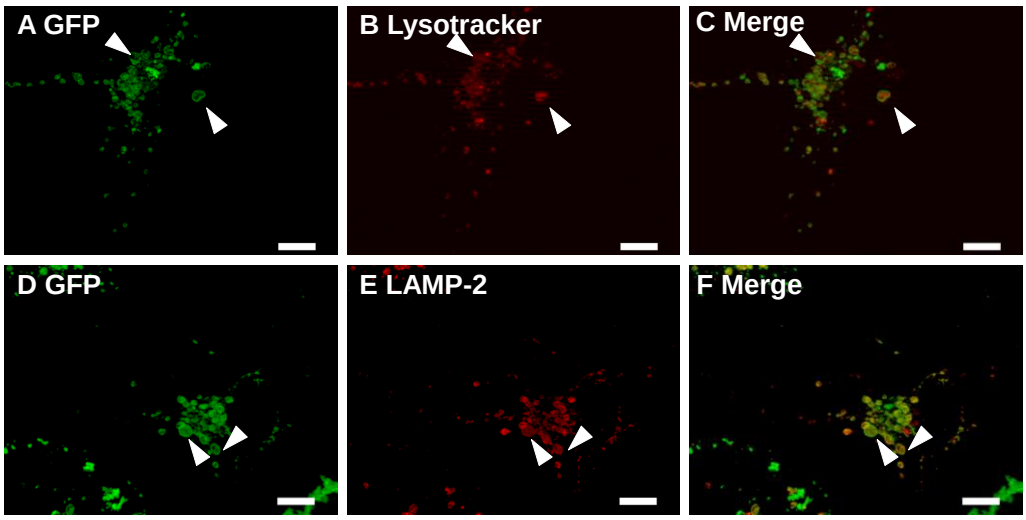

Figure 3.17 Large acidic organelle formations upon overexpression of GFP-DIRC2.

Cos7 cells were transfected with N-terminally GFP-tagged DIRC2 (GFP-DIRC2, Figure 3.1 C). Cells were fixed two days after transfection. Acidic organelles were detected with lysotracker (B-C), and lysosomes were stained with anti-LAMP-2 followed by a fluorophore conjugated secondary antibody (E-F). Bars represent 10 µm.

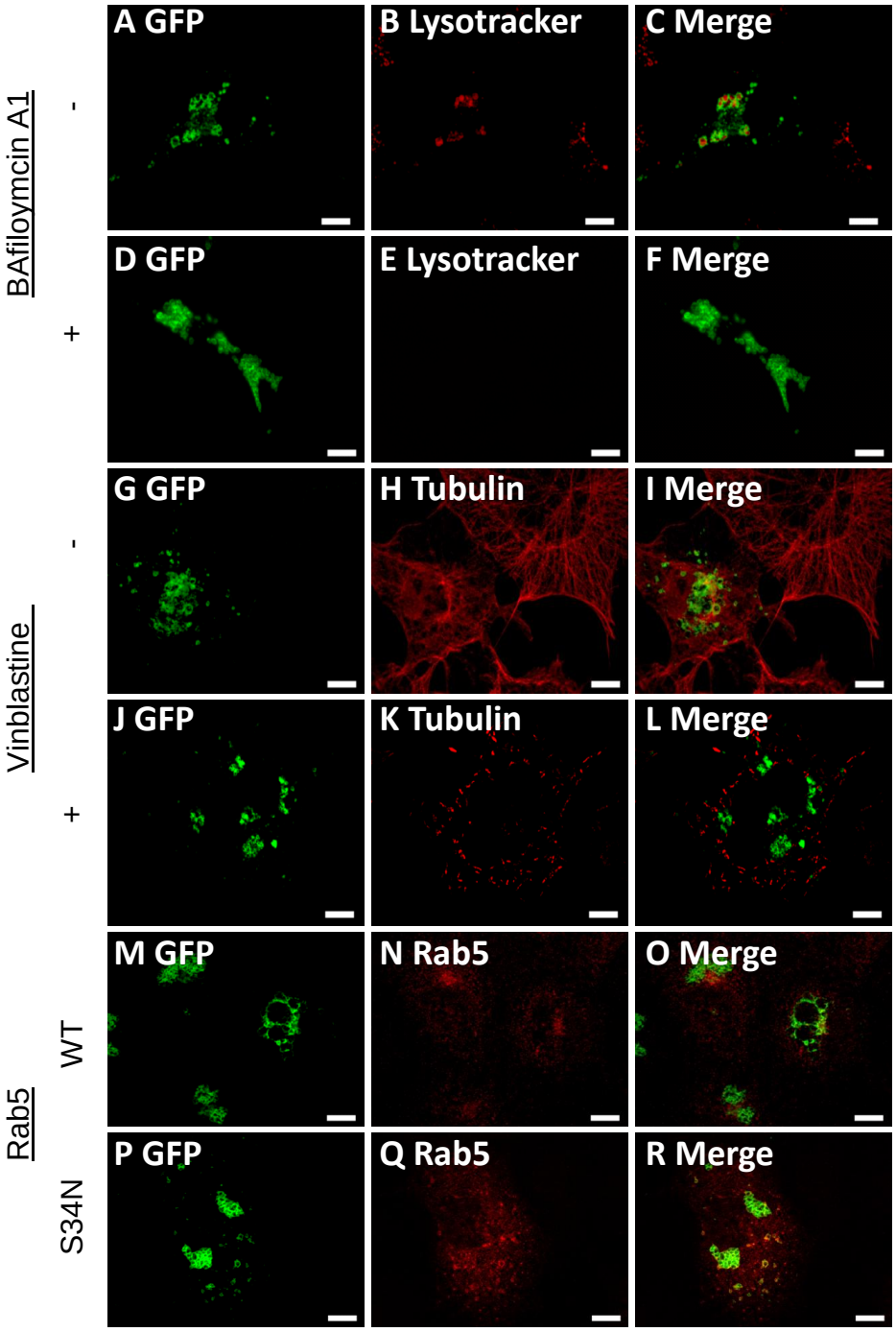

Figure 3.18 Effect of bafilomycin A1, vinblastine and Rab5 on the formation of large organelles.
Cos7 cells were transfected with DIRC2-GFP. Acidic organelles were detected with lysotracker in the absence of bafilomysin A1 (A-C) or in the presence of 20 nM bafilomycin A (D-F). Bafilomycin was added 3 hours prior to fixation. Depolymeration of tubulin is visualized by anti-tubulin antibody (K, L). G-I are untreated controls, whereas J-L are cells treated with 50 μM vinblastine 3 hours prior to fixation. Effects of co-expression of DIRC2-GFP with the wild-type Rab5 and dominant negative form of Rab5 (Rab5S34N) are shown in M-R. Both wild-type Rab5 and Rab5S34N were detected by anti-Rab5 antibody followed by Alexa fluor 594 conjugated secondary antibody. Bars represent 10 μm.

It has long been known that distribution or movement of lysosomes within a cell can be interfered by drugs or chemicals acting on microtubule or cell skeleton. One of these drugs is vinblastine, a chemotherapeutic agent used to treat numerous cancers, such as Hodgkin´s disease and testicular germ-cell cancer (Jordan and Wilson 2004). It acts by binding tubulin, thereby preventing the assembly of microtubules.

In order to check whether the administration of vinblastine has an effect to the formation of enlarged or clustered organelles, DIRC2-GFP transfected Cos7 cells (Figure 3.1. C) were incubated with 50 µM vinblastine 3 hours prior to fixation. It is shown in the Figure 3.18 that treatment of the cells with 50 µM vinblastine had no obvious effect on the vacuolation, indicating that the vacuolation and organelle cluster formation does not depend on the integrity of microtubules.

Kuronita et al (Kuronita et al 2002) have reported that co-expression of LIMP-2 with the dominant negative form of small GTPase Rab5 can abolish the formation of large endosome/lysosomes compartment induced by overexpression of LIMP-2. It was emphasized that the GTP-bound form of Rab5 is important for the formation of large endosome/lysosome. Therefore, it was tested whether co-expression of the dominant negative form of Rab5 can also interfere with the formation of enlarged or clustered vacuoles induced by the overexpression of DIRC2. Figure 3.18 P-R shows that co-expression of DIRC2-GFP with Rab5S34N allowed the formation of cluster of organelles, similar to the result obtained by co-expression of wild-type Rab5 (M-O), thus indicating that the formation of enlarged or clustered of organelles is independent of Rab5.

4. Discussion

4.1 DIRC2 is a novel lysosomal protein

From its first report (Bodmer et al 2002), DIRC2 has readily been predicted from its sequence to be a member of the major facilitator superfamily. However, the cellular localization of DIRC2 was not resolved. In a further work by Schroeder (Schroeder et al 2007), DIRC2 was identified as a putative member of lysosomal membrane proteins. By using an indirect immunofluorescence and subcellular fractionation, it was demonstrated that DIRC2 is a lysosomal/late endosomal protein. This protein was shown to colocalize with lysosomal associated membrane protein type 2 (LAMP-2) and β-glucocerebrosidase (βGC), as well as with a late endosomal lipid lysobiphosphatidic acid (LBPA) in immunofluorescence analysis. In addition, DIRC2 was co-sedimenting with LAMP-2, βGC and cathepsin D in subcellular fractionation experiments.

Like many other lysosomal membrane proteins, lysosomal targeting of DIRC2 was found to rely on a well known dileucine motif [DE]XXXL[LI] at its N-terminus. Two putative tyrosine-based lysosomal sorting motifs YXXØ are also identified at the C-terminus of DIRC2, but they were shown to be irrelevant for lysosomal targeting of DIRC2 (Dr. Schroeder, unpublished results). Most dileucine motifs of lysosomal proteins are located in close proximity (around 6 to 11 residues) to a transmembrane domain (Bonifacino and Traub 2003). The short distance is thought to be important for the interaction between the dileucine signals with adaptor proteins (APs) which later forms complexes with clathrin. However, the dileucine motif in DIRC2 is 37 residues apart from the adjacent transmembrane segment. It is conceivable that interaction of the dileucine motif of DIRC2 with an AP complex is facilitated by a lipid modification. An example of this facilitation mechanism has been reported for mucolipin-1 which undergoes palmitoylation that promotes its endocytosis. Lipid modification exemplified here is thought to bring peptide sorting signals closer to the membrane (Vergarajauregui and Puertollano 2006, Braulke and Bonifacino 2009). Indeed, DIRC2 has a putative myristoylation modification site at Gly-2 which may help to activate the dileucine signal. However, experimental evidence is required to validate this presumption.

In a preliminary study, overexpression of GFP-tagged constructs of DIRC2 in different cell lines led to formation of enlarged and/or clustered lysosomes. These morphological alterations were shown to be independent of lysosomal acidification, integrity of microtubules or active form of Rab5. However, overexpression of DIRC2 with a triple myc tag showed no enlargement and/or clustering of lysosomes. It is likely that the formation of enlarged and/or

clustered lysosomes resulting from overexpression of GFP-DIRC2 constructs was mainly caused by the appended GFP tags, although the mechanism is not clear.

4.2 DIRC2 is a glycoprotein

DIRC2 was demonstrated to be a glycoprotein with N-glycosylation of Asn-209. It was also shown that DIRC2 acquires its core glycan moiety in the ER which is further processed in a post ER compartment. It has been reported in an N-glycosylation scanning study that arginine residues require a minimum distance of 12-14 residues to the membrane to be efficiently used for glycosylation or, in the context of polytopic membrane proteins, the loop segments must be longer than 30 residues in order to harbor N-glycans (Cheung and Reithmeier 2007). According to the predicted topology, the N-glycosylation site of DIRC2 (Asn-209) is located in close proximity to the transmembrane segment in loop5 which is predicted to consist of only 16 residues. This may imply that the algorithm used to predict the protein topology may not precisely define the transmembrane and loop segments of DIRC2. It could also imply that the short glycosylation site distance to the closest transmembrane segment of DIRC2 is an exception from the general rule derived from the N-glycosylation scanning study described above. In comparison, a newer protein structure prediction software, I-TASSER (Zhang 2008; Roy et al 2010), would predict the N-glycosylation motif of DIRC2 to be located in the middle region of its putative loop5 (Figure 4.1). However, the overall topology of DIRC2 described in this study is supported by the luminal residence of Asn-209 as well as cytosolic localization of the dileucine targeting motif at the N- terminus (Figure 3.1 B).

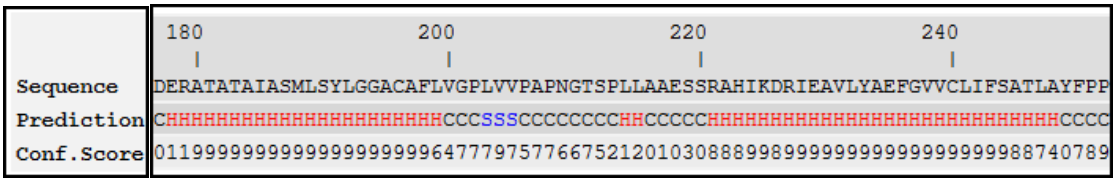

Figure 4.1 Secondary structure prediction of DIRC2 generated by I-TASSER program.

An alternative bioinformatics analysis of DIRC2 generated by I-TASSER program (http://zhanglab.ccmb.med.umich.edu/, Zhang 2008, Roy et al 2010) shows that the putative N-glycosylation site Asn-209 is located approximately in the middle of two hydrophobic stretches corresponding to TM5 and TM6 of DIRC2. (Legends: C = coil, H = helix, S = scramble, Conf. Score = confidence score range from 0 to 9).

The unusual large carbohydrate moiety attached to Asn-209 of DIRC2 resembles that observed in the GLUT8 protein, a membrane protein of twelve transmembrane spanning domains. GLUT proteins are known to play a role in glucose/fructose transport across the membrane. Unlike its related proteins such as GLUT1-4 which were reported to localize in plasma membranes, GLUT8 was identified to localize in late endosomes/lysosomes. An apparent molecular weight shift of more than 10 kDa was reported upon PNGase digestion of GLUT8 which has only one N-linked glycosylation site in a loop between transmembrane 9 and 10 (Augustin et al 2005). By the use of brefeldin A1, it could be shown DIRC2 acquires its core N-glycan in the ER and this glycan is further modified in a post-ER compartment.

4.3 DIRC2 is proteolytically processed

Lysosomes are known to be the degradation compartment of many macromolecules. This function is carried out by hydrolases within the lumen of lysosomes. Lysosomes are also the site for degradation of many plasma membrane proteins, including transporter proteins, after endocytic internalization (Schulze et al 2009). In this study, DIRC2 was shown to be proteolyzed in lysosomes. In the context described above, processing of DIRC2 in lysosomes may theoretically be regarded as the beginning of total degradation of DIRC2 proteins after serving their so far unknown function. However, since both overexpressed and endogenous DIRC2 showed an enormous stability in lysosomes, it seems likely that the observed processing of DIRC2 might represent a limited processing event rather than degradation. Moreover, the data in this study also revealed that endogenous DIRC2 was almost exclusively present in its proteolyzed form.

Many examples of proteolytic events have recently been reported for numerous membrane proteins, including transporter proteins. Specific proteolytic cleavage of membrane proteins may negatively or positively modulate their functions. Glycine transporter 2 (GlyT2) for example, a member of of Na^+/Cl^- -dependent plasma membrane transporters, which exhibits a cytoplasmic N-terminus that is at least three times longer than that of other members of neurotransmitter transporter family (Liu et al 1993), is cleaved by calpain proteases. The main cleavage site of this transporter protein is located in the N-terminal segment, and the remaining transmembrane fragment of the cleavage has a molecular weight of 70 kDa which is similar to other members of this protein family. The truncated GlyT2 displays full transport activity and it was suggested that the processing may contribute to the regulation of GlyT2

trafficking and/or function in the neuronal plasma membrane (Baliova et al 2004). Toll-like receptor 9 (TLR9), a pattern-recognition receptor localized in lysosomes/late endosomes, was reported to acquire its function and trigger signaling cascades activity in truncated form, although the full-length of TLR9 also exhibits significant activity. Cathepsin L and additional lysosomal proteases were suggested to be involved in the processing of TLR9 (Park et al 2008).

The current understanding of MFS proteins is deduced from high resolution structural data obtained for the lactose permease (LacY) (Abramson et al 2003) and the *E. coli* glycerol-3-phosphate transporter (GlpT) (Huang et al 2003). Structural analysis of MFS proteins has revealed that the 12 transmembrane domains of MFS proteins are clustered into two halves of 6 transmembrane-domains. The two clusters are pseudo-symmetric to each other with a pore between the two halves which is essential for substrate binding (Law et al 2008). In the case of LacY, it was demonstrated that the continuity of the polypeptide chain of the MFS protein is not essential for its activity. The two clusters of LacY can be expressed separately as non-overlapping fragments and they are capable of reconstituting its transport activity comparable to the wild type protein (Weinglass and Kaback 2000). In addition, many studies have shown that the substrate binding site and the catalytic site of MFS proteins are largely determined by charged side chains of amino acid residues within transmembrane domains (reviewed by Law et al 2008). This may explain the persistent activity of discontinous clusters of LacY. Among MFS proteins, DIRC2 is the first protein reported to undergo proteolysis. While the function of DIRC2 is currently unknown, the need for (or the consequence of) DIRC2 proteolysis remains still illusive. Taken together, the enormous stability of proteolytic fragments of DIRC2 in lysosomes and the fact that MFS protein, as exemplified by LacY protein, may preserve it activity as discontinuous fragments, proteolytically processed DIRC2 may possess transport activity.

4.4 Cathepsin L is involved in the processing of DIRC2

In order to answer the question where the proteolysis of DIRC2 takes place and which protease(s) play(s) a role in the proteolysis of DIRC2, DIRC2 was overexpressed in HeLa cells in the presence or absence of different types of inhibitors. It is demonstrated that treatment of transfected HeLa cells with NH_4Cl was able to prevent DIRC2 processing. NH_4Cl is known to interfere with lysosomal acidification (Misinzo et al 2008). This result,

together with the data obtained from subcellular fractionation analysis, demonstrated that processing of DIRC2 is likely to take place in lysosomes.

Inhibitory profiling of DIRC2 fragmentation with E-64, an inhibitor of cysteine proteases, revealed that DIRC2 is likely to be processed by this class of proteases. The possible involvement of cathepsin B and cathepsin L, two major lysosomal cysteine proteases, was investigated by addition of CA-074-Me and Z-FY-CHO, respectively, to HeLa cells transfected with DIRC2. It could be revealed that both cysteine protease inhibitors were able to prevent proteolysis of DIRC2.

Historically, it has been commonly believed that lysosomal cathepsins may have common substrates. However, more recent findings indicated non-redundant functions of individual cathepsins (Roth et al 2000, Nagler and Menard 2003, Brix 2005). TRP-ML1, a lysosomal monovalent cation channel was reported to undergo proteolytic cleavage which was impaired by inhibition of cathepsin B (Kiselyov et al 2005). The pore-forming protein perforin precursor was reported to be activated by proteolytic cleavage, in part, by cathepsin L but not by cathepsin B (Konjar et al 2010). A further dissection of the role of cathepsin B and cathepsin L in the processing of DIRC2 was carried out by overexpressing human DIRC2 in cathepsin deficient MEFs. In contrast to the result described from the inhibitory profiling of DIRC2 processing, expression of DIRC2 in cathepsin deficient MEFs showed that cathepsin L, but not cathepsin B, is involved in the processing of DIRC2. This divergent observation is most likely due to an overlapping specificity of cathepsin B inhibitor CA-074-Me (Ebert et al 2002, Montaser et al 2002).

The sensitivity of DIRC2 to Z-FY-CHO treatment and the fact the DIRC2 is not proteolyzed in cathepsin L deficient MEF underlined the critical role of cathepsin L in the processing of DIRC2. However, it was revealed that only small amounts of DIRC2 remain unprocessed in livers of cathepsin L deficient mice. This result indicated that the role of cathepsin L in the processing of DIRC2 in mice liver is compensated by unknown proteases which are either absent or inactive in MEF cells. The fact that individual cathepsins contribute to certain functions in a tissue and cell type specific manner is highlighted by the proteolysis of invariant chain (li) which plays a role in the targeting of MHCII complexes in the thymus and antigen-presenting cells. In cathepsin L deficient mice, the role of cathepsin L in the processing of li in peripheral antigen-presenting cells such as dendritic cells, B-lymphocytes and macrophages is compensated by cathepsin S and cathepsin F which results in no

impairment of li processing in these cell types in cathepsin L deficient mice (Reinheckel et al 2001).

4.5 Cleavage site of DIRC2

To address the question where exactly DIRC2 is cleaved, several mutants of DIRC2 were generated and expressed in HeLa cells. The fragmentation pattern of overexpressed wild type DIRC2 and the $N_{209}A$ mutant as well as the pattern of DIRC2 after PNGase F digestion indicated that DIRC2 is cleaved asymmetrically. Insertion of HA tags adjacent to residue 214 and residue 261 within loop5 and loop6, respectively, more specifically showed that fragmentation of DIRC2 takes place between these two residues. Inhibitory profiling of the proteases involved in the processing of DIRC2 showed the important role of cathepsin L, a cysteine protease localized within the lumen of lysosomes.

Together, the above described results narrowed down the likely cleavage site of DIRC2 within its loop5. According to the predicted DIRC2 topology, loop5 is limited by residues 210 to 229 connecting TM5 and TM6. As it would be expected for a cysteine protease, cathepsin L may cleave diverse peptide sequences. Nevertheless, a number of studies involving positional scanning synthetic combinatorial libraries (PS-SCL) of protease substrates have analyzed the preference cleavage sites of cathepsin L (examples are given in Table 4.1).

One possible cleavage site within the loop5 by cathepsin L is the peptide bond between two alanine residues (-A_{216}-A_{217}-). Two leucine residues at the P2 and P3 positions are among the preferred target sites of cathepsin L (Choe et al 2006). However, mutation of amino acid at these positions with alanines in A1 mutant (A1: $_{211}$-TSPLLAAESS-$_{220}$ → $_{211}$-TAAAAAAESS-$_{220;}$ Figure 4.2) did not alter the processing of DIRC2. Oligopeptide sequence with an Arg at position P1` was reported to be a potential cleavage site for cathepsin L (Table 4.1; Melo et al 2001). Mutation of Arg-221 along with 3 amino acids at N-terminal of Arg-221 in the A2 mutant (A2: $_{216}$-AAESSRAH-$_{223}$ → $_{216}$-AAAAAAAAH-$_{223;}$ Figure 4.2) did also not prevent proteolysis of DIRC2. Both mutants are shown to be localized in lysosomes and processed by cathepsin L.

Interestingly, substitution of a short luminal sequence directly bordering loop5 and TM6 with oligo-alanines resulted in a DIRC2 mutant (A3: $_{224}$-IKDRIEA-$_{230}$ → $_{224}$-

AAAAAAA-$_{230;}$ Figure 4.2) which is partially localized in ER and lysosomes. Oligopeptide sequence with Lys and Arg in the position P3 and P1, respectively, are preferable for cathepsin L cleavage. However, Asp and Glu at position P2 and P1´ are not favorable for cathepsin L digestion (Puzer et al 2004, Choe et al 2006). The fraction which reaches lysosomes is still processed in this compartment. In contrast, the fraction which is retained in the ER is not processed. An ER localization was also observed for the DIRC2 mutant where its TM6 sequence was replaced with a comparable TM6 sequence from an unrelated lysosomal MFS member CLN7 (data not shown). These results nevertheless underlined the critical role of amino acid residues bordering the TM6 for lysosomal localization or correct folding and membrane insertion of DIRC2.

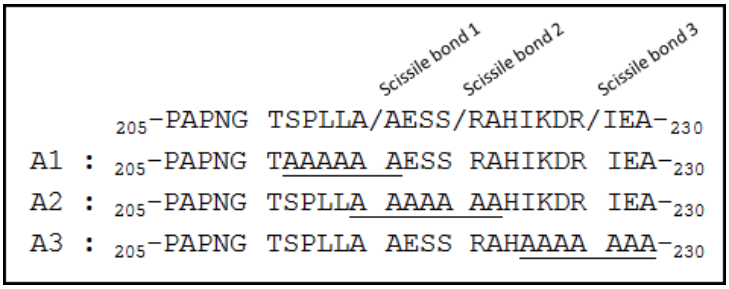

Figure 4.2 Sequence of loop5 of DIRC2 and alanine scanning mutants.
The sequence of loop5 of DIRC2 with predicted cleavages sites. Three alanine scanning mutation (A1, A2 and A3) used to analyse the cleavage site of DIRC2 are depicted.

Table 4.1 Combinatorial substrate analyses of cathepsin L.
Cleavage sequence preferences of human cathepsin L generated by positional scanning synthetic combinatorial libraries (PS-SCL) studies (adapted from http://merops.sanger.ac.uk/). Positions of amino acid residues are indicated by P4 to P1 and P1´to P4´ for amino acid residues at the N- and C-terminal from scissile sites and cleavages are taken place between P1 and P1´.

Specificity from combinatorial peptides								Optimal substrate	Note/reference
P4	P3	P2	P1	P1´	P2´	P3´	P4`		
-	-	-	-	R/A/K	-	-	-	XXXX/RXXX	Melo et al 2001
-	K/R	F	R	H/S	S/H	-	-	XKFR/HSXX	Puzer et al 2004
H/broad	K/R/M/L	F/W/Y	R/K	-	-	-	-	HKFR/XXXX	Choe et al 2006

4.6 Putative function of DIRC2

Upon downregulation of DIRC2 with siRNAs in HeLa cells, no alterations in lysosomal enzyme activities or expression of lysosomal proteins was observed (Figure 3.8) was observed. In a collaborative work with Prof. Bruno Gasnier (CNRS Paris), it was suggested that DIRC2 may function as an electrogenic metabolite transporter. The experimental set-up led to this conclusion is described as follows: the dileucine mutant of DIRC2 was expressed in *Xenopus oocytes* which allows a plasma membrane expression of the full length form of DIRC2. Electrophysiological transport activity was detected by two-electrode voltage clamp applied on the *oocytes* in an acidic medium (pH 5.0) which was supplemented with a metabolic mixture (Bacto Yeast Extract, BYE). Application of this metabolic mixture induced a significant outward current. Since the extracellular medium is topologically equivalent to the lysosomal lumen in a whole cell set up, DIRC2 might facilitate transport of anions from lysosomes or exchange cations from the cytosol into lysosomes (Figure 4.3).

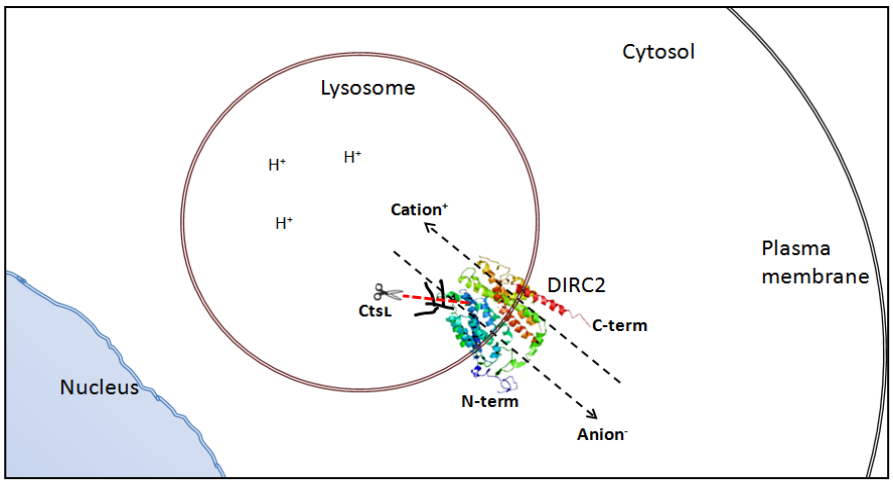

Figure 4.3 Putative role of DIRC2 as an electrogenic metabolite transporter.
A possible transport function of DIRC2, as described in the text, was analyzed by expression of a dileucine mutant of DIRC at the plasma membrane of *Xenopus oocytes*. An equivalent situation in a whole cell where DIRC2 localizes to lysosomes is described in this figure. A three dimensional model of DIRC2, generated with I-TASSER program, shows both N- and C-termini in the cytosolic environment and N-glycosylation site at the loop5 of DIRC2 within the lumen of lysosome. Cleavage site of DIRC2 by cathepsin L is presumably C-terminal from the glycosylation site. Outward current evoked by metabolites in the experiment with *X. oocytes* suggested an inward current from lysosomes. This may indicate that the substrates within the lysosomes are anions which counterbalance cations transport from the cytosol.

The model described above with a current toward lysosomes or anions are being transported out of lysosomes is somehow surprising since lysosomal transporters are generally coupled with a proton efflux from lysosomes and counterbalanced with an outward current. Nevertheless, the possibility that anions efflux from lysosomes accounting for DIRC2 activity is also supported by the fact that a high concentration of chloride ions was observed within lysosomes, as recently reported by Weinert and co-workers (Weinert et al 2010). It is also plausible that the DIRC2 operates as a symporter where the outward current from lysosomes is coupled with the efflux of catabolic products from lysosomes.

4.7 Outlook

It was shown in this study that DIRC2 is a lysosomal membrane protein. It is subject to proteolytic processing within the lysosomes which leads to fragmentation of DIRC2 into two asymmetric fragments. The cleavage site of DIRC2 is not yet clear. Scanning of amino acids in the loop5 which are adjacent to TM6 may reveal the exact cleavage site of DIRC2. Alternatively, the C-terminal fragment from overexpressed DIRC2-3xmyc can be purified by immunoaffinity chromatography and its N-terminal end representing the cleavage site by cathepsin L can be determined by Edman degradation of the amino terminus.

Cathepsin L was shown to play a role in the processing of DIRC2. However, it is not clear whether cathepsin L directly cleaves DIRC2 or indirectly cleaves DIRC2 through activation of another protease(s). *In vitro* cleavage assay of DIRC2 with a recombinant cathepsin L was not successful (data not shown). Optimization of such an *in vitro* cleavage assay may be necessary by modifying both DIRC2 preparation and/or cleavage conditions. Upon successful *in vitro* cleavage assay, the DIRC2 fragments can be analyzed by MALDI-TOF to determine the exact mass of each fragments from which the cleavage site of DIRC2 can be deduced.

Bioinformatic analysis of DIRC2 as well as results shown for the biochemical characterization of DIRC2 are in agreement that DIRC2 is a member of MFS proteins residing in the lysosomal membrane. However what function it plays in lysosomes is not clear. As current, there is no knock out mouse available to analyze the functional relevance of DIRC2 *in vivo*. Hence, preparation and analysis of such a DIRC2 knock out mouse is a promising strategy to identify the physiological role of DIRC2.

In an initial characterization of DIRC2 function by expression of a dileucine mutant of DIRC2 at the plasma membrane of *Xenopus oocytes* and testing its ability to take up metabolites, it was found that DIRC2 may act as an electrogenic transporter. It showed an outward current which counteracts influx of metabolites from the acidic, rich extracellular medium. This process is equivalent to efflux of catabolites from lysosomes and inward current into the lysosomes. By using the same approach, selective uptake of metabolites from the medium by DIRC2 expressed on the surface of *Xenopus oocytes* could be the method of choice to unravel the substrate of DIRC2.

Upon identification of the substrate of full length form of DIRC2, it is of interest to analyze the influence of proteolytic processing on the function of DIRC2. A possible interaction between the DIRC2 fragments and the relevance its function could also provide valuable information in order to have a more comprehensive description of this transporter protein.

Bibliography:

Abramson, J. Smirnova, I., Kasho, V., Verner, G., Kaback, H.R., and Iwata, S. (*2*003) Structure and mechanism of the lactose permease of *Escherichia coli*. *Science* **301**, 610-*615.*

Aoyagi, T., Takeuchi, T., Matsuzaki, A., Kawamura, K. and Kondo, S. (1969) Leupeptins, new protease inhibitors from *Actinomycetes*. *Journal of Antibiotics* **22**, 283-286.

Augustin, R., Riley, J. and Moley, K.H. (2005) GLUT8 contains a [DE]XXXL[LI] sorting motif and localizes to a late endosomal/lysosomal compartment. *Traffic* **6**, 1196-1212.

Bagshaw, R.D., Mahuran,D.J. and Callahan, J.W. (2005) A proteomic analysis of lysosomal integral membrane proteins reveals the diverse composition of the organelle. *Mol. Cell. Proteomics*, **4**, 133-143.

Baliova, M., Betz, H. and Jursky, F. (2004) Calpain-mediated proteolytic cleavage of the neuronal glycine transporter, GlyT2. *Journal of Neurochemistry* **88**, 227-232.

Bang, B., Baadsgaard, O., Skov, L., and Jaattela, M. (2004) Inhibitors of cysteine cathepsin and calpain do not prevent ultraviolet-B-induced apoptosis in human keratinocytes and HeLa cells. *Arch. Dermatol. Res*. **296**, 67-73.

Barrett, A.J., Kembhavi, A.A., Brown, M.A., Kirschke, H., Knight, C.G., Tamai, M., and Hanada, K. (1982) L-trans-Epoxysuccinyl-leucylamido(4-guanidino)butane (E-64) and its analogues as inhibitors of cysteine proteinases including cathepsins B, H and L. *Biochem. J*. **201**, 189-198.

Barrett, A.J., Rawlings, N.D. and Woessner, J.F. Jr. (eds). (1998) Handbook of Proteolytic Enzymes. Academic Press, London, UK.

Bodmer, D., Eleveld, M., Kater-Baats, E., Janssen, I., Janssen, B., Weterman, M., Schoenmakers, E., Nickerson, M., Linehan, M., Zbar, B., and van Kessel, A.G. (2002) Disruption of a novel MFS transporter gene, DIRC2, by a familial renal cell carcinoma-associated t(2;3)(q35;q21). *Hum .Mol. Gen.* **11**,641-649.

Bonifacino J.S. and Traub, L.M. (2003) Signals for sorting of transmembrane proteins to endosomes and lysosomes. *Annu. Rev. Biochem.* **72**, 395-447.

Braulke, T. and Bonifacino, J.S. (2009) Sorting of lysosomal proteins. *Biochim. Biophys. Acta* **1793**, 605-614.

Braulke, T., Gartung, C., Hasilik, A., von Figura, K. (1987) Is movement of mannose 6-phosphate-specific receptor triggered by binding of lysosomal enzymes? *J. Cell Biol*. **104,** 1735–1742.

Breuer, P., Körner, C., Böker, C., Herzog, A., Pohlmann, R., Braulke, T. (1997) Serine phosphorylation site of the 46-kDa mannose 6-phosphate receptor is required for transport to

the plasma membrane in Madin-Darby canine kidney and mouse fibroblast cells. *Mol. Biol. Cell* **8**, 567–576.

Brix, K. (2005) Lysosomal protease: revival of the sleeping beauty. *Eurekah Bioscience* **1**, 259-264.

Brooks, N.L., Corey, M.J., and Schwalbe, R.S. (2006) Characterization of N-glycosylation consensus sequences in the Kv3.1 channel. *FEBS Journal* **273**, 3287-3300.

Cheung, J.C. and Reithmeier, R.A.F. (2007) Scanning N-glycosylation mutagenesis of membrane proteins. *Methods* **41**, 451-459.

Chiechanover, A. (2005) Proteolysis: from the lysosome to ubiquitin and the proteasome. *Nat. Rev. Mol. Cell Biol*. **6**, 79-86.

Choe, Y., Leonetti, F., Greenbaum, D.C., Lecaille, F., Bogyo, M., Broemme, D., Ellman, J.A., and Craik, C.S. (2006) Substrate profiling of cysteine proteases using a combinatorial peptide library identifies functionally unique specificities. *J. Biol. Chem.* **281**,12824-12832.

Cuervo, A. M. and Dice, J. F. (1998) Lysosomes, a meeting point of proteins, chaperones, and proteases. *J. Mol. Med.* **76**, 6-12.

Dahl, S.W., Halkier, T., Lauritzen, C., Dolenc, I., Pedersen, J., Turk, V., and Turk, B. (2001) Human recombinant pro-dipeptidyl peptidase I (cathepsin C) can be activated by cathepsins L and S but not by autocatalytic processing. *Biochemistry* **40**, 1671-1678.

Damme, M., Morelle, W., Schmidt, B., Andersson, C., Fogh, J., Michalski, J-C. and Luebke, T. (2010) Impaired lysosomal trimming of N-linked oligosaccharides leads to hyperglycosylation of native lysosomal proteins in mice with α-mannosidosis. *Mol. Cell. Biol.* **30**, 273-283.

de Duve, C. (1959) in *Subcellular Particles* (Hayashi, T., ed) The Ronald Press Co., New York, 128-159.

de Duve, C., Pressman, B.C., Gianetto, R., Wattiaux, R., and Appelmans, F. (1955) Tissue fractionation studies. 6. Intracellular distribution patterns of enzymes in rat-liver tissue. *Biochem. J*. **60**, 604–617.

De Strooper, B., Annaert, W., Cupers, P., Saftig, P., Craessaerts, K., Mumm, J.S., Schroeter, E.H., Schrijvers, V., Wolfe, M.S., Rayk, W.J., Goatek, A., and Kopan, R. (1999) A presenilin-1-dependent γ-secretase-like protease mediates release of Notch intracellular domain. *Nature* **398**, 518-522.

Dennemärker, J., Lohmüller, T., Müller, S., Aguilar, S.V., Tobin, D.J., Peters, C., and Reinheckel, T. (2010) Impaired turnover of autophagolysosomes in cathepsin L deficiency. *Biol. Chem.* **391**, 913-22.

Deussing, J., Roth,W., Saftig, P., Peters, C., Ploegh, H.L., and Villadangos, J.A. (1998) Cathepsins B and D are dispensable for major histocompatibility complex class II-mediated antigen presentation. *Proc. Natl. Acad. Sci. USA.* **95**, 4516-4521.

Dittmer, F., Ulbrich, E.J., Hafner, A., Schmahl, W., Meister, T., Pohlmann, R., and von Figura, K. (1999) Alternative mechanisms for trafficking of lysosomal enzymes in mannose 6-phosphate receptor-deficient mice are cell type-specific. *J. Cell Sci.***112**, 1591-1597.

Drose, S. and Altendorf, K. (1997) Bafilomycins and concanamycins as inhibitors of V-ATPase and P-ATPase. *J. Exp. Biol*. **200**, 1-8.

Ebert, D. H., Deussing, J., Peters, C., Dermody, T. S. (2002) Cathepsin L and Cathepsin B mediate reovirus disassembly in murine fibroblast cells. *J. Biol. Chem.* **277**, 24609-24617.

Eskelinen, E-L., Tanaka, Y. and Saftig, P. (2003) At the acidic edge: Emerging functions for lysosomal membrane proteins. *Trends Cell Biol.* **13**, 137-145.

Felbor, U., Kessler, B., Mothes, W., Goebel, H.H., Ploegh, H.L., Bronson, R.T., and Olsen, B.R. (2002) Neuronal loss and brain atrophy in mice lacking cathepsins B and L. *Proc. Natl. Acad. Sci. USA* ***99***, 7883-7888.

Foghsgaard, L., Wissing, D., Mauch, D., Lademann, U., Bastholm, L., Boes, M., Elling, F., Leist, M., and Jäättelä, M. (2001) Cathepsin B acts as a dominant execution protease in tumor cell apoptosis induced by tumor necrosis factor. *J. Cell Biol.* **153**, 999-1010.

Gahl, W. A., Bashan, N., Tietze, F., Bernardini, I., and Schulman, J. D. (1982) Cystine transport is defective in isolated leukocyte lysosomes from patients with cystinosis. *Science* **217**, 1263-1265.

Gahl, W.A. and Tietze, F. (1985) pH effects on cystine transport in lysosome-rich leucocyte granular fractions. *Biochem. J*. **228**, 263-267.

Galbiati, F., Volonte., Minetti, C., Bregman, D.B. and Lisanti, M.P. (2000) Limb-girdle muscular dystrophy (LGMD-1C) mutants of caveolin-3 undergo ubiquitination and proteasomal degradation. Treatment with proteasomal inhibitors blocks the dominant negative effect of Lgmd-1c mutants and rescues wild-type caveolin-3. *J. Biol. Chem.* **275**, 37702-37711.

Gelfman, C. M., Vogel, P., Issa, T.M., Turner, C.A., Lee, W-S., Kornfeld, S., and Rice, D.S. (2007) Mice lacking α/β subunits of GlcNAc-1-phosphotransferase exhibit growth retardation, retinal degeneration, and secretory cell lesions. *Invest. Ophthalmol. Vis. Sci*. **48**, 5221–5228.

Ghosh, P., Dahms, N.M. and Kornfeld, S. (2003) Mannose 6-phosphate receptors: new twists in the tale. *Nat. Rev. Mol. Cell Biol*. **4**, 202-212.

Goulet, B., Baruch, A., Moon, N-S., Poirier, M., Sansregret, L-L., Erickson, A., Bogyo, M., and Nepveu, A. (2004) A cathepsin L isoform that is devoid of a signal peptide localizes to the nucleus in S phase and processes the CDP/Cus transcription factor. *Mol. Cell* **14**, 207-219.

Guicciardi, M.E., Miyoshi, H., Bronk, S.F., and Gores, G.J. (2001) Cathepsin B Knockout Mice Are Resistant to Tumor Necrosis Factor-α-Mediated Hepatocyte Apoptosis and Liver Injury: Implications for Therapeutic Applications. *Am. J. Pathol.* **159**, 2045-2054.

Gupta, R., Jung, E., and Brunak, S. (2004) Prediction of N-glycosylation sites in human protein, in preparation.

Halangk, W., Lerch, M.M., Brandt-Nedelev, B., Roth, W., Ruthenbuerger, M., Reinheckel, T., Domschke, W., Lippert, H., Peters, C., and Deussing, J. (2000) Role of cathepsin B in intracellular trypsinogen activation and the onset of acute pancreatitis. *J. Clin. Invest.* **106,** 773-781.

Hirai, T. and Subramaniam, S. (2004) Structure and transport mechanism of the bacterial oxalate transporter OxlT. *Biophys. J.* **87**, 3600-7.

Hrebicek, M., Mrazova, L., Seyrantepe, V., Durand, S., Roslin, N.M., Noskova, L., Hartmannova, H., Ivanek, R., Cizkova, A., Poupetova, H., Sikora, J., Urinovska, J., Stranecky, V., Zeman, J., Lepage, P., Roquis, D., Verner, A., Ausseil, J., Beesley, C.E., Maire, I., Poorthuis, B.J., van de Kamp, J., van Diggelen, O.P., Wevers, R.A., Hudson, T.J., Fujiwara, T.M., Majewski, J., Morgan, K., Kmoch, S., Pshezhetsky, A.V. (2006) Mutations in TMEM7 cause mucopolysaccharidosis IIIC (Sanfilippo C syndrome). *Am. J. Hum. Genet*. **79**, 807-819.

Huang, Y., Lemieux, M.J., Song, J., Auer, M., and Wang, D.N. (2003) Structure and mechanism of the glycerol-3-phosphate transporter from *Escherichia coli*. *Science* **301**, 616-620.

Janvier, K. and Bonifacino, J. S. (2005) Role of the endocytic machinery in the sorting of lysosome-associated membrane proteins. *Mol. Biol. Cell* **16**, 4231-4242.

Jonas, A. J., Greene, A. A., Smith, M. L., and Schneider, J. A. (1982) Cystine accumulation and loss in normal, heterozygous, and cystinotic fibroblasts. *Proc. Natl. Acad. Sci. U.S.A.* **79**, 4442-4445.

Jordan, A.M and Wilson, L. (2004) Microtubules as a target for Anticancer drugs. *Nat. Rev. Cancer* **4,** 253-265.

Journet, A., Chapel, A., Kieffer, S., Roux, F., and Garin, J. (2002) Proteomic analysis of human lysosomes: Application to monocytic and breast cancer cells. *Proteomics* **2**, 1026-1040.

Kaback, H.R., Sahin-Tóth, M., and Weinglass, A.B. (2001) The kamikaze approach to membrane transport. *Nat. Rev. Mol. Cell Biol.* **2,** 610–620.

Kalatzis, V., Cherqui, S., Antignac, C., and Gasnier, B. (2001) Cystinosin, the protein defective in cystinosis, is a H(+)-driven lysosomal cystine transporter. *EMBO J.* **20**, 5940-5949.

Katunuma, N. and Kominami, E. (1995**)** Structure, properties, mechanisms, and assays of cysteine protease inhibitors: Cystatins and E-64 derivatives. *Methods Enzymol*. **251**, 382-397.

Keel, S.B., Doty, R.T., Yang, Z., Quigley, J.G., Chen, J., Knoblaugh, S., Kingsley, P.D., De Domenico, I., Vaughn, M.B., Kaplan, J., Palis, J., and Abkowitz, J.L. (2008) A heme export protein is required for red blood cell differentiation and iron homeostasis. *Science* **319**, 825-828.

Kiselyov, K., Chen, J., Rbaibi, Y., Oberdick, D., Tjon-Kon-Sang, S., Shcheynikov, N., Muallem, S., and Soyombo, A. (2005) TRP-ML1 is a lysosomal monovalent cation channel that undergoes proteolytic cleavage. *J. Biol. Chem.* **280**, 43218-43223.

Klemencic, I., Carmona, A. K., Cezari, M. H., Juliano, M. A., Juliano, L., Guncar, G., Turk, D., Krizaj, I., Turk, V., and Turk, B. (2000) Biochemical characterization of human cathepsin X revealed that the enzyme is an exopeptidase, acting as carboxymonopeptidase or carboxydipeptidase. *Eur. J. Biochem.* **267**, 5404-5412.

Kollmann, K., Mutenda, K.E., Balleininger, M., Eckermann, E., von Figura, K., Schmidt, B., and Lübke, T. (2005) Identification of novel lysosomal matrix proteins by proteome analysis. *Proteomics* **5**, 3966-3978.

Konjar, S., Sutton V.R., Hoves, S., Repnik, U., Yagita, H., Reinheckel, T., Peters, C., Turk, V., Turk, B., Trapani, J.A. and Kopitar-Jerala, N. (2010) Human and mouse perforin are processed in part through cleavage by the lysosomal cysteine proteinase cathepsin L. *Immunology* **131**, 257-67.

Kornfeld, S. and Mellman, I. (1989) The biogenesis of lysosomes. *Annu. Rev. Cell Biol.* **5**, 483-525.

Kornfeld, S. and Sly, W.S. (2001) I-cell disease and pseudo-Hurler polydystrophy: disorders of lysosomal enzyme phosphorylation and localization, in: C.R. Scriver, A.L.Beaudet,W.S. Sly, D. Valle (Eds.), The Metabolic and Molecular Bases of Inherited Disease, McGraw-Hill, New York, 3421–3452

Krogh, A., Larsson, B., von Heijne, G., and Sonnhammer, E.L.L. (2001) Predicting transmembrane protein topology with a Hidden Markov model: application to complete genomes. *J.Mol. Biol.* **305**, 567-580.

Kuronita, T., Eskelinen, E-L., Fujita, H., Saftig, P., Himeno, M. and Tanaka, Y. (2002) A role for the lysosomal membrane protein LGP85 in the biogenesis and maintenance of endosomal and lysosomal morphology. *J. Cell Sci*. 115, 4117-4131.

Law, C.J., Maloney, P.C., and Wang, D.N. (2008) Ins and outs of major facilitator superfamily antiporters. *Annu. Rev. Microbial.* **62,** 289-305.

Lefrancois, S., Zeng, J., Hassan, A., Canuel, M, Morales, C. (2003) The lysosomal trafficking of sphingolipid activator proteins (SAPs) is mediated by sortilin. *EMBO J.* **22**, 6430–6437.

Letourneur, F. and Klausner, R.D. (1992) A novel di-leucine motif and a tyrosine-based motif independently mediate lysosomal targeting and endocytosis of CD3 chains. *Cell* **69,** 1143-1157.

Lin, C.W., Sasaki, M.m Orcutt, M.L., Miyayama, H. and Singer, R.M., (1976) Plasma membrane localization of alkaline phosphatase in HeLa cells. *J. Histochem. Cytochem.* **24**, 659-667.

Liu, Q.-R., Lopez-Corcuera, B., Mandiyan, S., Nelson, H., and Nelson, N. (1993) Cloning and expression of a spinal cord- and brain-specific glycine transporter with novel structural features. *J. Biol. Chem*. **268**, 22802-22808.

Lübke, T., Lobel, P. and Sleat, D.E. (2009) Proteomics of the lysosome. *Biochim. Biophys. Acta* **1793**, 625-635.

Maiden, M.C.J., Davis, E.O., Baldwin, S.A., Moore, D.C.M., and Henderson, P.J.F. (1987) Mammalian and bacterial sugar-transport proteins are homologous. *Nature* **325**, 641-43.

Medzihradszky, K.F. (2008) Post-translational modification of proteins: tools for functional proteomics, Book Title in Series: *Methods in Molecular Biology*, Springer, **446**; 293-316.

Mellman, I., Fuchs, R. and Helenius, A. (1986) Acidification of the endocytic and exocytic Pathways. *Ann. Rev. Biochem*. **55**, 663-700.

Melo, R.L., Alves, L.C., Del Nery, E., Juliano, L., and Juliano, M.A. (2001) Synthesis and hydrolysis by cysteine and serine proteases of short internally quenched fluorogenic peptides. *Anal. Biochem.* **293**, 71-77.

Misinzo, G., Delputte, P.L. and Nauwynck, H.J. (2008) Inhibition of endosome-lysosome system acidification enhances porcine circovirus 2 infection of porcine epithelial cells. *Journal of Virology* **82**, 1128-1135.

Misumi, A., Misumi, Y., Miki, K., Takasugi, A., Tamura, G., and Ikehara, Y. (1986) Novel blockade by brefeldin A of intracellular transport of secretory protein in cultured rat hepatocytes. *J. Biol. Chem.* **261**, 11398-11403.

Montaser, M., Lalmanach, G. and Mach, L. (2002) CA-074, but not its methyl ester CA-074Me, is a selective inhibitor of cathepsin B within living cells. *Biol. Chem.* **383**, 1305-1308.

Morin, P., Sagné, C. and Gasnier, B. (2004) Functional characterization of wild-type and mutant human sialin. *EMBO J.* **23**, 4560-4570.

Musil, D., Zucic, D., Turk, D., Engh, R.A., Mayr, I., Huber, R., Popovic, T., Turk, V., Towatari, T., and Katunuma, N. (1991) The refined 2.15 A X-ray crystal structure of human liver cathepsin B: the structural basis for its specificity. *EMBO J.* **10**, 2321-2330.

Nagler, D.K. and Menard, R. (2003) Family C1 cysteine proteases: Biological diversity of redundancy? *Biol. Chem.* **384,** 837-843.

Nägler, D., Tam, W., Storer, A.C., Krupa, J.C., Mort, J.S., and Menard, R. (1999) Human cathepsin X: a cysteine protease with unique carboxypeptidase activity. *Biochemistry* **38**, 4868-4874.

Nakagawa, T., Roth, W., Wong, P., Nelson, A., Farr, A., Deussing, J., Villadangos, J.A., Ploegh, H., Peters, C., and Rudensky, A.Y. (1998) Cathepsin L: critical role in Ii degradation and CD4 T cell selection in the thymus. *Science* **280**, 450-453.

Ni, X. and Morales, C. (2006) The lysosomal trafficking of acid sphingomyelinase is mediated by sortilin and mannose 6-phosphate receptor. *Traffic* **7**, 889–902.

Pao, S.S., Paulsen, I.T. and Saier, M.H. (1998) Major facilitator superfamily. *Microbiol. Mol. Biol. Rev.* **62**,1-34.

Park, B., Brinkmann, M.M., Spooner, E., Lee, C.C., Kim, Y. and Ploegh, H.L. (2008) Proteolytic cleavage in an endolysosomal compartment is required for activation of Toll-like receptor 9. *Nat. Immun.* **9**, 1407-1414.

Peters, C., Braun, M., Weber, B., Wendland, M., Schmidt, B., Pohlmann, R., Waheed, A., and von Figura, K. (1990) Targeting of a lysosomal membrane protein: a tyrosine-containing endocytosis signal in the cytoplasmic tail of lysosomal acid phosphatase is necessary and sufficient for targeting to lysosomes. *EMBO J.* **9**, 3497-3506.

Pisoni, R.L. and Thoene, J.G. (1991) The transport systems of mammalian lysosomes. *Biochim. Biophys. Acta* **1071**, 351-373.

Puzer, L., Cotrin, S.S., Alves, M.F.M., Egborge, T., Araujo, M.S., Juliano, A.A., Juliano, L., Broemme, D., and Carmona, A.K. (2004) Comparative substrate specificity analysis of recombinant human cathepsin V and cathepsin L. *Arch. Biochem. Biophys.* **430**, 274-283.

Reczek, D., Schwake, M., Schröder, J., Hughes, H., Blanz, J., Jin, X., Brondyk, W., van Patten, S., Edmunds, T., Saftig, P. (2007) LIMP-2 is a receptor for lysosomal mannose-6-phosphate-independent targeting of beta-glucocerebrosidase. *Cell* **131**, 770–783.

Reinheckel, T., Deussing, J., Roth, W., and Peters, C. (2001) Towards specific functions of lysosomal cysteine peptidases: phenotypes of mice deficient for cathepsin B or cathepsin L. *Biol. Chem.* **382**, 735-741.

Reiser, J., Adair, B. and Reinheckel, T., (2010) Specialized roles for cysteine cathepsins in health and disease. *J. Clin. Invest.* **120**, 3421-3431.

Rickles, R.J., Botfield, M.C., Weng, Z., Taylor, J.A., Green, O.M., Brugge, J.S., and Zoller,M.J. (1994) Identification of Src, Fyn, Lyn and Abl SH3 domain ligands using phage display libraries. *EMBO J.*, **13**, 5598-5604.

Roth, W., Deussing, J., Botchkarev, V.A., Pauly-Evers, M., Saftig, P., Hafner, A., Schmidt, P., Schmahl, W., Scherer, J., Anton-Lamprecht, I., von Figura, K., Paus, R. and Peters, C. (2000) Cathepsin L deficiency as molecular defect of furless: hyperproliferation of keratinocytes and pertubation of hair follicle cycling. *FASEB J.* **14**, 2075-2086.

Roy, A., Kucukural, A. and Zhang, Y. (2010) I-TASSER: a unified platform for automated protein structure and function prediction. *Nature Protocols* **5**, 725-738.

Ruivo, R., Anne, C., Sagné, C., Gasnier, B. (2009) Molecular and cellular basis of lysosomal transmembrane protein dysfunction. *Biochim. Biophys. Acta* **1793**, 636-649.

Saftig, P., Hetman, M.m Schmahl, W., Weber, K., Heine, L., Mossmann, H.m Koester, A., Hess, B., Evers, M., von Figura, K., and Peters, C. (1995) Mice deficient for the lysosomal proteinase cathepsin D exhibit progressive atrophy of the intestinal mucosa and profound destruction of lymphoid cells. *EMBO J.* **14**, 3599-3608.

Saftig, P and Klumperman, J. (2009) Lysosome biogenesis and lysosomal membrane proteins: trafficking meets function. *Nat. Rev. Mol. Cell Biol.* **10**, 623-635.

Sagné, C. and Gasnier, B. (2008) Molecular physiology and pathophysiology of lysosomal membrane transporters. *J. Inherit. Metab. Dis*. **31**, 258-266.

Saier, M.H. Jr., Beatty, J.T., Goffeau, A., Harley, K.T., Heijne, W.H.M., Huang, S-C., Jack, D.L., Jähn, P.S., Lew, K., Liu, J., Pao, S.S., Paulsen, I.T., Tseng, T-T., and Virk, P.S. (1999) The Major Facilitator Superfamily. *J. Mol. Microbiol. Biotechnol*. **1**, 257-279.

Saier, M.H. (2003) Tracing pathways of transport protein evolution. *Mol. Microbiol.* **48**, 1145-56.

Schroeder, B., Wrocklage, C., Pan, C., Jäger, R., Kösters, B., Schafer, H., Elsässer, H.P., Mann, M., and Hasilik, A. (2007) Integral and associated lysosomal membrane proteins. *Traffic* **8**, 1676-1686.

Schulze, H., Kolter, T., and Sandhoff, K. (2009) Principles of lysosomal membrane degradation. Cellular topology and biochemistry of lysosomal lipid degradation. *Biochim. Biophys. Acta* **1793**, 674–683.

Sevenich, L., Pennacchio, L.A., Peter, D., and Reinheckel, T. (2006) Human cathepsin L rescues the neurodegeneration and lethality in cathepsin B/L double-deficient mice. *Biol. Chem*. **387**,885-891.

Siintola, E. (2008) Identification of two novel human neuronal ceroid lipofuscinosis genes. Helsinki University Biomedical Dissertations No. 107, Finland.

Sleat, D.E., Lackland, H., Wang, Y., Sohar, I., Xiao, G., Li, H., Lobel, P. (2005) The human brain mannose 6-phosphate glycoproteome: a complex mixture composed of multiple isoforms of many soluble lysosomal proteins. *Proteomics* **5**, 1520–1532.

Storch, S. and Braulke, T. (2005) Transport of lysosomal enzymes. In: Lysosomes (P. Saftig, ed). Georgetown: Landes Bioscience: Springer Science+Business Media, New York, 17-26.

Tedelind, S., Poliakova, K., Valeta, A., Hunegnaw, R., Yemanaberhan, E-L., Heldin, N-E., Kurebayashi, J., Weber, E., Kopitar-Jerala, N., Turk, B., Bogyo, M., and Brix, K. (2010) Nuclear cysteine cathepsin variants in thyroid carcinoma cells. *Biol. Chem*. **391**, 923-935.

Maley, F., Trimble, R.B., Tarentino, A.L., and Plummer, Jr., T.H. (1989) Characterization of glycoproteins and their associated oligosaccharides through the use of endoglycosidases. *Anal. Biochem.* **180**, 195-2004.

Turk, V., Turk, B. and Turk, D. (2001) Lysosomal cysteine proteases: facts and Opportunities. *EMBO J*. **20**, 4629-4633.

Turk, B., Turk, D. and Turk, V. (2000) Lysosomal cysteine proteases: more than scavengers. *Biochim. Biophys. Acta* **1477**, 98-111.

Umezawa, H., Aoyagi, T, Morishima, H., Matsuzaki, M. and Hamada, M. (1970) Pepstatin, a new pepstin inhibotor produced by Actinomycetes. *Journal Antibiotics* **23**, 259-262.

Vardy, E., Arkin, I.T., Gottschalk, K.E., Kaback, H.R., and Schuldiner, S. (2004) Structural conservation in the major facilitator superfamily as revealed by comparative modeling. *Protein Science* **13**, 1832–1840.

Vergarajauregui, S. and Puertollano, R. (2007) Two di-leucine motifs regulate trafficking of mucolipin-1 to lysosomes. *Traffic* **6**, 337-353.

von Figura, K. and Hasilik, A. (1986) Lysosomal enzymes and their receptors. *Annu. Rev. Biochem*. **55**, 167-193.

Waheed, A., Pohlmann, R., Hasilik, A., von Figura, K., van Elsen, A., and Leroy, J.G. (1982) Deficiency of UDP-N-acetylglucosamine: lysosomal enzyme N-acetylglucosamine-1-phosphotransferase in organs of I-cell patients. *Biochem. Biophys. Res. Commun.* **105**, 1052–1058.

Weinert, S., Jabs, S., Supanchart, C., Schweizer, M., Gimber, N., Richter, M., Rademann, J., Stauber, T., Kornak, U., and Jentsch, T. J. (2010) Lysosomal Pathology and Osteopetrosis upon Loss of H^+-Driven Lysosomal Cl^- Accumulation. *Science* **328**, 1401-1403.

Weinglass, A.B. and Kaback, H.R. (2000) The central cytoplasmic loop of the major facilitator superfamily of transport proteins governs efficient membrane insertion. *Proc. Natl. Acad. Sci. USA* **97,** 8938-8943.

Williams, M.A. and Fukuda, M. (1990) Accumulation of membrane glycoproteins in lysosomes requires a tyrosine residue at a particular position in the cytoplasmic tail. *J. Cell Biol*. **111**, 955-966.

Wreden, C.C., Wlizla, M. and Reimer, R.J. (2005) Varied mechanisms underlie the free sialic acid storage disorders. *J. Biol. Chem.* **280**, 1408 -1416.

Yin, Y., He, X., Szewczyk, P., Nguyen, T., and Chang, G. (2006) Structure of the multidrug transporter EmrD from *Escherichia coli*. *Science* **312**, 741-744.

Zhang, Y. (2008) I-TASSER server for protein 3D structure prediction. *BMC Bioinformatics* **9**, 1-8.

CURRICULUM VITAE

Personal data:

Name : Lalu Rudyat Telly Savalas, B.Sc., M.Sc

Place and date of birth: Lombok, Indonesia, June 26th 1975

Nationality: Indonesian

Education:

1. Master degree with thesis, with grade of 'Excellent', Department of Chemistry, Faculty of Mathematics and Natural Sciences, ITB, with major in Biochemistry, 2002.
2. Bachelor degree with thesis, with grade of 'very good', Department of Chemistry, Faculty of Mathematics and Natural Sciences, ITB, 1999.

Award: Awardee of the Germany Academic Exchange Service (DAAD) scholarship and Overseas PhD Scholarship from the Department of Education and Cultural, Republic of Indonesia to undertake PhD study in Germany.

Working Experiences:

1. Lecturer in biochemistry, University of Mataram, Indonesia, since 2004.
2. Research Assistant, Protein and Enzyme Research Group and Genetic Engineering Laboratory, Biotechnology Research and Development Center, ITB, 2000-2003.
3. Teaching Assistant, Biochemistry Laboratory, Department of Chemistry, ITB, 1997-2002.

Attended Courses/Seminars:

1. International Summer School on Pathogen-Host-Interplay, Center of Infection Biology and Immunity, July 20-24, 2009, Charite´, Berlin.
2. Attending the Summer School in Graduate Frontier of Biosciences, Osaka University, Japan (July - Aug 2004), and assigned in Prof. Hiroshi Nojima's lab (Research Institute of Microbial diseases)
3. The 3rd Sanbe Teaching and Laboratory Course on Diagnostic with DNA Probes and Monoclonal Antibodies (Genetic Cardiology), Bandung, Indonesia, 17-18 February 2003.
4. The 5th ITB-UKM Joint Seminar, Malacca, Malaysia, 16-17 July 2002.
5. National Seminar on Chemistry, Institut Teknologi Sebelas November Surabaya, Indonesia, August 24 1999.